

**PERFORMANCE IMPROVEMENT OF
ANTENNA ARRAY COMMUNICATIONS
THROUGH TIME SHIFTED SAMPLING
FOR OFDM SYSTEMS**

A THESIS

SUBMITTED TO THE SCHOOL OF INTEGRATED
DESIGN ENGINEERING OF KEIO UNIVERSITY
IN PARTIAL FULFILLMENT OF THE REQUIREMENTS
FOR THE DEGREE OF
DOCTOR OF PHILOSOPHY

By

Refik Caglar KIZILIRMAK

September, 2010

ABSTRACT

PERFORMANCE IMPROVEMENT OF ANTENNA ARRAY COMMUNICATIONS THROUGH TIME SHIFTED SAMPLING FOR OFDM SYSTEMS

Refik Çağlar KIZILIRMAK

Supervisor: Assoc. Dr. Yukitoshi Sanada

Recent developments in wireless communications have shown that, by applying diversity techniques, it is possible to provide link improvement without increasing transmission power and bandwidth. A commonly used method for achieving diversity employs multiple antennas at the receiver end. Usually a separation of a few wavelengths is required between two antennas in order to obtain signals that fade independently. In this work, a new technique called Time Shifted Sampling (TSS) to improve the performance of transmission with the correlated fading signals for Orthogonal Frequency Division Multiplexing (OFDM) is proposed. OFDM has emerged as a promising air-interface technique and has been adopted by many wireless standards. OFDM divides the available spectrum into many subcarriers and each subcarrier is assigned some data to transmit.

Chapter 1 gives the detailed introduction on antenna array communications, OFDM and spatial correlation is given in.

Chapter 2 proposes the TSS technique. TSS is a signal processing technique that takes the benefit of multipath diversity and improves the performance of correlated antenna arrays. In conventional array systems, individual receivers of an array start sampling the received signals at the same time with the same sampling rate. On the other hand, in the proposed scheme, the received signals are again sampled with the same rate. However, the sampling points are shifted in each receiver. Numerical results through computer simulation show that with correlated received signals, by applying the proposed technique the correlation for some subcarriers can be reduced to a sufficient level for diversity reception.

In Chapter 3, an adaptive modulation scheme for orthogonal frequency division multiplexing (AOFDM) that provides efficient data transmission for correlated receiver antenna arrays is proposed. In the AOFDM transmission, each carrier in the OFDM system can transmit different modulation schemes depending on its channel condition where in the conventional OFDM systems fixed modulation across all the subcarriers is used. Previously reported adaptive modulation schemes generally select the modulation scheme based on the estimated carrier-to-noise ratio (CNR) on each subcarrier. However, in antenna array communication in addition to the CNR, the spatial fading correlation should also be considered to evaluate the system performance. Especially, when the Time Shifted Sampling (TSS) technique is applied which overcomes the spatial correlation for some subchannels of an OFDM symbol, the spatial correlation varies dramatically through subcarriers. In this Chapter, modulation scheme is selected based on the CNR and the spatial correlation coefficient for each subcarrier when the TSS technique is employed at the receiver. Numerical results through computer simulation show that the proposed scheme outperforms the conventional systems in achieving a target bit-error-rate (BER) and establishing reliable communication while having almost the same transmission rate.

Chapter 4 analyzes the performance of the OFDM diversity system with the spatial fading correlation when the network includes an RF repeater. In this chapter, a multipath channel is constructed by the repeated signal instead of natural multipath due to cluttered environments and the system performance with spatial correlation per subcarrier is evaluated. Numerical results indicate that the TSS technique is also effective in reducing the effect of correlation for the multipath channels constructed by the repeaters.

Chapter 5 summarizes each chapter and concludes this dissertation.

Keywords: Spatial Fading Correlation, Orthogonal Frequency Division Multiplexing, Time Shifted Sampling, Antenna Arrays, Adaptive Modulation, Relay Networks, Amplify and Forward.

Contents

List of Acronyms	xv
List of Notations	xvii
1 Introduction	1
1.1 Antenna Arrays in the Evolution of Wireless Technologies	1
1.2 A Physical Limit on the Antenna Array Communications: Spatial Correlation	5
1.2.1 Impact of the Correlation on the Performance	6
1.2.2 Spatial Channel Model	7
1.3 Orthogonal Frequency Division Multiplexing (OFDM)	10
1.3.1 Historic Background	10
1.3.2 Transmission Methodology	11
1.3.3 Adaptive OFDM (AOFDM)	14
1.3.4 OFDM in Repeater Wireless Networks	15
1.3.5 OFDM in Spatially Correlated Antenna Arrays	16

1.4	Motivation of this Research	17
1.4.1	Overview of Chapter 2	18
1.4.2	Overview of Chapter 3	22
1.4.3	Overview of Chapter 4	23
	References	25
2	Multipath Diversity Through Time Shifted Sampling for Spatially Correlated OFDM Antenna Array Systems	32
2.1	Introduction	33
2.2	Spatially Correlated Rayleigh Channel Model	34
2.2.1	Single Path Ring Model for Antenna Arrays	35
2.2.2	Multipath Ring Model for Antenna Arrays	37
2.3	Time Shifted Sampling	39
2.4	Numerical Results	44
2.5	Discussions and Conclusion	54
	References	57
3	Adaptive Modulation Scheme Incorporating Spatial Fading Correlation for OFDM with Time Shifted Sampling	60
3.1	Introduction	61
3.2	Subcarrier-by-Subcarrier Spatial Correlation for TSS Receivers	63
3.3	Proposed Adaptive Modulation Scheme	65

3.3.1	Conventional Modulation-Scheme Selection Chart	66
3.3.2	Proposed Modulation-Scheme Selection Chart	66
3.4	Performance of the Proposed Scheme	68
3.4.1	Simulation Conditions	68
3.4.2	Channel Models	69
3.4.3	Effect of Time Shifted Sampling for 2 path Rayleigh Channel	71
3.4.4	Performance of the Proposed Adaptive Modulation Scheme for 2 path Rayleigh Channel	73
3.4.5	Effect of Time Shifted Sampling for 6-ray GSM Channel Model	77
3.4.6	Performance of the Proposed Adaptive Modulation Scheme for 6-ray GSM Channel Model	80
3.5	Effect of Error Correcting Code	82
3.6	Discussions and Conclusion	82
	References	86
4	Performance Analysis of OFDM Repeater Networks with Spatial Fading Correlation	90
4.1	Introduction	91
4.2	System Model	93
4.2.1	Amplify-and-Forward Repeater System	93
4.2.2	Spatial Correlation on the Direct-Path (ρ_d)	97
4.2.3	Spatial Correlation on the Relayed-Path (ρ_r)	98

4.3	Signal Model	98
4.4	Numerical Results	101
4.4.1	Impact of the Repeater	101
4.4.2	Impact of Location of the Source	107
4.5	Conclusion	110
	References	111
5	Conclusions	115
	Acknowledgements	119
	List of Achievements	120

List of Figures

1.1	Bandwidth requirement needed to support 1 Gbps link speed as a function of the number of the antenna elements at the receiver array for a Rayleigh fading NLOS link.	4
1.2	Illustration of combining two independent fading signals.	5
1.3	Impact of the spatial correlation on the BER performance of PSK modulation for 2 branch diversity under Rayleigh fading.	6
1.4	Clustered channel for uniform linear array with antenna spacing of δ	8
1.5	Spatial correlation in magnitude for different clusters.	9
1.6	Real portion of the spatial correlation for different clusters.	9
1.7	Imaginary portion of the spatial correlation for different clusters.	10
1.8	Maintaining orthogonal subcarriers.	12
1.9	OFDM Transmitter Architecture.	13
1.10	OFDM Receiver Architecture.	13
1.11	Adaptive OFDM transceiver.	15
1.12	RF Repeater deployment for coverage extension.	16

1.13	Channel taps corresponding to the same time delays will be correlated according to their clusters.	17
1.14	Chapter 2 proposes novel Time Shifted Sampling (TSS) technique to combat the degradations due to the spatial fading correlation.	18
1.15	Block diagram for OFDM Antenna Array Receiver with TSS. . .	19
1.16	Block diagram for Oversampling OFDM.	20
1.17	Reception with polarization diversity. $\chi= \alpha_V ^2/ \alpha_H ^2$	21
1.18	Chapter 3 proposes an adaptive OFDM scheme incorporating the spatial fading correlation when the TSS is applied to receiver array.	23
1.19	Chapter 4 analyzes the performance of correlated OFDM base station when the network includes an RF repeater. TSS is also found effective in Repeater networks.	24
2.1	Jakes' ring model for antenna arrays.	35
2.2	Far scatterers are modeled as another ring that circles the existing ring.	37
2.3	Spatial fading correlation relationships between received signals by each antenna.	38
2.4	Fading envelopes generated for the first and second antennas from both rings for maximum Doppler shift of 100 Hz.	39
2.5	Block diagram for OFDM Antenna Array Receiver with TSS. . .	40
2.6	Illustration of TSS for two elements antenna array in the delay domain.	42

2.7	Spatial fading correlations on each subcarrier for the arrays employ TSS technique and for the conventional arrays. Spatial parameters of the Channel Model-1 are considered. Delay of the second path is $T_s/2$. Sampling delay at the second antenna is $T_s/2$	46
2.8	BER performance improvement with TSS for two elements antenna array for 2-path Rayleigh channel. Spatial parameters for the Channel Model-1 and Model-2 are given in Table 2.2. Delay of the second path is $T_s/2$. Sampling delay at the second antenna is $T_s/2$	47
2.9	BER performance improvement with TSS for Channel Model-2 vs. Antenna Separation. E_b/N_0 is 20 dB. Spatial parameters for the Channel Model-2 is given in Table 2.2. Delay of the second path is $T_s/2$. Sampling delay at the second antenna is $T_s/2$	48
2.10	BER performance improvement with TSS for Channel Model-2 vs. Angular Spread. E_b/N_0 is 20 dB. Spatial parameters for the Channel Model-2 is given in Table 2.2. Delay of the second path is $T_s/2$. Sampling delay at the second antenna is $T_s/2$	49
2.11	BER performance improvement with TSS vs. Angle of Arrival. E_b/N_0 is 20 dB. Spatial parameters for the Channel Model-1 is given in Table 2.2. Delay of the second path is $T_s/2$. Sampling delay at the second antenna is $T_s/2$	50
2.12	Effect of the Normalized Doppler Frequency on the BER Performance. E_b/N_0 is 20 dB. Spatial parameters for the Channel Model-1 and Model-2 are given in Table 2.2. Delay of the second path is $T_s/2$. Sampling delay at the second antenna is $T_s/2$	51
2.13	BER performance improvement with TSS for Channel Model-1. Spatial parameters for the Channel Model-1 is given in Table 2.2. Delay of the second path is taken as $T_s/4$ and $3T_s/4$. Sampling delay at the second antenna is $T_s/2$	52

2.14	BER performance improvement with TSS for Channel Model-1 for different sampling delay at the second antenna. E_b/N_0 is 20 dB. Spatial parameters for the Channel Model-1 is given in Table 2.2. Delay of the second path is taken as $T_s/2$	53
2.15	BER performance improvement with TSS for four elements antenna array. Spatial parameters for the Channel Model-1 and Model-2 are given in Table 2.2. Delay of the second path is $T_s/2$. Sampling delays at the second, third and fourth antennas are $T_s/4$, $2T_s/4$ and $3T_s/4$ respectively.	54
2.16	Comparison of 2 element antenna array with TSS and Oversampling with ratio of 2. Discrete sequences to be transformed into the frequency domain and then combined are pointed as circles and squares.	55
3.1	Signaling scenario in proposed scheme.	67
3.2	Proposed Modulation-Scheme Selection Chart based on CNR and correlation coefficient for target BER 10^{-3}	68
3.3	2 path Rayleigh fading model with uniform delay spread.	69
3.4	6-ray GSM Typical Urban model.	70
3.5	Correlation coefficient over subcarriers for 2-path Rayleigh channel.	72
3.6	Impact of TSS on system throughput performance for 2-path Rayleigh channel Case-1.	73
3.7	BER performance of the proposed scheme for 2-path Rayleigh channel Case-1.	74
3.8	Throughput performance of the proposed scheme for 2-path Rayleigh channel Case-1.	75

3.9	BER performance of the proposed scheme for 2-path Rayleigh channel Case-2.	76
3.10	Throughput performance of the proposed scheme for 2-path Rayleigh channel Case-2.	77
3.11	Correlation coefficient over subcarriers for 6-ray GSM Channel Model.	78
3.12	Impact of TSS on system throughput performance for 6-ray GSM Channel Model.	79
3.13	BER performance of the proposed scheme for 6-ray GSM Channel Model.	80
3.14	Throughput performance of the proposed scheme for 6-ray GSM Channel Model.	81
3.15	BER performance of the proposed scheme with error correcting code for 2-path Rayleigh Case-1.	83
3.16	The probability distribution function of the CNR at the output of MRC combiner for different correlation coefficients. The mean of CNR is 20 dB.	84
3.17	Comparison of the throughput performances of the proposed scheme based on long-term CNR and correlation information and the conventional scheme based on instantaneous channel information. 2-path Rayleigh channel Case-1 is considered.	85
3.18	Comparison of the BER performances of the proposed scheme based on long-term CNR and correlation information and the conventional scheme based on instantaneous channel information. 2-path Rayleigh channel Case-1 is considered.	86
4.1	Transmission model.	93

4.2	Multipath delay profile at adjacent antennas.	95
4.3	Simplified illustration of antenna separation, angular spread and angle of arrival.	96
4.4	Spatial fading correlation coefficient (ρ_d) between the antennas for the direct path.	97
4.5	Wireless repeater channel and singlehop reference channel models. Double lines indicate multi-antenna channel links.	102
4.6	BER performance improvement with TSS for repeater wireless channel.	104
4.7	Different placements of the repeater and the source.	105
4.8	Spatial fading correlation between the subcarriers for repeater wireless channel.	106
4.9	BER performance improvement with TSS for different transmission powers in terms of ϵ for the source and the repeater terminals. The gray surface is the performance for the TSS receiver. The black grid is the performance for the conventional receiver.	107
4.10	BER performance improvement with TSS for repeater wireless channel.	108
4.11	Spatial fading correlation between the subcarriers for repeater wireless channel.	109
4.12	Spatial fading correlations for subcarriers $k=0, \pm N/4$ and $\pm N/2$ vs. different source locations.	110

List of Tables

1.1	History of OFDM	11
2.1	Simulation Conditions	44
2.2	Spatial Channel Models Considered in Simulations	45
3.1	Conventional Modulation-Scheme Selection Chart based on CNR for target BER 10^{-3}	66
3.2	Simulation Conditions	69
3.3	Spatial Channel Models Used for 2 Path Rayleigh Channel	70
3.4	6-ray GSM Typical Urban Model	71
4.1	OFDM Parameters	101
4.2	Channel Parameters	103

List of Acronyms

OFDM	orthogonal frequency division multiplexing
OOFDM	oversampled orthogonal frequency division multiplexing
TSS	time shifted sampling
1G	first-generation cellular networks
2G	second-generation cellular networks
3G	third-generation cellular networks
4G	fourth-generation cellular networks
3GPP	the 3rd generation partnership project
IMT-Advanced	international mobile telecommunications-advanced
ITU	International Telecommunication Union
HSDPA	high speed downlink packet access
WLAN	wireless local area networks
WiMAX	worldwide interoperability for microwave access
MIMO	multiple-input-multiple-output
IEEE	intitule of electrical and electronics engineers
SNR	signal-to-noise ratio
CNR	carrier-to-noise ratio
LOS	line-of-sight
NLOS	non-line-of-sight
SC	selection combining
MRC	maximum ratio combining
EGC	equal gain combining
BER	bit-error-rate
BPSK	binary phase shift keying
QPSK	quadrature phase shift keying
QAM	quadrature amplitude modulation
DMT	discrete multitone
ADSL	asymmetric digital subscriber line
HDSL	high-bit-rate digital subscriber line
VDSL	very-high-speed digital subscriber line

DAB	digital audio broadcasting
DVB-T	digital video broadcasting for terrestrial television
DVB-H	digital video broadcasting for handheld terminals
BRAN	broadband radio access networks
DFT	discrete fourier transform
IDFT	inverse discrete fourier transform
GI	guard interval
ISI	inter-symbol interference
DAC	digital-to-analog converter
ADC	analog-to-digital converter
P/S	parallel-to-serial converter
S/P	serial-to-parallel converter
PAPR	peak-to-average power ratio
FS	fractional sampling
AOFDM	adaptive orthogonal frequency division multiplexing

List of Notations

f_c	carrier frequency
R	radius of the scattering ring
d	distance between the transmitter and the receiver
s	scatterer index
ψ_s	nominal angle of the scatterer s
w_s	Doppler shift for the scatterer s
c	the speed of light
f	frequency
ζ	nominal angle of motion of the mobile
θ_s	random phase shift of the scatterer s
λ	wavelength
δ	antenna separation(λ)
Δ	angular spread($^\circ$)
ϕ	angle of arrival($^\circ$)
L	number of multipath components
ℓ	path index of multipath channel
Δ_ℓ	angular spread($^\circ$) of the ℓ^{th} path
ϕ_ℓ	angle of arrival($^\circ$) of the ℓ^{th} path
M	number of antennas at the receiver antenna array
M_R	number of antennas at the receiver site of MIMO transmission
M_T	number of antennas at the transmitter site of MIMO transmission
m	antenna index at the receiver side
$\tau_{m,\ell}$	delay of the ℓ^{th} path
ρ	correlation coefficient
ρ_ℓ	correlation coefficient for the ℓ^{th} path
$\alpha_{m,\ell}$	complex channel gain for the ℓ^{th} path at the receiver antenna m
γ_m	SNR at the m^{th} antenna
\mathbf{I}	identity matrix
$\mathbb{E}[\cdot]$	statistical mean operator
$(\cdot)^H$	hermitian operator
$\text{Cov}[\cdot]$	covariance operator
$\text{Re}\{\cdot\}$	real portion of the complex quantity
$\text{Im}\{\cdot\}$	imaginary portion of the complex quantity

j	$\sqrt{-1}$
$e^{(\cdot)}$	exponential operator
$\log_2(\cdot)$	logarithm operator based 2
$\det(\cdot)$	determinant operator
\mathbf{H}	$M \times 1$ channel vector
E_s	symbol energy
E_b	bit energy
N_0	noise density
P_b	bit-error probability
$Q(\cdot)$	gaussian Q-function
$p(\cdot)$	probability distribution function
T_s	sampling interval
k	subcarrier index
$s[k]$	transmitted information symbol
N	DFT length
$p(t)$	impulse response of the pulse shaping filter
$p_2(t)$	auto correlation of $p(t)$
n	DFT index
P	sum of the DFT length and the cyclic prefix
\star	convolution operator
$v_m(t)$	additive noise at the receiver antenna m
$h_m[n]$	$1 \times N$ channel gain vector in time domain at the receiver antenna m
$H_m[k]$	$1 \times N$ channel gain vector in frequency domain at the receiver antenna m
$\rho[k]_{m,m'}$	correlation between the m^{th} and m'^{th} antennas for the subcarrier k
R_c	coding rate
K_c	constraint length of the encoder
S	source terminal in relay topology
R	repeater terminal in relay topology
D	destination terminal in relay topology
$S \rightarrow R$	from the source to the repeater
$R \rightarrow D$	from the repeater to the destination
$S \rightarrow D$	from the source to the destination
K	rician K-factor

ε	power of the transmitted signal
$r_{d1}^{(m)}$	received signal at the destination antenna m from the source
$n_{d1}^{(m)}$	noise added to the destination antenna m when the source transmits
r_r	received signal at the repeater from the source
n_r	noise added to the repeater
τ	delay added by the repeater
$r_{d2}^{(m)}$	received signal at the destination antenna m from the repeater
$n_{d2}^{(m)}$	noise added to the destination antenna m when the repeater transmits
G	amplification gain at the repeater
h_{sd}	complex channel gain between the source and the destination
h_{sr}	complex channel gain between the source and the repeater
h_{rd}	complex channel gain between the repeater and the destination
ρ_d	correlation coefficient for the direct path
ρ_r	correlation coefficient for the relayed path
d_{sd}	distance between the source and the destination
d_{sr}	distance between the source and the repeater
d_{rd}	distance between the repeater and the destination
η	propagation exponent
T_{fb}	feedback information period
χ	cross-polarization discrimination

Chapter 1

Introduction

This Chapter covers the background and the motivation of the work done in this dissertation. In Section 1.1 the need for antenna arrays as a spatial diversity method and its place in the evolution of wireless technologies are mentioned. Then in Section 1.2 spatial fading correlation which dramatically limits the performance of antenna array communications is presented as the primary problem. In Section 1.3 Orthogonal Frequency Division Multiplexing (OFDM) as a promising scheme for the forthcoming wireless technologies and its applications with antenna arrays are given. Finally, we give our motivation in Section 1.4 which is to combat the performance degradations for the correlated OFDM antenna arrays.

1.1 Antenna Arrays in the Evolution of Wireless Technologies

Over the last two decades, the cellular communication technology has experienced a significant growth in terms of both the technological development and the increase in number of mobile subscribers. The cellular wireless technologies were first upgraded from the first-generation (1G) analog networks to the second-generation (2G) digital ones. These 2G technologies became popular worldwide

including GSM (Global System for Mobile Communications) in Europe, IS-136 (also known as US-TDMA and Digital AMPS) in the U.S., and PDC (Personal Digital Communications) in Japan. The traffic volume in 2G networks was clearly dominated by voice traffic. The introduction of the third-generation (3G) networks with High Speed Downlink Packet Access (HSDPA) has boosted data usage in mobile networks and data traffic in mobile networks has exceeded voice traffic [1.1]. Meanwhile, the number of mobile subscribers has exceeded 1 billion globally in 2002, two billion in 2005, three billion in 2007 and four billion in 2008 [1.2]. The forthcoming fourth-generation (4G) mobile telephone technology aims to provide on-demand high quality video and audio services. 4G refers to IMT-Advanced (International Mobile Telecommunications Advanced) standards defined by ITU-R. According to ITU, an IMT-Advanced cellular system must reach data rates of up to approximately 100 Mbit/s for high mobility and up to approximately 1 Gbit/s for low mobility. The name LTE is usually branded as pre-4G and the forthcoming LTE-Advanced standard submitted by 3GPP is expected to fully satisfy IMT-Advanced 4G requirements.

In addition to the cellular systems, recently the popularity of the Internet combined with the portable laptop computers caused Wireless Local Area Networks (WLANs) to become an important and rapidly growing part of the wireless communications world. In 1997, the first WLAN technology was standardized in the IEEE 802.11 specifications with 2 Mbps user data rates. In 1999, IEEE 802.11b was approved, providing new data rate capabilities of 11 Mbps. Later, 802.11g and 802.11n standards were ratified with higher user data rates in 2003 and 2009, respectively. Today, the latest wireless Internet access technology is WiMAX (Worldwide Interoperability for Microwave Access) which is based on the IEEE 802.16 family. The standard 802.16-2004 is sometimes referred as "Fixed WiMAX" and it has no support of mobility. 802.16e introduced support of mobility and it is known as "Mobile WiMAX". Mobile WiMAX has the most commercial interest and it is the basis of future revisions of WiMAX. It aims to provide high speed wireless internet connections over long distances.

Both the forthcoming 4G and WiMAX technologies require high data rates to meet the end users' demands for various applications. How high should the

data rate be to satisfy the user's demand? In fact, the demand can be unlimited. For instance, one can easily demand to send his photo album of 1 Gigabyte size to his friend in a few seconds with his mobile device. 1 Gbps data rate service can be reasonable for this purpose and a user can reach his goal in 8 seconds. In order to achieve 1 Gbps data rate, consider a system that realizes a nominal spectrum efficiency of 4 bps/Hz over 250 MHz bandwidth, so that the data rate is 1 Gbps. 250 MHz band is not feasible in the spectrum range below 6 GHz, but it can be obtained over 40 GHz spectrum. However, the communication range of the system dramatically reduces due to the propagation characteristics at this frequency and the power constraints on the mobile devices. Moreover when cellular system is considered, the network requires a total bandwidth of many times the link bandwidth in order to support a cellular reuse plan. This example clearly states the unreachable bandwidth requirements for Gbps data rates.

While traditional single antenna communication systems fail to achieve higher data rates, multi-antenna systems constitute a technological breakthrough that will allow Gbps data speeds. By introducing an array of antenna elements to the both receiver and transmitter ends, the channel capacity of the system can grow linearly with the number of antennas under ideal conditions. This system with multiple antennas at the both ends is termed as MIMO (multiple-input multiple-output) system. The capacity of multi-antenna fading channels applying antenna arrays at both ends was first published by Winters in 1987 [1.3]. However, the theoretical background was later developed by Foschini and Gans [1.4][1.5], and Telatar [1.6]. In particular, with M_T antennas at the transmitter and M_R antennas at the receiver, $\min(M_T, M_R)$ independent data streams can be supported. Alternatively, diversity combining of the transmit and receive antenna signals can be used to reduce the impact of multipath fading on bit-error-rate. Multiple antennas can not achieve multiplexing and diversity simultaneously. Hence, there is a fundamental tradeoff between diversity and multiplexing gains and both are interest of system designers. [1.7].

The upper bound for the capacity of SIMO channel follows as [1.6]

$$C = E[\log_2 \det(\mathbf{I}_M + \frac{E_s}{N_0} \mathbf{H}\mathbf{H}^H)] \quad (\text{bps/Hz}) \quad (1.1)$$

where \mathbf{H} is the $M \times 1$ channel matrix, M is the number of antenna elements at the receiver site, \mathbf{I}_M is the identity matrix of size $M \times M$, E_s/N_0 is the total average symbol energy to noise ratio at the each receiver antenna element. $E[\cdot]$ is the statistical mean operator and $(\cdot)^H$ is the Hermitian operator. Now consider a Rayleigh fading NLOS link with an average signal-to-noise ratio (SNR) of 20 dB. According to Eq. (1.1), Fig. 1.1 plots the bandwidth requirement to support 1 Gbps link speed as a function of the number of the antenna elements at the receiver array. Clearly, employing an antenna array reduces the bandwidth requirement and makes Gbps data rates possible for future applications.

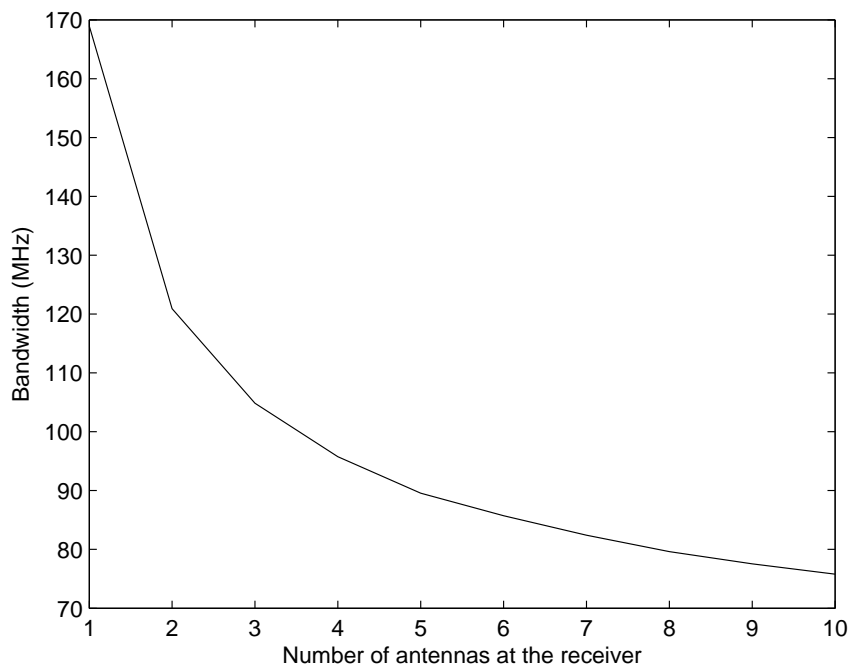


Figure 1.1: Bandwidth requirement needed to support 1 Gbps link speed as a function of the number of the antenna elements at the receiver array for a Rayleigh fading NLOS link.

In February 2007, NTT DoCoMo announced the completion of a 4G trial where they achieved a maximum packet transmission rate of approximately 5 Gbps in the downlink using 100 MHz frequency bandwidth to a mobile station moving at 10 km/h by employing 12×12 MIMO [1.8]. Because of its high potential to increase the capacity of the system, MIMO is included in both forthcoming cellular Long-Term Evolution (LTE) and WiMAX standards.

1.2 A Physical Limit on the Antenna Array Communications: Spatial Correlation

Knowing that the capacity of the antenna array systems increases with the number of antennas, one can try to place as many antennas as possible. Is there any limit to it? The main problem is that the correlation arises when the antenna elements are placed very close to each other and there is a lack of scatterers in the environment [1.9]. The correlation phenomenon is more likely to occur in the uplink since the base station is on high vantage point and very far from the mobile unit [1.10]. The problem is not so severe for mobile devices since they are usually located in high scattering environment.

Figure 1.2 shows an antenna array with two elements at a receiver having two independent replica of the transmitted signal and combining them with a combiner circuit. For the successful implementation of the antenna diversity systems, low correlation between the antenna elements is an essential condition. This is because if the correlation is too high, then deep fades will occur simultaneously at different antennas, accordingly combined signal would fade at that instant.

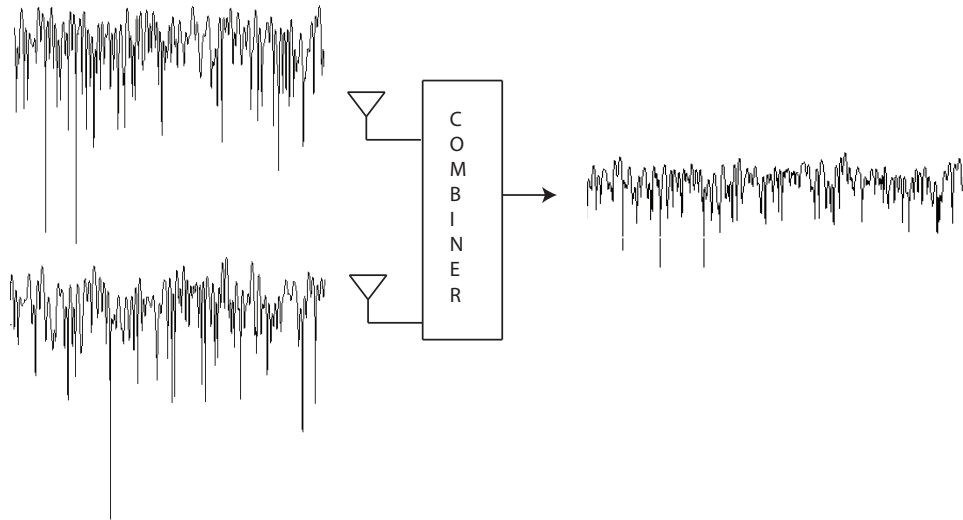


Figure 1.2: Illustration of combining two independent fading signals.

The traditional types of combining schemes are selection combining (SC), maximum ratio combining (MRC), and equal gain combining (EGC) [1.11].

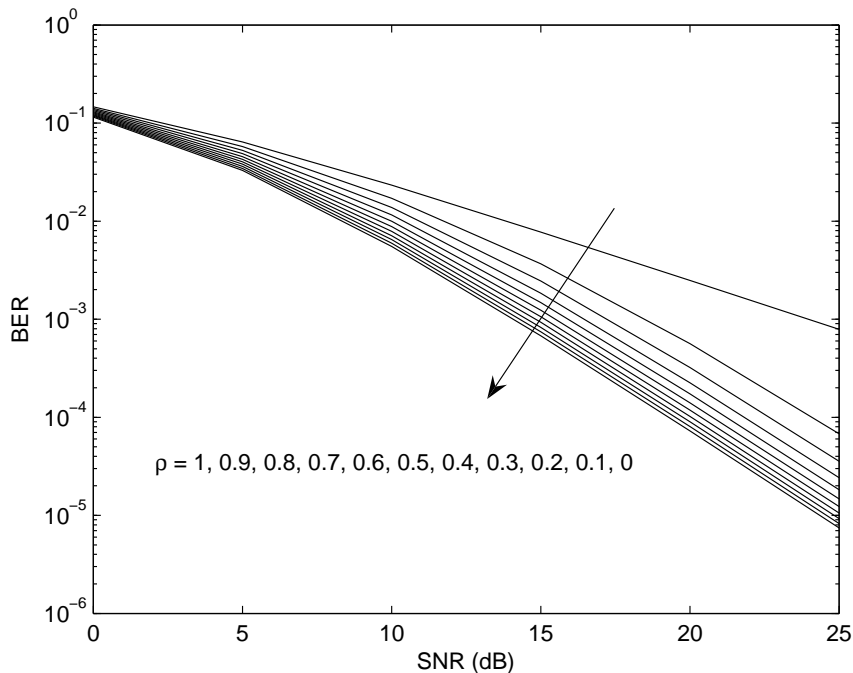


Figure 1.3: Impact of the spatial correlation on the BER performance of PSK modulation for 2 branch diversity under Rayleigh fading.

Among these, MRC is the optimum combiner for independent AWGN channels where received signals are weighted proportional to their signal level and then summed. In selection combining, the receiver selects the antenna which has the highest signal level. In equal gain combining, all the received signals are summed coherently.

1.2.1 Impact of the Correlation on the Performance

In a general form, regardless of the fading statistics (Rayleigh, Rice, Nakagami etc.), for MRC diversity schemes, the bit-error-rate (BER) for two antenna case is given by [1.12]

$$P_b = \int_0^\infty Q(\sqrt{2g\gamma_t}) p_{\gamma_t}(\gamma_t) d\gamma_t \quad (1.2)$$

where γ_t is the total SNR per symbol at the output of the MRC combiner (for 2 antenna elements $\gamma_t = \gamma_1 + \gamma_2$). $g=1$ for coherent BPSK and $Q(\cdot)$ is Gaussian

Q-function. If both antennas have correlated Rayleigh fading with equal average SNRs $\bar{\gamma}$, the probability distribution of the total SNR is [1.12]

$$p(\gamma_t) = \frac{1}{2\sqrt{\rho\bar{\gamma}}} \exp\left[-\frac{\gamma_t}{(1+\sqrt{\rho})\bar{\gamma}}\right] - \exp\left[-\frac{\gamma_t}{(1-\sqrt{\rho})\bar{\gamma}}\right], \quad \gamma_t \geq 0. \quad (1.3)$$

where ρ is the correlation coefficient which gives the statistical dependence of two fading signals.

Figure 1.3 shows the BER performance of the antenna array with 2 elements for different correlation coefficient values for phase shift keying (PSK) modulation. As seen in Figure 1.3, while the correlation decreases, the BER performance is increased. Therefore, the spatial correlation is one of the significant limitations on the system performance and likely to happen in low scattering environment and when there is insufficient antenna separation.

1.2.2 Spatial Channel Model

The fading correlation between the channel fading distributions seen by the receiver antennas depends on the physical channel parameters such as antenna separation (δ), angular spread (Δ) and the angle of arrival (ϕ). The effects of angular spread, angle of arrival and the antenna separation requirement on the spatial fading correlation have been shown by Lee in 1973 [1.9] both theoretically and experimentally. Lee [1.9] and later Adachi [1.13] found that the correlation between the signals received at two base station antennas increases as the angle spread decreases.

There are many spatial channel models proposed in literature for antenna array communications. A very detailed survey can be found in [1.14]. Choosing an efficient and accurate spatial channel model for the system under consideration is important to predict the performance of the antenna array communications. The widely used scattering model is the Lee model where the scatterers around the receiver are placed on a ring. Then the angle of arrival ϕ and the angular spread Δ are obtained according to the geometry of the physical link. Figure 1.4

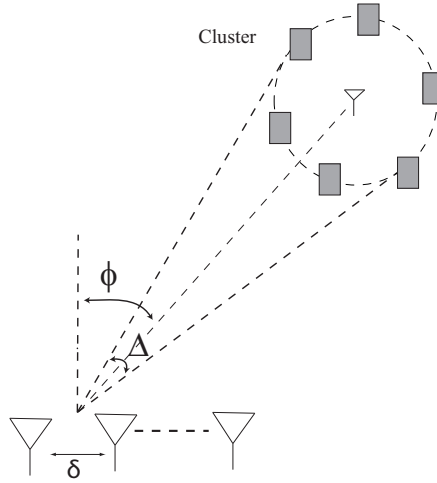


Figure 1.4: Clustered channel for uniform linear array with antenna spacing of δ .

illustrates these parameters.

The fading correlation between the path components at the adjacent antennas significantly depends on these physical channel parameters. i.e. for low correlation, antennas should be well separated, Δ should be wide and ϕ should be close to the broadside angle 0° . In addition to theoretical approaches, a set of correlated Rayleigh waveforms can be generated by [1.15] which follows the Lee model and the spatial correlation can be obtained numerically for different physical channels. Spatial fading correlation coefficient is a complex number and its real and imaginary parts can be either positive or negative depending on the cluster properties [1.16]. Figure 1.5 shows the correlation coefficient in magnitude for different antenna separation, angles of arrival and angular spreads. Figures 1.6 and 1.7 show the real and imaginary portions of the correlation, respectively. When the signal is coming from broadside angle, imaginary portion of the correlation vanishes, which is previously reported in [1.16].

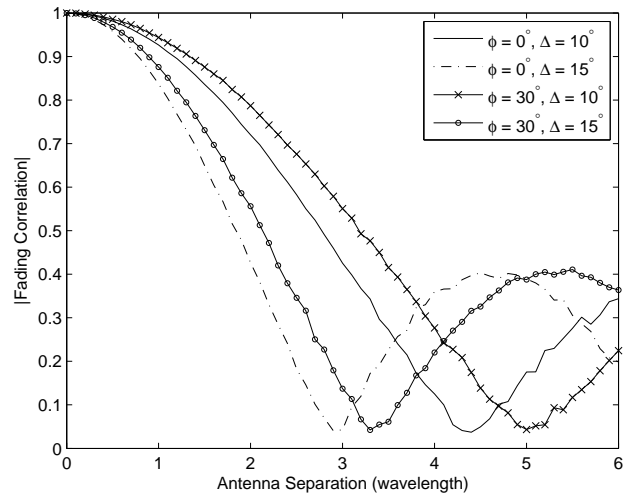


Figure 1.5: Spatial correlation in magnitude for different clusters.

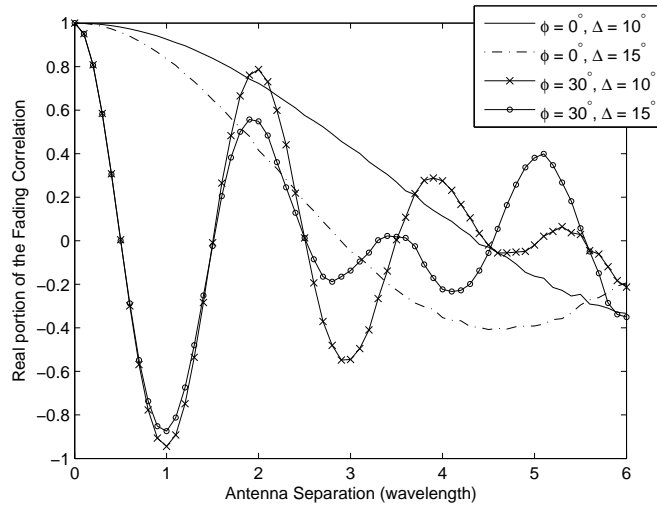


Figure 1.6: Real portion of the spatial correlation for different clusters.

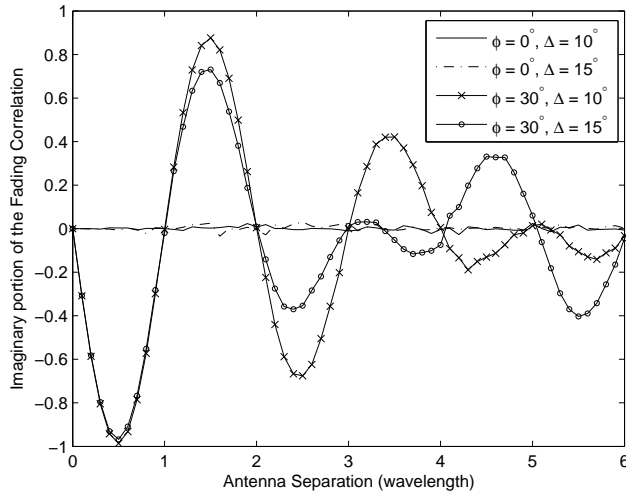


Figure 1.7: Imaginary portion of the spatial correlation for different clusters.

1.3 Orthogonal Frequency Division Multiplexing (OFDM)

1.3.1 Historic Background

In recent years OFDM has emerged as a promising air-interface technique. It is also used in wired communications where it is known as Discrete Multitone (DMT) transmission and is employed in Asymmetric Digital Subscriber Line (ADSL), High-bit-rate Digital Subscriber Line (HDSL) and Very-High-speed Digital Subscriber Line (VDSL). In wireless communications, it has been adopted by many standards such as Digital Audio Broadcasting (DAB), Digital Video Broadcasting for Terrestrial Television (DVB-T), Digital Video Broadcasting for Handheld Terminals (DVB-H), Broadband Radio Access Networks (BRANs) and Wireless Local Area Networks (WLANs).

The first proposal of the OFDM scheme dates back to 1960s [1.17][1.18]. In OFDM, frequency domain bandwidth is divided into non-overlapping subchannels, each of which referred as a subcarrier. The early OFDM systems used banks of sinusoidal subcarrier generators and modulators/demodulators which imposed

high implementation complexity. Since Weinstein and Ebert [1.19] proposed the use of Discrete Fourier Transform (DFT) to reduce the complexity, more practical OFDM research has been carried out. Table 1.1 gives the historic development of the OFDM in the wireless world.

Table 1.1: History of OFDM

Year	Development
1966	First proposal of OFDM by Chang. [1.17]
1970	U.S. patent on OFDM approved. [1.20]
1971	Weinstein and Ebert applied DFT to OFDM. [1.19]
1980	Hirosaki designed subcarrier based equalizer [1.21]. Keasler et al. described OFDM modem for telephone networks [1.22].
1985	OFDM is investigated for mobile communications [1.23].
1987	Alard and Lasalle employed OFDM for digital broadcasting [1.24].
1991	ADSL standard [1.25]
1994	HDSL standard [1.26]
1995	DAB standard [1.27]
1996	WLAN standard [1.28]
1997	DVB-T standard [1.29]
1998	VDSL standard [1.30] BRAN standard [1.31]
1999	IEEE 802.11a WLAN standard [1.32]
2003	IEEE 802.11g WLAN standard [1.33]
2004	DVB-H standard [1.34] IEEE 802.16 WMAN standard (WiMAX) [1.35]
2008	3GPP Release 8 - LTE standard [1.36]
2009	IEEE 802.11n standard [1.37]

1.3.2 Transmission Methodology

OFDM is a multicarrier transmission technique, which divides the available spectrum into many carriers, each one being modulated by a low rate data stream. OFDM uses the spectrum more efficiently by spacing the channels closer to each other. This is done by making all the carriers orthogonal to one another which prevents interference between closely spaced carriers. The orthogonal channels means that the spectrum of each carrier has a null at the center frequency of each of the other carriers in the system as shown in Fig. 1.8. All the narrow band

carriers experience a flat fading which provides resistance to frequency selective wideband channels. This is generally counted as the greatest advantage of the OFDM.

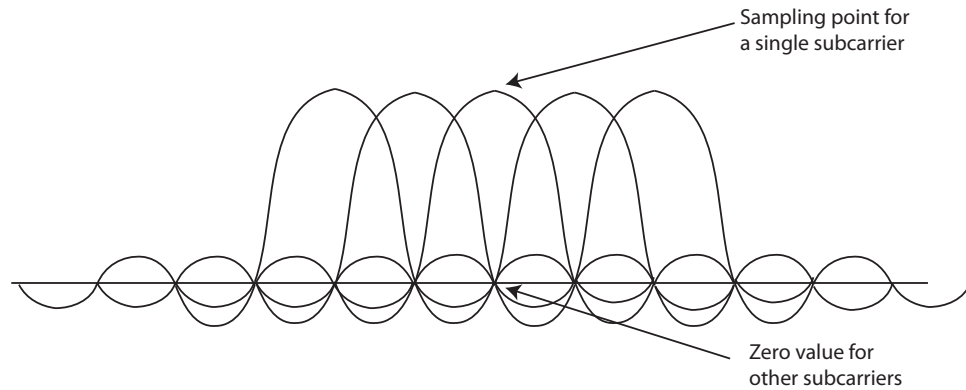


Figure 1.8: Maintaining orthogonal subcarriers.

Each carrier of the OFDM symbol is assigned some data to transmit. Based on the modulation scheme (typically BPSK, QPSK or QAM), the required amplitude and phase of the carrier are then calculated. The complex time domain signal is generated using an IDFT. The IDFT is an efficient way for this transformation and provides a simple way of ensuring the orthogonality of the carrier signals. After generating OFDM signal, a guard interval (GI) (also called cyclic prefix) is added to suppress inter-symbol interference (ISI) caused by multipath distortion. It is usually the replica of the last part of the OFDM symbol. The guard interval guarantees a time for the multipath signals from the previous symbol to be suppressed before the information from the current symbol arrives. If the delay spread of the channel is longer than the guard interval, then ISI is caused. Then OFDM symbol with the GI is first converted to analog domain by digital-to-analog converters (DACs), the analog signal is then used to modulate cosine and sine waves at the carrier frequency, respectively. These signals are then summed to give the transmission signal. Figure 1.9 shows the OFDM transmitter architecture.

The receiver picks up the signal and transforms it to its baseband form using cosine and sine waves at the carrier frequency. The baseband signals are then sampled using analog-to-digital converters (ADCs), and a forward DFT is used

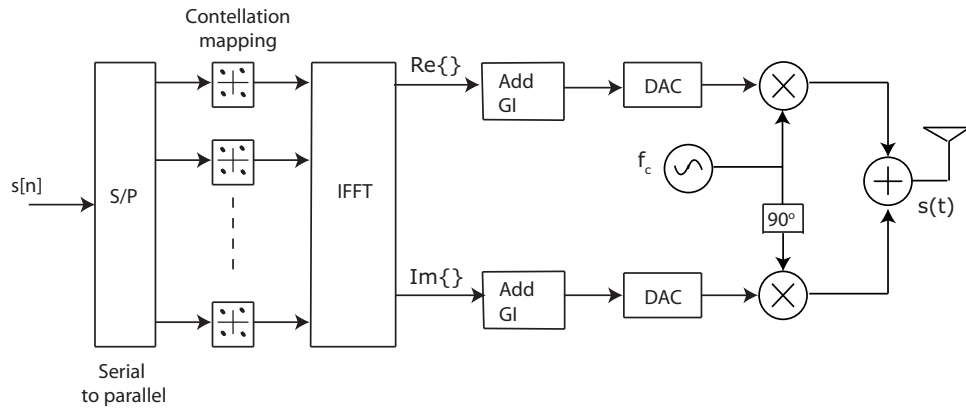


Figure 1.9: OFDM Transmitter Architecture.

to convert it back to the frequency domain. This gives parallel streams, each of which is converted to a binary stream using an appropriate symbol demodulator. These streams are then converted to a serial stream, which is an estimate of the original binary stream at the transmitter. Figure 1.10 shows the OFDM receiver architecture.

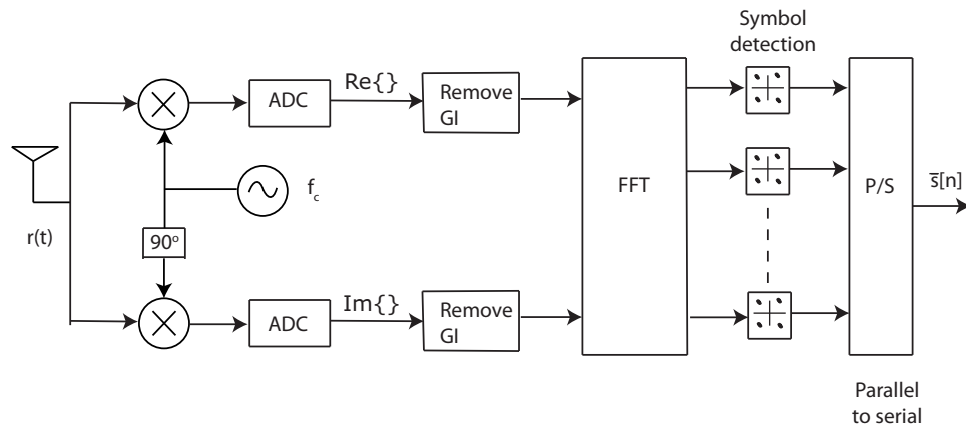


Figure 1.10: OFDM Receiver Architecture.

In summary, the main advantages of OFDM are; it can easily adapt severe channel conditions without complex equalization, it is robust to errors caused by multipath propagation and it is efficient to implement using DFTs. For these reasons, OFDM has been adopted in many wireless standards such as DAB/DVB-T, 802.11 WLAN and 802.16 WiMAX. The OFDM is also well suited for MIMO communications [1.38]. Some disadvantages can be counted as; it has high peak to average power ratio (PAPR)[1.39], loss of resource caused by using a cyclic

prefix, and its sensitivity to frequency offset and phase noise [1.40][1.41].

1.3.3 Adaptive OFDM (AOFDM)

Adaptive modulation scheme is an efficient way to increase the transmission rate by changing the channel modulation scheme according to the channel state information. Most OFDM systems use a fixed modulation scheme over all carriers. However, each carrier in an OFDM system has a potential to use a different modulation scheme depending on its channel condition. Different QAM modulation formats can be selected such as BPSK, QPSK, 8PSK, 16-QAM, 32-QAM, 64-QAM, 128-QAM and 256-QAM. This means that 1, 2, 3, ... 8 bit per subcarrier [1.42].

AOFDM transmission can be applied to duplex communication systems since it requires additional signaling including steps;

- (i) transmitter should reliably estimate the channel quality
- (ii) transmitter should select the appropriate modulation scheme
- (iii) receiver should know which modulation scheme is applied to which subcarrier.

For the step (i); the channel quality should be predicted reliably in order to select the transmission parameters. In previous literatures, there are works related to AOFDM for reliable channel condition prediction [1.43][1.44][1.45]. Then in the step (ii), with the obtained channel knowledge, an appropriate modulated scheme has to be chosen. Each modulation scheme provides a tradeoff between spectral efficiency and a target BER. Choosing the highest modulation scheme that will give an acceptable BER would maximize the spectral efficiency. At the final step (iii), for successful demodulation, the receiver has to be informed as which modulation scheme parameters are used at the transmitter site. This can be done by transmitting this information directly to receiver with the cost of transmission capacity or the receiver may attempt to estimate which modulation scheme is used by itself. Figure 1.11 illustrates the AOFDM transceiver.

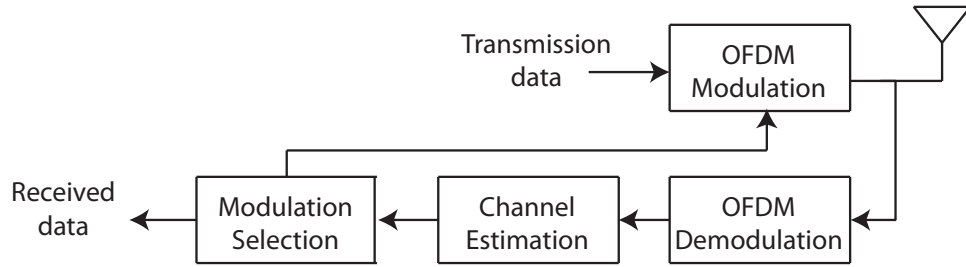


Figure 1.11: Adaptive OFDM transceiver.

1.3.4 OFDM in Repeater Wireless Networks

Next generation wireless systems are expected to operate at higher frequency ranges which will cause high propagation losses between the terminals. In order to increase the uplink coverage while maintaining a high bit rate level, repeaters are employed in the networks. The concept of repeater can be found in cellular systems, WLANs, and digital broadcasting systems which are based on OFDM [1.45]-[1.52].

An RF repeater receives and amplifies the signal almost at the same time. The delay between the reception and the transmission is as low as 5-6 μsec [1.51]. In some applications, the replica of the transmitted signal may reach the destination from the direct path. Therefore, the received signal consists of the signal from the main transmitting station and the signal from the repeater, and each regarded as delayed multipath signal [1.52][1.53]. Hence, the repeater channel can be considered as an artificial multipath channel if the signal reaches the destination from both the source (direct path) and the repeater (repeated path). Figure 1.12 shows a deployment RF repeater scenario for coverage extension. Depending on the mobile user's location, base station can have the replica of the transmitted signal from both mobile user and the repeater terminal. When OFDM is considered, guard interval should be long enough to mitigate the intersymbol interference due to the delay of the relayed path [1.53].

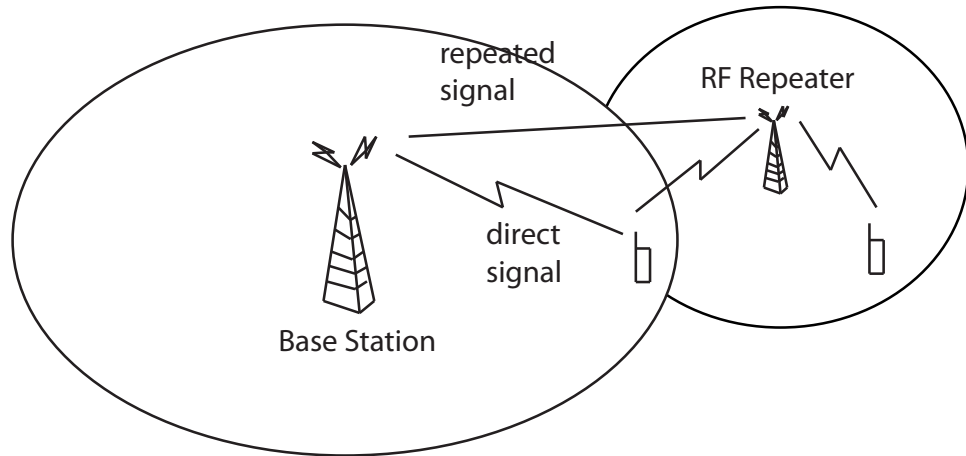


Figure 1.12: RF Repeater deployment for coverage extension.

1.3.5 OFDM in Spatially Correlated Antenna Arrays

When an antenna array is employed at the receiver site, the spatial fading correlation will be the significant concern for the successful diversity reception for OFDM communications as well. Fading correlation keeps its significance for any of the systems described above; either fixed/adaptive modulation is used or the network includes an RF repeater.

In the studies related to OFDM, the fading correlation between antenna elements is usually considered constant for all subcarriers. However, this is the case when the channel is flat during an OFDM symbol. In this thesis, it is shown that in multipath channels spatial correlation varies over subcarriers depending on the transmit pulse shaping filter, channel delay profile and the spatial correlation between each individual delayed paths. Since the combining scheme is usually employed in the frequency domain for OFDM, the spatial correlation for each subcarrier will affect the system performance. Each delayed path component of a multipath channel will be correlated depending on their angle of arrivals and angular spreads. Figure 1.13 illustrates the multipath channel with different correlations on each tap.

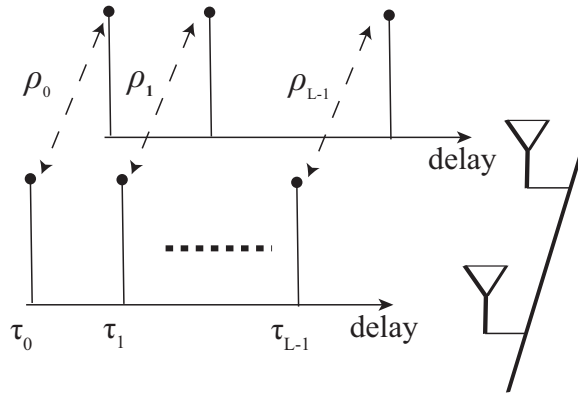


Figure 1.13: Channel taps corresponding to the same time delays will be correlated according to their clusters.

1.4 Motivation of this Research

Future wireless systems are expected to provide high data rates in the order of more than 100 Mbps. In order to satisfy this demand, antenna diversity has been proposed which provides link improvement without increasing the transmission power and bandwidth [1.3]. An essential condition for the antenna array systems to work properly is that the fading distributions are independent at each antenna branch of the receiver [1.4]. The correlation depends on the displacement between the antennas and the spatial properties of the wireless channel. In short, for uncorrelated received signals, one or more of the following conditions should be met

- A separation of a few wavelengths between the antennas.
- Wide angular spread.
- Arriving angle is close to front angle.

In some practical applications, antennas can not be placed sufficiently apart due to the physical limitations, or angular spread is very small due to the low scattering environment [1.54][1.55]. Therefore, the spatial fading correlation can occur and it is the main parameter to combat in antenna array communications.

1.4.1 Overview of Chapter 2

In Chapter 2, a novel technique called Time Shifted Sampling (TSS) to improve the performance of transmission with the correlated fading signals for Orthogonal Frequency Division Multiplexing (OFDM) is proposed. Figure 1.14 shows the place of proposed Time Shifted Sampling scheme in literature. It is known that antenna array improves the system performance. However, if the antennas are correlated, some of the diversity gain is lost. When TSS is applied to the receiver array, the correlation for some subcarriers is reduced to a sufficient level for diversity reception and overall system performance improves.

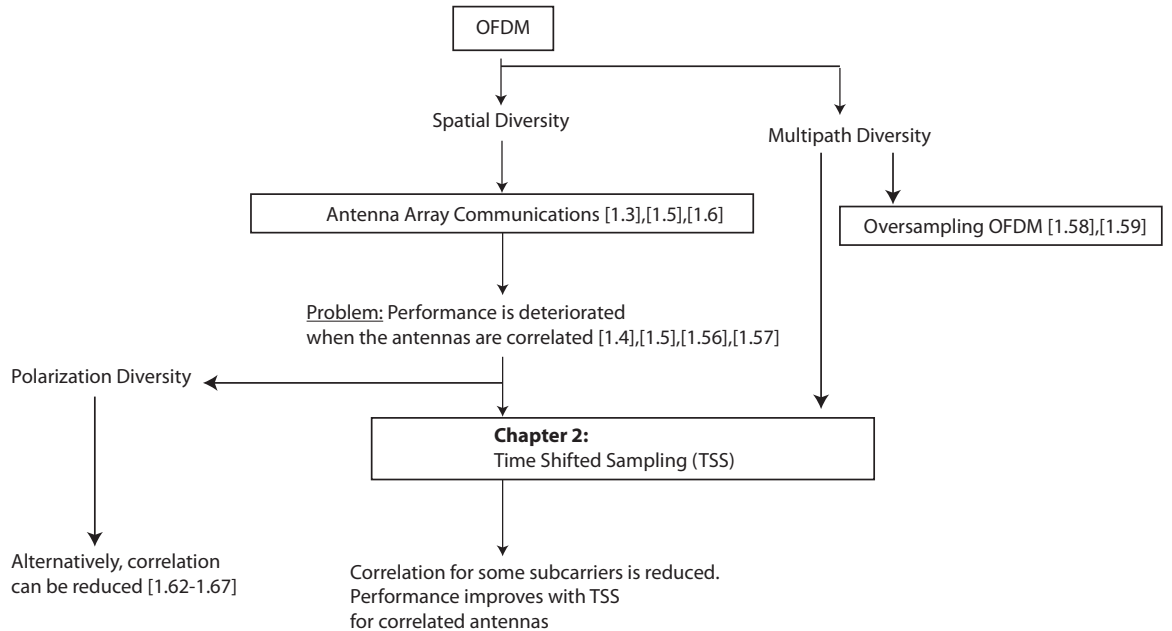


Figure 1.14: Chapter 2 proposes novel Time Shifted Sampling (TSS) technique to combat the degradations due to the spatial fading correlation.

TSS is a sampling technique which exploits the multipath diversity by oversampling the channel with the aid of multiple antennas. Figure 1.15 shows the block diagram of the TSS receiver. Oversampling is achieved by shifting the sampling points at each antenna while sampling at the Nyquist rate. Since the antennas are still at Nyquist rate, no additional multipath diversity gain is obtained for each antenna. However, shifting the sampling points at each antenna

provides different replicas of the multipath channel for each antenna. These different replicas are uncorrelated and the exploited multipath diversity by TSS comes from this uncorrelated channels. If the antennas are already uncorrelated, no additional gain is obtained with TSS. Therefore, TSS provides diversity gain only for correlated antennas and its basis relies on the multipath diversity.

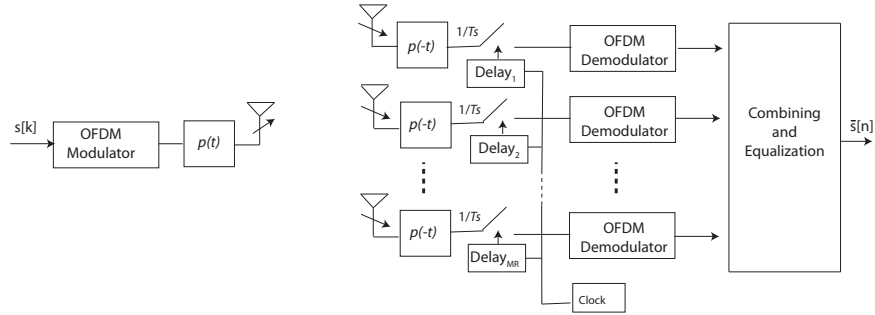


Figure 1.15: Block diagram for OFDM Antenna Array Receiver with TSS.

TSS can be related to number of previous works including Oversampling OFDM (OOFDM) and non-uniform sampling for OFDM which are based on the multipath diversity and also correlation reduction techniques such as polarization diversity.

1.4.1.1 Oversampling

Multipath diversity for OFDM is usually a subject to single antenna systems. Oversampling (sometimes called Fractional Sampling) techniques are proposed to achieve multipath diversity with a single antenna [1.58][1.59]. In a conventional single antenna OFDM receiver, the sampling is carried out at the baud rate of $1/T_s$ (T_s is the sampling interval). On the other hand, in OOFDM systems, a received signal is sampled at the multiples of baud rate (G/T_s , where G is some integer) and the resultant sampled signals are combined at the receiver. Hence, the system benefits from multipath diversity and leads to SIMO.

However, oversampling requires analog-to-digital converters with higher sampling rates which cause high power consumption [1.60]. It also suffers from intercarrier interference if the sampling rate is higher than the Nyquist rate. Also,

when the number of multipaths is low, the achievable diversity order by oversampling is limited. Also, it should be noted that the discrete-time noise samples are mutually correlated. The noise samples should be whitened which increases the complexity of the receiver. Hence, in some real wireless scenarios, employing antenna arrays is more effective solution to exploit diversity and overcome the fading errors. Figure 1.16 shows the block diagram of the OOFDM receiver.

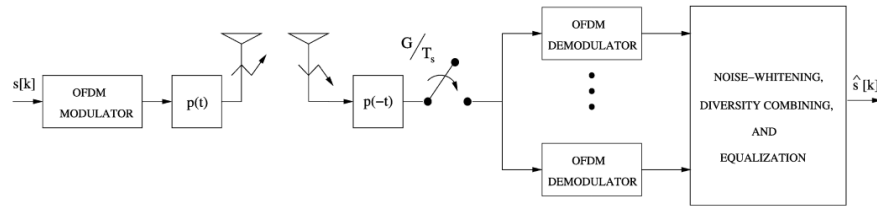


Figure 1.16: Block diagram for Oversampling OFDM.

Both TSS and OOFDM take the benefit of multipath diversity. In TSS receiver multipath diversity helps reducing the correlation between the antennas and the performance gain comes from this reduced correlation. On the other hand, in OOFDM systems multipath diversity provides an additional gain however it increases the complexity of the receiver.

1.4.1.2 Non-Uniform Sampling

In usual OOFDM systems, sampling intervals are fixed for each demodulation branches and when the sampling speed is large, more path diversity can be obtained. This leads to the increase of a circuit size for demodulation in a mobile terminal. Instead of that, sampling points can be optimized according to the frequency response of the channel [1.61]. This scheme is called Non-Uniform Sampling. With Non-Uniform Sampling, the number of demodulation branches can be halved as compared to conventional OOFDM to achieve the same bit-error-rate. Moreover, the complexity and accordingly the power consumption of the receiver are also reduced.

The results of the previous literature for Non-Uniform Sampling can be applied to TSS receivers in which the shifts for the sampling points are fixed. In single antenna OOFDM systems, Non-Uniform Sampling optimizes the sampling points and it can reduce the number of demodulation branches, complexity and power consumption. Since the TSS technique is already proposed for antenna arrays, applying Non-Uniform Sampling would not change the number of antenna elements and the power consumption. In this thesis, TSS is proposed for fixed time shifts for each antenna and discussions are kept limited to reducing the spatial fading correlation.

1.4.1.3 Polarization Diversity

Polarization diversity is an alternative means of increasing the diversity order [1.62] with less correlation between the branches. Moreover, employing dual-polarized antennas consumes less space than the antenna arrays [1.63]. The characteristics of PD have been described by the envelope correlation ρ and the cross-polarization discrimination χ . The ρ is the correlation between the polarizations and the χ is the power ratio of the polarizations. The best performance is expected to occur when there is no correlation between the polarizations $\rho=0$ and the received powers by the polarizations are equal $\chi=0$ dB (2 branch equal SNR uncorrelated spatial diversity receiver). Figure 1.17 shows the reception with dual polarized antenna.

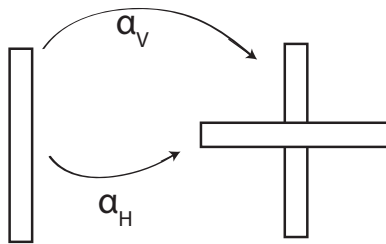


Figure 1.17: Reception with polarization diversity. $\chi=|\alpha_V|^2/|\alpha_H|^2$.

However, such a system is ideal and is unlikely to occur in practical wireless systems. Moreover, χ in urban environments, given that the transmitter is vertically polarized, is 6 dB in average [1.64] while in rural areas χ is more than 10

dB [1.65] due to the lack of obstacles that couple polarizations. Experimental data have shown that typical correlation value between horizontal and vertical polarized receive antennas is generally less than 0.2 [1.64-1.67].

Placing dual polarized antennas is an alternative way to reduce the spatial correlation. However, received SNRs are unlikely to be equal due to the factor χ . Also, if one places an array of dual polarized antennas [1.63], the same polarized components in the array will be correlated.

1.4.2 Overview of Chapter 3

Chapter 3 proposes Adaptive OFDM scheme which chooses the modulation scheme for each subcarrier based on joint effect of the CNR and correlation coefficient to achieve the target BER. In Section 1.3.3 the transmission rate improvement with adaptive OFDM (AOFDM) schemes have been discussed. In conventional AOFDM systems, the modulation scheme for each subcarrier is decided according to its channel quality (usually carrier-to-noise ratio (CNR)) to achieve the target BER. Employing antenna array at the receiver end will help the system to achieve the target BER with less SNR due to the diversity gain. Therefore, modulation selection chart should be updated for the the combined CNR. However, when the antennas are correlated, this diversity gain vanishes and AOFDM system fails to achieve target BER. Since the TSS technique is effective to combat the degradations due to the spatial correlation, one can implement it into AOFDM antenna array systems and increases the system performance. As mentioned earlier, when the TSS is employed, spatial correlation is reduced for some subcarriers. For correlated arrays (also when TSS is employed), in order to optimize the transmission rate, AOFDM systems should select the modulation scheme for each subcarrier based on not only combined CNR but also the correlation coefficient for that subcarrier. Figure 1.18 summarizes the development of the proposed scheme.

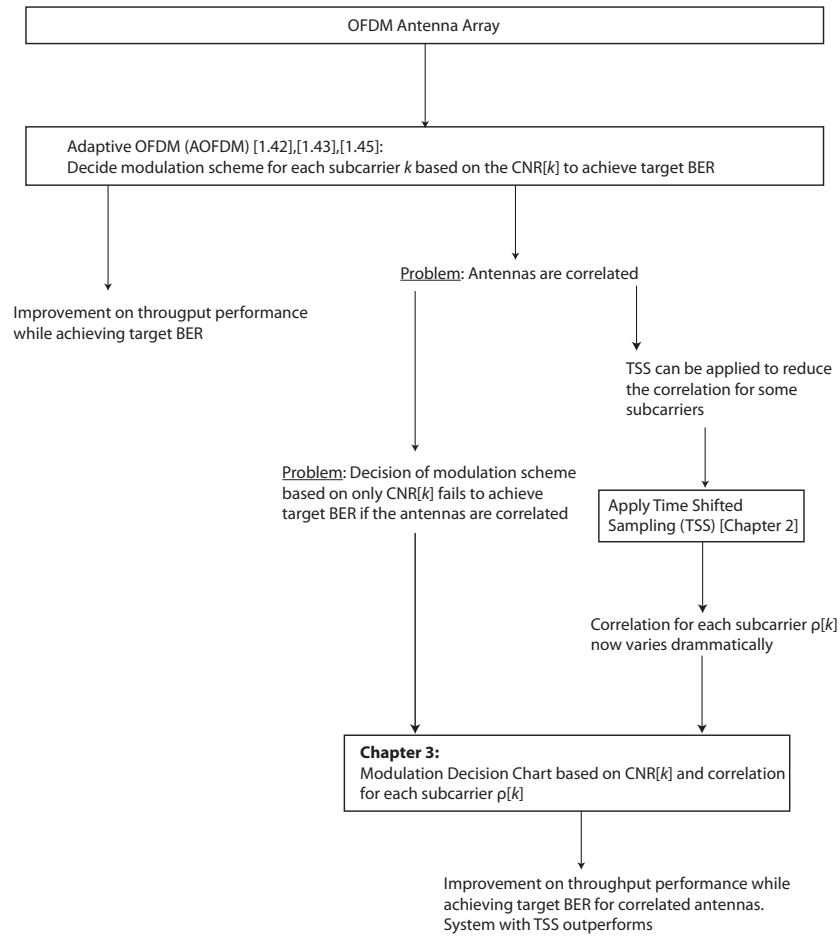


Figure 1.18: Chapter 3 proposes an adaptive OFDM scheme incorporating the spatial fading correlation when the TSS is applied to receiver array.

1.4.3 Overview of Chapter 4

In Chapter 4, due to the recent interest in wireless repeater/relaying networks, spatial correlation at the base station is analyzed when the network includes an RF repeater. For the wireless channels without repeaters, spatial fading correlation is well studied in literature. In this work, a multipath channel is generated with the aid of the repeated signal, the spatial fading correlation per each subcarrier at the destination antenna array is investigated for different placements of the repeater and the mobile user. The Time Shifted Sampling is also found to be effective when the network includes an RF Repeater. Figure 1.19 summarizes the work done in Chapter 4.

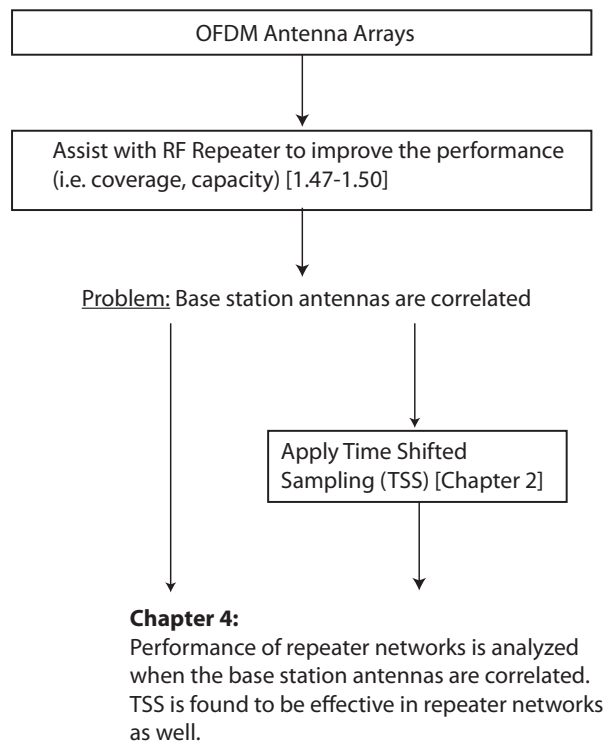


Figure 1.19: Chapter 4 analyzes the performance of correlated OFDM base station when the network includes an RF repeater. TSS is also found effective in Repeater networks.

References

- [1.1] T.S. Rappaport, “Wireless Communications: Principles and Practice,” Prentice Hall PTR, Upper Saddle River, NJ, 2002.
- [1.2] “ITU Corporate Annual Report 2008,”
<http://www.itu.int/dms-pub/itu-s/opb/conf/s-conf-arep-2008-E06-pdf-e.pdf>.
- [1.3] J. H. Winters, “On the capacity of radio communication system with diversity in a Rayleigh fading environment,” *IEEE Journal on Selected Areas in Communications*, vol. 5, No. 5, pp. 871-878, Nov. 1981.
- [1.4] G. J. Foschini, M. J. Gans, “On limits of wireless communication in a fading environment when using multiple antennas,” *Wireless Personal Commun.*, vol. 6, No. 3, pp. 311-335, Mar. 1998.
- [1.5] G. J. Foschini, “Layered space-time architecture for wireless communication in a fading environment when using multi-element antennas,” *Bell Labs Tech. J.*, vol. 1, No. 2, pp. 41-59, Mar. 1996.
- [1.6] E. Telatar, “Capacity of multi-antenna Gaussian channels,” *European Transactions on Telecommunications*, 10(6):585-596, 1999.
- [1.7] L. Zheng, D. Tse, “Diversity and Multiplexing: A Fundamental Tradeoff in Multiple Antenna ,” *IEEE Trans. Inform. Theory*, vol. 49, No.5, pp. 1073-1096, May 2003.
- [1.8] 4G field experiment, NTT DoCoMo. <http://www.nttdocomo.com/pr/2007/001319.html>.
- [1.9] W. C. Y. Lee, “Effects on correlation between two mobile radio basestation antennas,” *IEEE Trans. Commun.*, vol. 21, pp. 1214-1224, Nov. 1973.

- [1.10] M. Jankiraman, "Space-time codes and MIMO systems," Artech House , Norwood, MA USA, 2004.
- [1.11] S.R. Saunders, "Antennas and propagation for wireless communication systems," Wiley, 1999.
- [1.12] M.K.Simon, M.S.Alouini, "Digital communication over fading channels," John Wiley & Sons , NY, USA, 2005.
- [1.13] F. Adachi et al., "Crosscorrelation between the envelopes of 900 MHz signals received at a mobile radio base station site," *IEE Proc. on Commun., Signal and Radar Processing*, vol. 133, No. 6, pp. 506-512, Oct. 1986
- [1.14] R. B. Ertel, P. Cardieri, K. W. Sowerby, T. S. Rappaport, J. H. Reed, "Overview of spatial channel models for antenna array communication systems," *IEEE Personal Commun.*, vol. 5, No.1, pp. 10- 21, Feb. 1998.
- [1.15] T. L. Fulghum, K. J. Molnar, A. Duel-Hallen, "Jakes Fading model for antenna arrays Incorporating Azimuth Spread," *IEEE Trans. Vehicular Technology*, vol. 51, No. 5, pp. 968-977, Sep. 2002.
- [1.16] J. Salz, J. H. Winters, "Effect of fading correlation on adaptive arrays in digital mobile radio," *IEEE Trans. Vehicular Technology*, vol. 43, No. 4, pp. 1049-1057, Nov. 1994.
- [1.17] R. W. Chang, "Synthesis of band-limited orthogonal signals for multichannel data transmission," *Bell System Tech. J.*, vol. 45, pp. 1775-1796, Dec. 1966.
- [1.18] B. R. Saltzberg, "Performance of an efficient parallel data transmission system," *IEEE Trans. Commun.*, vol.15, No. 6, pp. 805-811, Dec. 1967.
- [1.19] S. B. Weinstein, P. M. Ebert, "Data transmission by frequency-division multiplexing using the Discrete Fourier Transform," *IEEE Trans. Commun.*, vol.19, No. 5, pp. 628-634, Oct. 1971.
- [1.20] R. W. Chang, "Orthogonal frequency division multiplexing," *U.S. Patent 3 488 445*, filed Nov. 14, 1966, issued Jan. 6, 1970.

- [1.21] B. Hirosaki, "An analysis of automatic equalizers for orthogonally multiplexed QAM systems," *IEEE Trans. Commun.*, vol.28, No. 1, pp. 73-83, Jan. 1980.
- [1.22] W. E. Keasler, D. L. Bitzer, P. T. Tucker, "High-speed modem suitable for operating with a switched network," *U.S. Patent 4 206 320*, filed Aug. 21, 1978, issued Jun. 3, 1980.
- [1.23] L. J. Cimini, Jr., "Analysis and simulation of a digital mobile channel using orthogonal frequency division multiplexing," *IEEE Trans. Commun.*, vol.33, No. 7, pp. 665-675, Jul. 1985.
- [1.24] M. Alard, R. Lassalle, "Principles of modulation and channel coding for digital broadcasting for mobile receivers," *EBU Tech. Rev.*, pp. 168-190, Aug. 1987.
- [1.25] A Multicarrier Primer, ANSI T1E1.4/91-157, Nov. 1991, J. M. Cioffi.
- [1.26] ANSI Committee T1-Telecommunications, "A technical report on high-bit-rate digital subscriber lines (HDSL)," *Tech. Rep.* 28, Feb. 1994.
- [1.27] European Telecommunication Standard Institute, Digital Audio Broadcasting (DAB); *DAB to Mobile, Portable and Fixed Receivers*, ETSI ETS 300 401 ed.1, Feb. 1995.
- [1.28] European Telecommunication Standard Institute, *Radio Equipment and Systems (RES); High Performance Radio Local Area Network (HIPERLAN) Type 1; Functional Specification*, ETSI ETS 300 652 ed.1, Oct. 1996.
- [1.29] European Telecommunication Standard Institute, *Digital Video Broadcasting (DVB); Framing Structure, Channel Coding and Modulation for Digital Terrestrial Television (DVB-T)*, ETSI ETS 300 744 ed.1, Mar. 1997.
- [1.30] European Telecommunication Standard Institute, *Transmission and Multiplexing (TM); Access Transmission Systems on Metallic Access Cables; Very High Speed Digital Subscriber Line (VDSL); Part 1: Functional requirements*, ETSI TS 101 270-1 V1.1.2, Jun. 1998.

- [1.31] European Telecommunication Standard Institute, *Broadband Radio Access Networks (BRAN); Inventory of Broadband Radio Technologies and Techniques*, ETSI TR 101 173 V1.1.1, May 1998.
- [1.32] Institute of Electrical and Electronics Engineers, *IEEE Standard 802.11a: Wireless LAN Medium Access Control (MAC) and Physical Layer (PHY) Specifications: High-Speed Physical Layer in the 5 GHz Band*, 1999.
- [1.33] Institute of Electrical and Electronics Engineers, *IEEE Standard 802.11g: Wireless LAN Medium Access Control (MAC) and Physical Layer (PHY) Specifications*, 2003.
- [1.34] European Telecommunication Standard Institute, *Digital Video Broadcasting (DVB); Transmission System for Handheld Terminals (DVB-H)*, ETSI EN 302 304 V1.1.1, Nov. 2004.
- [1.35] Institute of Electrical and Electronics Engineers, *IEEE Standard 802.16: Air Interface for Fixed Broadband Wireless Access Systems*, 2004.
- [1.36] 3GPP Technical Report, TR 36.913, "Requirements for Further Advancements for E-UTRA (LTE-Advanced)", 3GPP TSG RAN, version 8.0.0, May 2008.
- [1.37] Institute of Electrical and Electronics Engineers, *IEEE Standard 802.11n: Enhancements for Higher Throughput in Wireless LANs* 2009.
- [1.38] H. Bolcskei, D. Gesbert, A. J. Paulraj, "On the capacity of OFDM-based spatial multiplexing systems," *IEEE Trans. on Communications*, vol. 50, No.2, pp. 225-234, Feb. 2002.
- [1.39] T. Ginige, N. Rajatheva, K.M. Ahmed, "Signal design and spectral efficiency in multi-carrier multiple access systems with PAPR as a parameter," in Proc. *IEEE Vehicular Technology Conf.*, pp. 1923-1927, vol.3, 2000.
- [1.40] P.H. Moose, "A technique for orthogonal frequency division multiplexing frequency offset correction," *IEEE Trans. on Communications*, vol. 42, No. 10, pp. 2908-2914, 1994.

- [1.41] P. Robertson, S. Kaiser, "Analysis of the effects of phase-noise in orthogonal frequency division multiplex (OFDM) systems," in Proc. *IEEE Int. Conf. Comm.*, pp. 1652-1657, vol.3, 1995.
- [1.42] A. Czylik, "Adaptive OFDM for wideband radio channels," in Proc. *IEEE Int. Global Telecom. Conference*, vol.1, pp. 713718, 1996.
- [1.43] C.J. Ahn, I. Sasase, "The effects of modulation combination, target BER, doppler frequency, and adaptive interval on the performance of adaptive OFDM in broadband mobile channel," *IEEE Trans. Consumer Electronics*, vol. 48, No.1, pp. 167-174, Feb. 2002.
- [1.44] H. Harada, T. Yamamura, Y. Kamito, M. Fujise, "Adaptive modulated OFDM radio transmission scheme using a new channel estimation method for future broadband mobile communication systems," *IEICE Trans. Commun.* VOL.E-85B, No.12, pp.2785-2796, Dec. 2002.
- [1.45] T. Keller, L. Hanzo, "Adaptive modulation techniques for duplex OFDM transmission," *IEEE Trans. Vehicular. Tech.*, vol.49, No.5 pp.1893-1906, Sep. 2000.
- [1.46] R. Raulefs, A. Damman, "Repeating or Relaying in Wireless Systems," in Proc. *IEEE Wireless Communications and Networking Conference*, pp. 506-510, 2008.
- [1.47] M. Qingyu, A. Osseiran, "Performance Comparison Between DF relay and RF Repeaters in the Cellular System," in Proc. *IEEE Vehicular Tech. Conference*, pp. 2021 - 2025, May. 2008.
- [1.48] K. Hiltunen, "Using RF Repeaters to Improve WCDMA Speech Coverage and Capacity Inside Buildings," in Proc. *IEEE Vehicular Tech. Conference*, pp. 1-5, Sep. 2006.
- [1.49] M. N. Patwary, P. B. Rapajic, I. Oppermann, , "Capacity and Coverage Increase with Repeaters in UMTS Urban Cellular Mobile Communication Environment," *IEEE Transactions on Communications*, Vol.53, No. 10, pp.1620-1624, October 2005.

- [1.50] W. Choi, B.Y. Cho, T.W. Ban, "Automatic on-off switch repeater for DS/CDMA reverse link capacity improvement," *IEEE Commun. Lett.*, vol. 4, No. 5, pp. 138-141, Apr. 2001.
- [1.51] "UTRA Repeater: Planning Guidelines and System Analysis," *3GPP TR 25.956*
- [1.52] S.W. Choi, H.J. Hong, "A Study on the Interference in Single Frequency Network and On-Channel Repeater," *Progress In Electromagnetics Research Symposium*, Cambridge, USA 2008
- [1.53] "Repeater issues for MBWA," *IEEE 802.20 Working Group on Mobile Broadband Wireless Access*
- [1.54] Y. Zhang, Z. Wang, D. Li, "A simulation study on the MIMO channel capacity for small angle spread correlated fading signals," in. Proc. *IEEE Int. Conf. on Communications, Circuits and Systems, ICCAS* vol. 1, pp. 158-161, 2000.
- [1.55] W.C. Jeong, J.M. Chung, "Analysis of macroscopic diversity combining of MIMO signals in mobile communications," *Int. Journal on Electron. Commun. (AEU)*, pp. 454-462, 2005.
- [1.56] L. Fang, B. Guoan, A.C. Kot, "New Method of Performance Analysis for Diversity Reception with Correlated Rayleigh-fading Signals," *IEEE Trans. on Vehicular Technology*, vol. 49, No. 5, pp. 1807-1812, Sept. 2000.
- [1.57] D. Shiu, G. J. Foschini, M. J. Gans, J. M. Kahn, "Fading Correlation and Its Effect on the Capacity of Multielement Antenna Systems," *IEEE Trans. on Communications*, vol. 48, pp. 502-5133, March 2000.
- [1.58] C. Tepedelenlioglu, R. Challagualla, "Low Complexity Multipath Diversity Through Fractional Sampling in OFDM," *IEEE Trans. on Signal Processing*, vol. 52, No. 11, pp. 3104-3116, Nov. 2004.
- [1.59] J. Wu, "Oversampled Orthogonal Frequency Division Multiplexing in Doubly Selective Fading," *IEEE Wireless and Communications Networks Conference WCNC*, pp. 177-181, 2008.

- [1.60] H. Nishimura, M. Inamori, Y. Sanada, , “Sampling Rate Selection for Fractional Sampling in OFDM,” in Proc. *Int. Symp. on Personal Indoor and Mobile Radio Communications*, pp. 1-5, Sept. 2007.
- [1.61] H. Nishimura, M. Inamori, Y. Sanada, M. Ghavami, “Non-uniform Sampling Point Selection in OFDM Receiver with Fractional Sampling,” in Proc. *IEEE PacRim Communications, Computers and Signal Processing*, pp. 837-842, 2009.
- [1.62] J. Jootar, J-F. Diouris, J.R. Zeidler, “Performance of polarization diversity in correlated nakagami-m fading channels,” *IEEE Trans. on Veh. Technology*, vol. 55, No. 1, pp. 128-136, 2006.
- [1.63] N.M. Das, M. Shinozawa, N. Miyadai, T. Taniguchi, Y. Karasawa, “Experiments on a MIMO system having dual polarization diversity branches,” *IEICE Trans. Commun.*, vol.E89-B, No. 9, pp. 2522-2529, 2006.
- [1.64] W.C.Y. Lee, Y.S. Yeh, “Polarization diversity system for mobile radio,” *IEEE Trans. on Commun.*, vol. 26, pp. 912-923, 1972.
- [1.65] R.G. Vaughan, “Polarization diversity in mobile communications,” *IEEE Trans. on Veh. Technology*, vol. 39, No. 3, pp. 177-186, 1990.
- [1.66] A.M.D. Turkmani, A. A. Arowojolu, P.A. Jefford, C.J. Kellet “An experimental evaluation of the performance of two-branch space and polarization diversity schemes at 1800 MHz,” *IEEE Trans. on Veh. Technology*, vol. 44, No. 3, pp. 319-326, 1995.
- [1.67] F. Lotse, J-E. Berg, U. Forssen, P. Idahl, “Base station polarization diversity reception in macrocellular systems at 1800 MHz,” in Proc. *IEEE Vehicular Technology Conf.*, pp. 1643-1646, 1996.

Chapter 2

Multipath Diversity Through Time Shifted Sampling for Spatially Correlated OFDM Antenna Array Systems

In Chapter 1, the importance of the spatial fading correlation for the diversity receivers has been mentioned. In this chapter, a novel method of diversity reception with correlated fading distributions for OFDM antenna array systems is proposed. Conventional OFDM diversity systems may suffer from the spatial correlation depending on the physical channel characteristics (such as insufficient antenna separation, small angular spread and when the angle of arrival is close to the array axis). In the proposed sampling scheme, the spatial correlation can be reduced in frequency domain partially for some subcarriers to a sufficient level for successful diversity combining.

In conventional array systems, individual receivers sample the received signals at the same time with the same sampling rate. In the proposed scheme, the received signals are again sampled at the same rate, however the sampling points are shifted in each receiver. This scheme is called Time Shifted Sampling (TSS).

This chapter is organized as follows. Introduction is given in Section 2.1. The method of generating correlated Rayleigh fading signals for antenna arrays is presented in Section 2.2. Then, the proposed TSS scheme is introduced in Section 2.3. Numerical results through computer simulation are presented in Section 2.4. Finally, the chapter is concluded in Section 2.5.

2.1 Introduction

Orthogonal Frequency Division Multiplexing (OFDM) has been adopted by many wireless standards such as digital video broadcasting, IEEE 802.11a. It is getting more popular because of its ability to convert a frequency selective multipath channel into a set of parallel frequency-flat fading channels. In case of a spatially multiplexed system, OFDM is found to be advantageous in terms of ergodic capacity in rich multipath environments [2.1]. For single antenna OFDM systems, it is also possible to extract multipath diversity through OOFDM[2.2]. In a usual single antenna OFDM receiver, the sampling is carried out at the baud rate of $1/T_s$ (T_s is the sampling interval). On the other hand, in OOFDM, a received signal is sampled at the multiples of baud rate (G/T_s , where G is some integer) and the resultant sampled signals are combined at the receiver. Hence, the system leads to SIMO and benefits from multipath diversity.

However, OOFDM requires analog-to-digital converters with higher sampling rates which cause high power consumption [2.3]. It also suffers from intercarrier interference if the sampling rate is higher than the Nyquist rate. Also, when the number of multipaths is low, the achievable diversity order by OOFDM is limited. Hence, in some real wireless scenarios, employing antenna arrays is more effective solution to overcome fading errors.

The capacity of antenna array systems is mainly limited by the spatial fading correlation between antenna elements [2.4]. This problem generally occurs on the uplink (between the antenna elements of a base station) since a mobile unit is usually surrounded by many scatterers which provide almost independent

reception, while the base station is not. It has been shown that when the fades are independent at each element, antenna arrays provide an impressive gain to the capacity of transmission [2.5]. The results of [2.6] states that when maximum ratio combining (MRC) is employed, when the spatial correlation is less than 0.5, signals can be considered as uncorrelated. However, in real wireless channels, especially in poor scattering environments, it is difficult to keep spatial correlation level less than 0.5. This might require larger antenna separation which is not desired when the space is limited.

In this chapter, a new method of diversity reception with correlated fading distributions for OFDM antenna array systems is proposed. In conventional array systems, individual receivers start sampling the received signals at the same time with the same sampling rate. In the proposed scheme, the received signals are again sampled at the same rate, however, sampling points are shifted in each receiver. We call this scheme Time Shifted Sampling (TSS). Numerical results through computer simulation show that, when the TSS is applied, spatial correlation between antenna elements can be reduced by exploiting multipath diversity.

2.2 Spatially Correlated Rayleigh Channel Model

The received signal is modeled as multiplication of transmitted signal and a Rayleigh fading waveform. In case of antenna arrays, a set of fading waveforms is needed for each receiver to generate individual received signals.

It is known that fading correlation between the antenna elements strongly depends on the spatial aspects of the channel. A number of previous works propose different approaches to model the spatial channel. Using a scatterer model is usually a simple way to characterize the channel. A very detailed overview of the scattering models can be found in [2.7].

In this work, in order to obtain a set of correlated Rayleigh fading waveforms, the scatterer model based on Jakes' ring model [2.8] is chosen.

2.2.1 Single Path Ring Model for Antenna Arrays

In [2.9], a method of generating correlated fading waveforms for antenna arrays, by extending the Jakes ring model, is introduced. Figure 2.1 illustrates the model. This model is basically a ray-tracing model which is based on the physical characteristics of the channel, such as antenna spacing (δ), antenna arrangement (linear, circular etc.), angle of arrival of cluster (ϕ) and angular spread of cluster (Δ). The amount of spread is determined by the radius of the ring (R) and the distance (d) between the receiver and the transmitter. The sum of each scattered signal is Rayleigh distributed. In case of multiple antennas, another correlated Rayleigh waveform can be generated by using the same scatterers. It is assumed that all rays arrive receiver array at the same time with equal power.

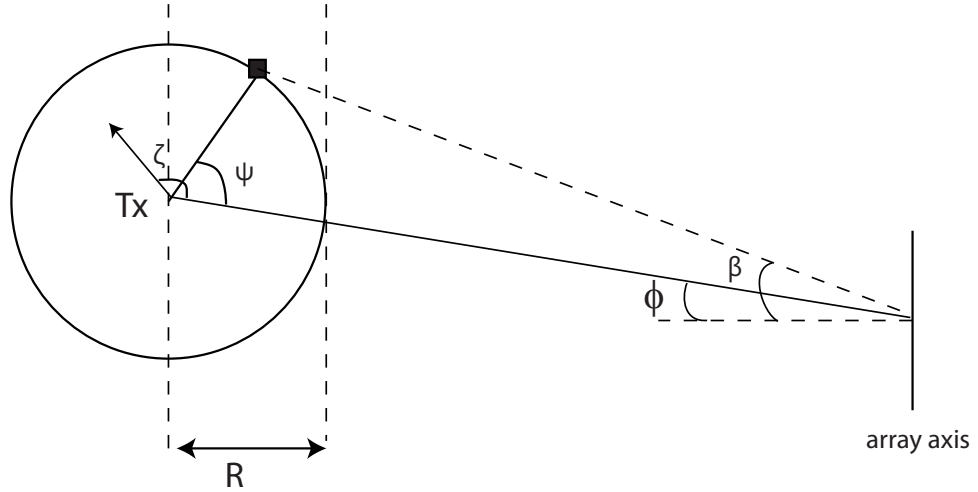


Figure 2.1: Jakes' ring model for antenna arrays.

The scatterers are placed uniformly on the ring. Angle ψ for each scatterer is given as;

$$\psi_s = \frac{2\pi(s - 0.5)}{S} \quad (2.1)$$

where S is the number of scatterers on the ring and s is the scatterer index. The Doppler frequency shift for each scattered signal is $w_s = 2\pi f \frac{v}{c} \cos(\psi_s - \zeta)$, where v is the speed of mobile, c is the speed of light, f is the frequency, and ζ is the angle of motion of the mobile as shown in Figure 2.1. In Eq. (2.1), the quantity 0.5 is

added in order to pretend placing a scatterer on the line between the transmitter and the receiver array (NLOS environment). Each scattered signal is summed to form a Rayleigh fading waveform. If one fading waveform experienced at one spot x along the axis of array is $T(t, x)$;

$$T(t, x) = \frac{1}{\sqrt{S}} \sum_{s=1}^S \exp(j(w_s t + \theta_s)) \quad (2.2)$$

where θ_s is the random phase $(0, 2\pi]$, then the waveform at the adjacent antenna which is separated by δ (wavelength) becomes

$$T(t, x + \delta) = \frac{1}{\sqrt{S}} \sum_{s=1}^S \exp(j(w_s t + \theta_s)) \exp(-j\delta 2\pi \sin(\beta_s)), \quad (2.3)$$

β_s is the arriving angle of the s^{th} scattered signal.

The correlation between $T(t, x)$ and $T(t, x + \delta)$ can be calculated as the time average product of the first waveform and the complex conjugate of the second waveform. In previous Chapter, Figure 1.5 showed the change in correlation coefficient with respect to antenna separation for different angle of arrivals and angular spreads. As seen in Figure 1.5, the fades between antennas become correlated as the antenna elements get closer to each other, the arriving angles of the scatterers get closer to the end-fire direction of the array or the angular spread of cluster decreases.

2.2.2 Multipath Ring Model for Antenna Arrays

Measurement results show that incoming signals arrive receiver generally within more than one cluster due to the far scattering environments [2.10]. In this chapter, a channel with two multipath components is used for simulating the performance of the proposed scheme in Section 2.4. The second Rayleigh component is generated by using another ring that circles the existing ring. Figure 2.2 illustrates this model. Following assumptions are made in this model.

- All rays from both rings arrive the receiver array with equal power.
- The rays from the second ring arrive receiver array with an equal delay.

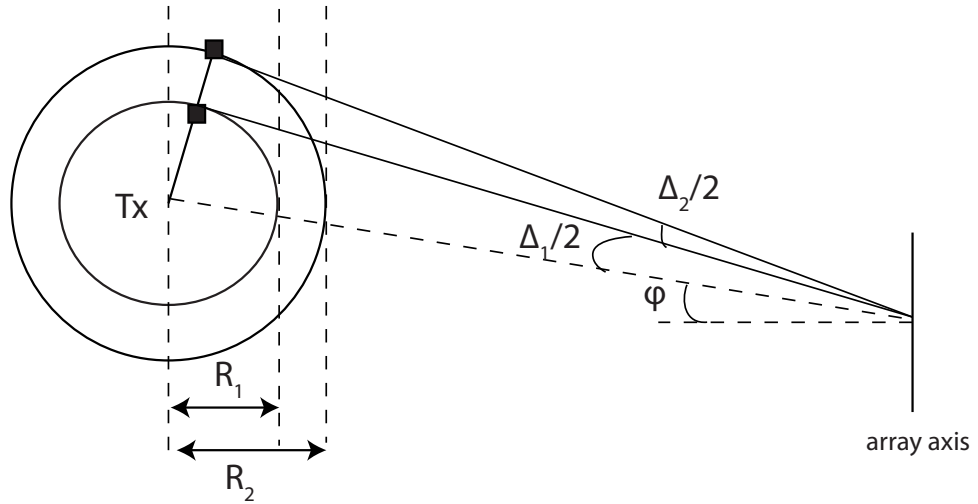


Figure 2.2: Far scatterers are modeled as another ring that circles the existing ring.

Fading waveforms are generated from both rings by the same procedure described in Section 2.2.1. Fading waveform generated by the inner ring is said to be the first multi-path component, and accordingly the outer ring is the second multi-path component.

Sample simulation is run for two antennas in linear arrangement with antenna separation equals to the transmission wavelength. The number of scatterers are chosen as 64 on both rings and the angle of arrival for both rings are set to 60

degrees. The angular spreads of the clusters from the inner and outer rings are taken as 5 and 10 degrees, respectively. (These parameters are referred as Channel Model-1 in Section 2.4). The results have shown that the fading correlation between the antenna elements of the same multipath components is high. The spatial fading correlation coefficient between the first multipath components is 0.98 and between the second multipath components is 0.96, since angular spread is a bit larger for the second path. On the other hand, the fading correlation between the first and the second multipath components is still low. In Figure 2.3, delay profiles of the multipath channel for the both antennas and the fading correlation relationships are illustrated.

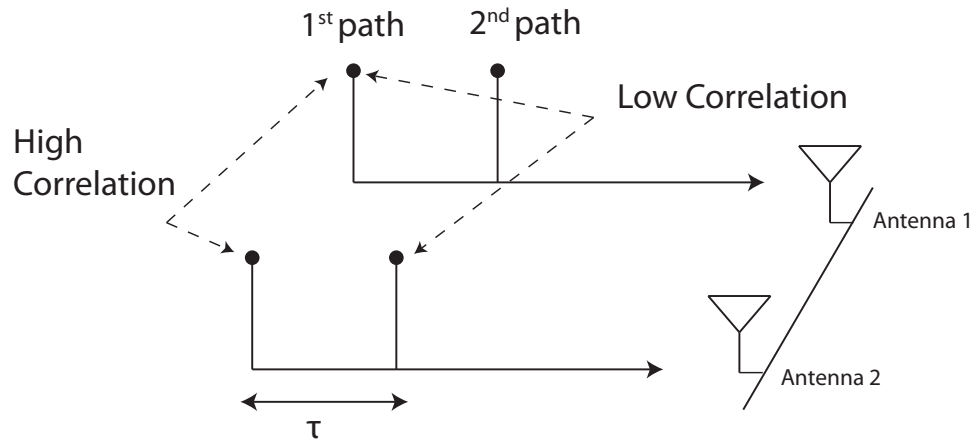


Figure 2.3: Spatial fading correlation relationships between received signals by each antenna.

The fading envelopes generated by the simulation are given in Figure 2.4. It can be seen that the fading correlation is high between the same multipath components at different antennas and it is low between the first and second multipath components.

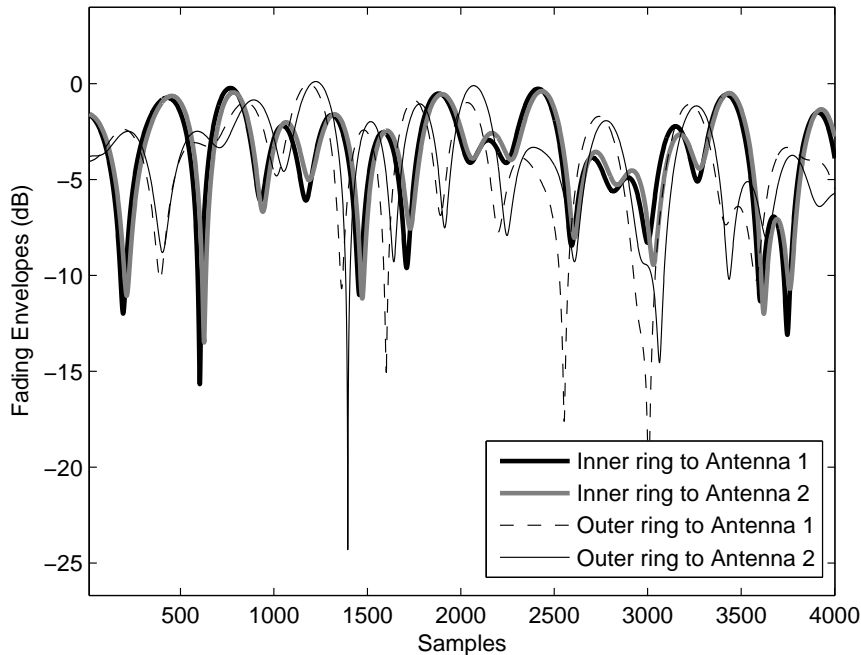


Figure 2.4: Fading envelopes generated for the first and second antennas from both rings for maximum Doppler shift of 100 Hz.

2.3 Time Shifted Sampling

TSS is a signal processing technique that takes the benefit of multipath diversity, which already exists in the channel, in order to improve the system performance with spatially correlated received signals. Figure 2.5 gives the complete block diagram of the receiver that employs TSS.

Suppose OFDM symbol is transmitted and the information symbol on the k^{th} subcarrier is $s[k]$ ($k = 0, 1, \dots, N - 1$). Then OFDM symbol is the IDFT of the information symbols,

$$u[n] = \frac{1}{N} \sum_{k=0}^{N-1} s[k] e^{j2\pi nk/N} \quad (2.4)$$

where n ($n = 0, 1, \dots, N - 1$) is the time index and N is the IDFT length. The baseband signal at the output of the filter is given by $x(t) = \sum_{n=0}^{P-1} u[n] p(t - nT_s)$ where $p(t)$ is the impulse response of the pulse shaping filter, T_s is the symbol duration and P is the sum of the IDFT length and the length of cyclic prefix. Then

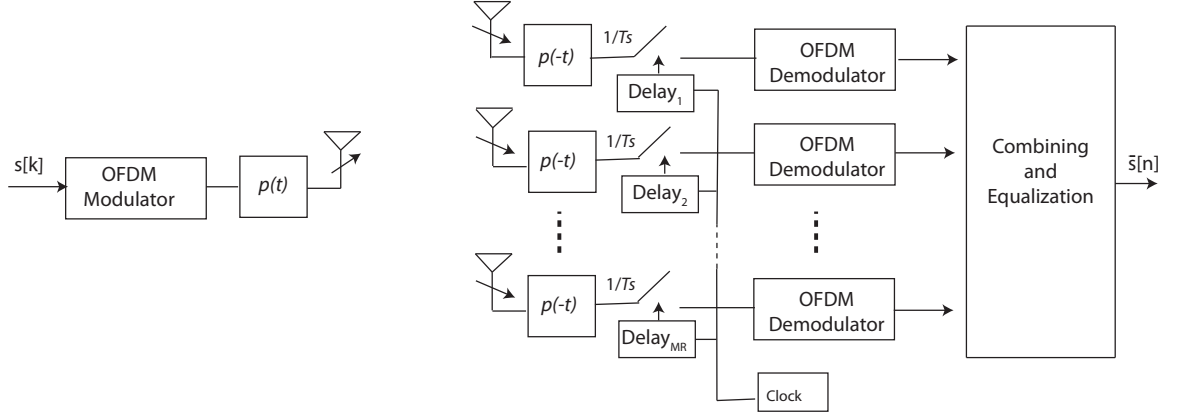


Figure 2.5: Block diagram for OFDM Antenna Array Receiver with TSS.

this signal is transmitted over different multi-path channels to different antennas m with impulse responses $c_m(t)$ and is matched to the transmitted pulse shape. The received signals by each antenna m then become

$$y_m(t) = \sum_{n=0}^{P-1} u[n]h_m(t - nT_s) + v_m(t) \quad (2.5)$$

where $h_m(t)$ is the impulse response of the channel seen by antenna m and is given by $h_m(t) = p(t) \star c_m(t) \star p(-t)$, \star denotes convolution. $v_m(t)$ is the additive white Gaussian noise at the receivers. $h_m(t)$ can be expressed in a baseband form as

$$h_m(t) = \sum_{\ell=0}^{L-1} \alpha_{m,\ell} p_2(t - \tau_{m,\ell}). \quad (2.6)$$

$p_2(t) = \int p(t')p(t+t')dt'$ is the auto correlation of $p(t)$, L is the number of multipath components, $\alpha_{m,\ell}$ is the complex gains of the ℓ^{th} component at the m^{th} antenna and $\tau_{m,\ell}$ is the path delay. Amplitudes of the channels are assumed time-invariant during one OFDM symbol.

When sampling is carried out at the baud rate of $1/T_s$ with a delay of $(m -$

1) T_s/M at antenna m over total of M antennas, the received signals in discrete-time are expressed as

$$y_m[n] = \sum_{l=0}^{P-1} u[l]h_m[n-l] + v_m[n] \quad (2.7)$$

where $y_m[n] = y_m(nT_s + (m-1)T_s/M)$, $h_m[n] = h_m(nT_s + (m-1)T_s/M)$, $v_m[n] = v_m(nT_s + (m-1)T_s/M)$. At each antenna, noise samples are still independent and white. However the fading correlation between any antenna elements m and m' , $h_m[n]$ and $h_{m'}[n]$, and accordingly between $y_m[n]$ and $y_{m'}[n]$, is reduced. Channel gains in discrete-time at each antenna are given by

$$h_m[n] = \sum_{\ell=0}^{L-1} \alpha_{m,\ell} p_2(nT_s + (m-1)T_s/M - \tau_{m,\ell}). \quad (2.8)$$

By taking the DFT of Eq. (2.8), the channel gains for each subcarrier in frequency domain are

$$H_m[k] = \sum_{n=0}^{N-1} e^{-j2\pi nk/N} \sum_{\ell=0}^{L-1} \alpha_{m,\ell} p_2(nT_s + (m-1)T_s/M - \tau_{m,\ell}) \quad (2.9)$$

where N is the DFT size.

Figure 2.6 illustrates the obtaining the frequency responses of the channels for each element of an antenna array with TSS. Assume, there are two elements in the array ($M=2$), the number of multipath components is two ($L=2$) and the delays of the second path are $T_s/2$ for both antennas. Pulse shaping filter $p_2(t)$ is a function with a length of $2T_s$. In TSS, the sampling points at the second receiver are shifted by a delay of $T_s/2$. Then, the sampled discrete-time channel gains are transformed into the frequency domain using the DFT. The shifted discrete sequence is no longer defined for the frequency range $0 \leq k \leq N-1$. Therefore, using the cyclic property of DFT, the index of shifted sequence is started from -1 to keep the shifted sequence in the range $0 \leq k \leq N-1$. As mentioned before, the fading correlation is low between the different multipath components. Hence, the correlation between the channel gains in the frequency domain is lowered for the array with TSS.

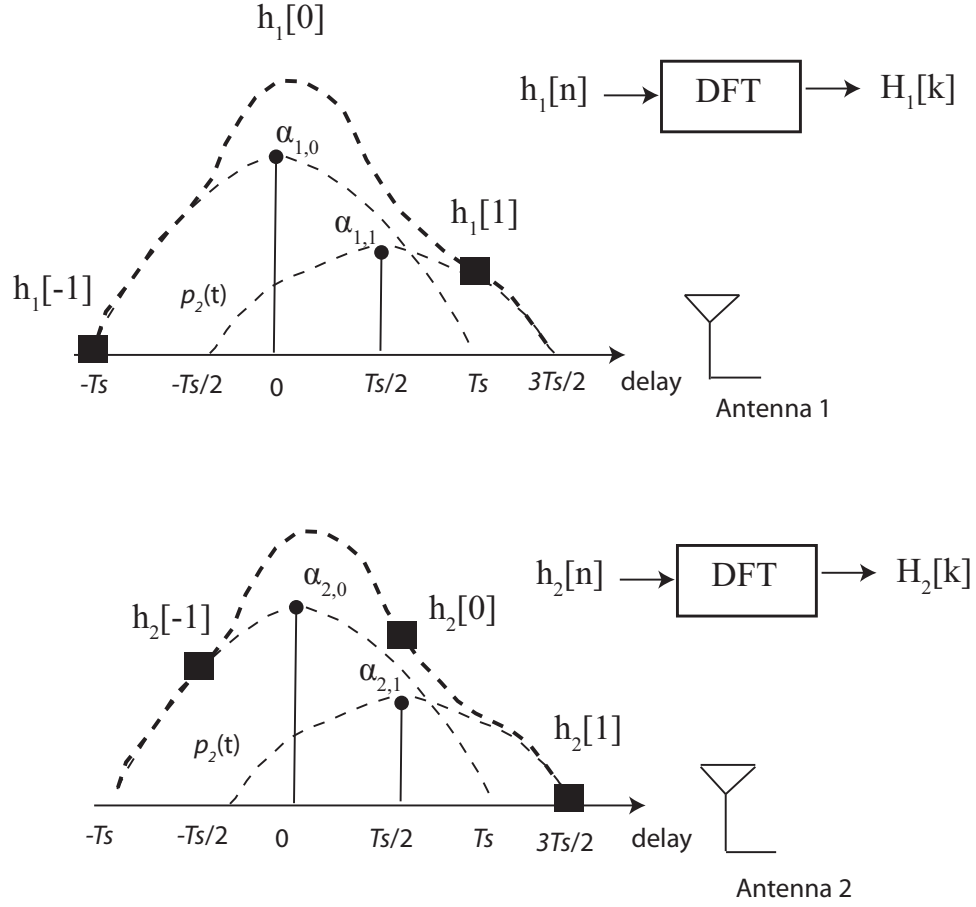


Figure 2.6: Illustration of TSS for two elements antenna array in the delay domain.

The basic input-output relationship in OFDM-antenna array systems is

$$\mathbf{z}[k] = \mathbf{H}[k]\mathbf{s}[k] + \mathbf{w}[k] \quad (2.10)$$

where $\mathbf{z}[k]$, $\mathbf{H}[k]$ and $\mathbf{w}[k]$ are the $M \times 1$ column vectors of the received symbols, the channel gains and the Gaussian noises at each subcarrier, respectively. Then the estimate of $s[k]$ through MRC combining is

$$\check{s}[k] = \frac{\check{\mathbf{H}}^H[k]\mathbf{z}[k]}{\check{\mathbf{H}}^H[k]\check{\mathbf{H}}[k]} \quad (2.11)$$

where $\check{\mathbf{H}}[k]$ is the estimated $M \times 1$ channel column vector. Since MRC is employed in frequency domain, the amount of spatial correlation should be calculated in

frequency domain. Spatial correlation between any antenna elements m, m' can be calculated as

$$\rho[k]_{m,m'} = \frac{\text{Cov}[H_m[k]H_{m'}[k]^*]}{\sqrt{\text{E}[|H_m[k]|^2]\text{E}[|H_{m'}[k]|^2]}} \quad (2.12)$$

where $\text{Cov}[\cdot]$ is the covariance operator. The covariance at the numerator of Eq.(2.12) can be written as

$$\begin{aligned} \text{Cov}[H_m[k]H_{m'}[k]^*] &= \text{E}\left[\sum_{n_1=0}^{N-1} \sum_{n_2=0}^{N-1} e^{-j2\pi(n_1-n_2)k/N} \right. \\ &\quad \times \sum_{\ell_1=0}^{L-1} \sum_{\ell_2=0}^{L-1} (\alpha_{m,\ell_1})p_2(n_1T_s + (m-1)T_s/M - \tau_{m,\ell_1}) \\ &\quad \left. \times (\alpha_{m',\ell_2})^*p_2(n_2T_s + (m'-1)T_s/M - \tau_{m',\ell_2})\right]. \end{aligned} \quad (2.13)$$

As seen in Eqs. (2.12) and (2.13), when TSS is applied, spatial correlation between the antennas depends on the carrier index k and the pulse shape $p_2(t)$. $\rho[k]_{m,m'}$ can be obtained by Monte Carlo simulations or by numerical computations.

If the example presented in Figure 2.6 is revisited, the channel gains in the frequency domain are; $H_1[k] = \alpha_{1,0} + \alpha_{1,1}p_2(-T_s/2) + e^{-j2\pi k/N}\alpha_{1,1}p_2(T_s/2)$ and $H_2[k] = e^{j2\pi k/N}\alpha_{2,0}p_2(-T_s/2) + \alpha_{2,0}p_2(T_s/2) + \alpha_{2,1}$. The covariance function $\text{Cov}[H_1[k]H_2[k]^*]$ then becomes

$$\begin{aligned} \text{Cov}[H_1[k]H_2[k]^*] &= \text{E}[e^{-j2\pi k/N}\alpha_{1,0}\alpha_{2,0}^*p_2(-T_s/2) + \alpha_{1,0}\alpha_{2,0}^*p_2(T_s/2) + \alpha_{1,0}\alpha_{2,1}^* \\ &\quad + e^{-j2\pi k/N}\alpha_{1,1}\alpha_{2,0}^*p_2(-T_s/2)^2 + \alpha_{1,1}\alpha_{2,0}^*p_2(-T_s/2)p_2(T_s/2) \\ &\quad + \alpha_{1,1}\alpha_{2,1}^*p_2(-T_s/2) + \alpha_{1,1}\alpha_{2,0}^*p_2(-T_s/2)p_2(T_s/2)e^{-j4\pi k/N} \\ &\quad + e^{-j2\pi k/N}\alpha_{1,1}\alpha_{2,0}^*p_2(T_s/2)^2 + e^{-j2\pi k/N}\alpha_{1,1}\alpha_{2,1}^*p_2(T_s/2)]. \end{aligned} \quad (2.14)$$

2.4 Numerical Results

Performance of the proposed TSS technique is evaluated through computer simulation. In each simulation, maximal ratio combining is employed and perfect channel estimation is performed. The pulse shaping filter $p_2(t)$ is chosen as truncated sinc pulse of length $2T_s$. Table 2.1 shows the other parameters that are used in each simulation.

Table 2.1: Simulation Conditions

Number of Antennas	2
Modulation Scheme	OFDM/QPSK
FFT size	64
Number of Subcarriers	64
Channel Model	2-path Rayleigh (Equal power)
Delay of Second Path	$T_s/2$
OFDM Symbol Duration	$64T_s$
Guard Interval	$16T_s$
Doppler Frequency ($f_D T_s$)	10^{-4}
Channel Estimation	ideal
Combining Scheme	MRC

Simulations are run for two different spatial channel models. Model-1 stands for a very high spatial correlation scenario (~ 0.98) and Model-2 is for more reasonable amount of correlation scenario (~ 0.85). In Model-1, antennas are displaced by 1λ (wavelength). Whereas in Model-2, the displacement is increased to 1.2λ which helps spatial correlation to reduce in Model-2. Measurement results in [2.11] show that when the base station is placed over the rooftop level, angular spread is usually less than 10° and when it is placed below the rooftop level, angular spread can be measured as high as 20° . Therefore, in Model-1, angular spreads are chosen less than 10° to increase the spatial correlation between array elements. On the other hand, angular spreads are considered as wider for Model-2. In practise, the angle of arrival depends on the mobile unit position. In Sections 1.2 and 2.2, it has been shown the spatial fading correlation is low when

the angle of arrival is close to the front direction ($\phi=0^\circ$) of the antenna array. Consequently, in Model-1 for very high spatial fading correlation, angle of arrival is chosen as 60° and in Model-2 in order to lower the amount of correlation, angle of arrival is chosen as 0° . Table 2.2 shows these two physical channel models that are used in simulations.

Table 2.2: Spatial Channel Models Considered in Simulations

	Model-1	Model-2
Antenna Separation (δ)	1λ	1.2λ
Angular Spread of First Path (Δ_1)	5°	10°
Angular Spread of Second Path (Δ_2)	10°	15°
Angle of Arrival of Paths (ϕ)	60°	0°

In Figure 2.7, for Channel Model-1, the spatial fading correlation coefficients between the antenna elements for each subcarrier are presented. When TSS is employed, correlation can be reduced to a sufficient level for uncorrelated reception. As seen in Fig. 2.7, the fading correlation is lowered mostly around $k = \pm N/2$. The channel delay profiles in the simulations are very similar to the ones presented in Figure 2.6. For that channel profile, the covariance of the frequency responses of the channels experienced by each antenna is given by Eq. (2.14). When $k = \pm N/2$, also remembering that the $e^{-j\pi} = -1$ and $p_2(t) = p_2(-t)$, all the terms except $\alpha_{1,0}\alpha_{2,1}^*$ will cancel each other. Therefore, the amount of spatial correlation on the subcarrier index $N/2$ equals to the correlation between the first multipath component of the first antenna ($\alpha_{1,0}$) and the second multipath component of the second antenna ($\alpha_{2,1}$) which is close to the zero as explained before. Hence, under this channel condition, the fading correlation is expected to be the lowest around $k = \pm N/2$.

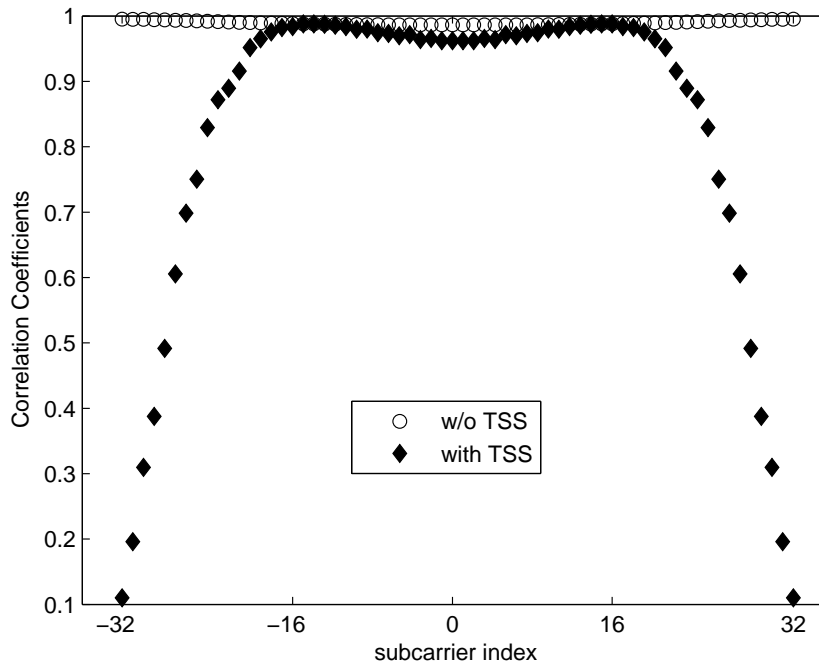


Figure 2.7: Spatial fading correlations on each subcarrier for the arrays employ TSS technique and for the conventional arrays. Spatial parameters of the Channel Model-1 are considered. Delay of the second path is $T_s/2$. Sampling delay at the second antenna is $T_s/2$.

Figure 2.8 shows the improvement in BER performance with TSS for both spatial channel models in Table 2.2. Performance improvement for the system under Channel Model-1 is observed higher than the one under Channel Model-2. This is because there is no linear relationship between correlation coefficient and system performance. For example, system performance difference between correlation values of 0.99 and 0.9 is much higher than the difference between 0.89 and 0.8. BER performances for some different correlation coefficients can also be found in [2.12].

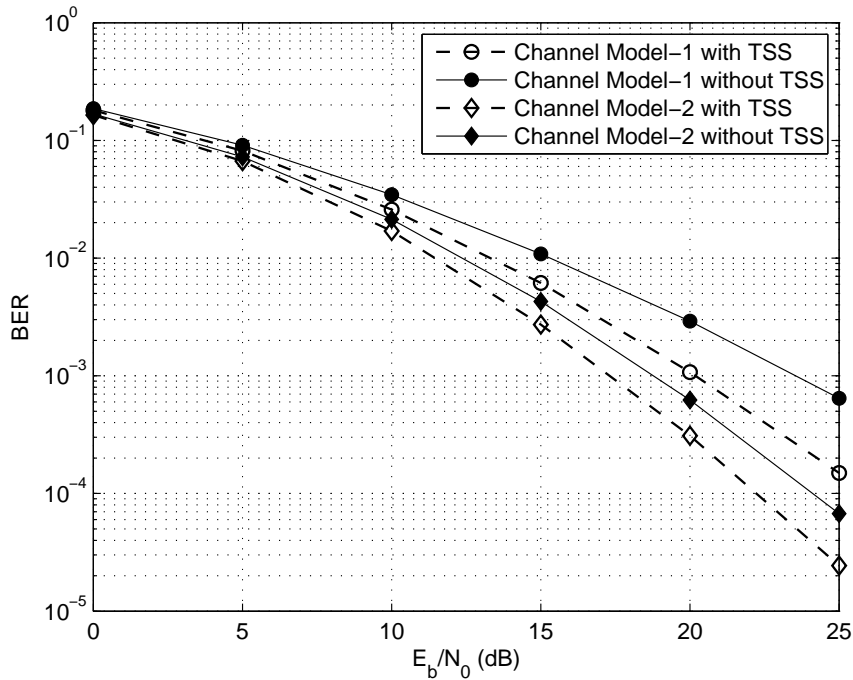


Figure 2.8: BER performance improvement with TSS for two elements antenna array for 2-path Rayleigh channel. Spatial parameters for the Channel Model-1 and Model-2 are given in Table 2.2. Delay of the second path is $T_s/2$. Sampling delay at the second antenna is $T_s/2$.

In Figure 2.9, Channel Model-2 is considered and antenna separation is changed from 0 to 9λ (wavelength). The system which employs TSS performs better than the conventional system until the separation of 4λ . For larger separations, the performances are almost the same. After 4λ , the spatial fading correlation between the antennas is already low enough for diversity reception and employing TSS can not improve the performance further.

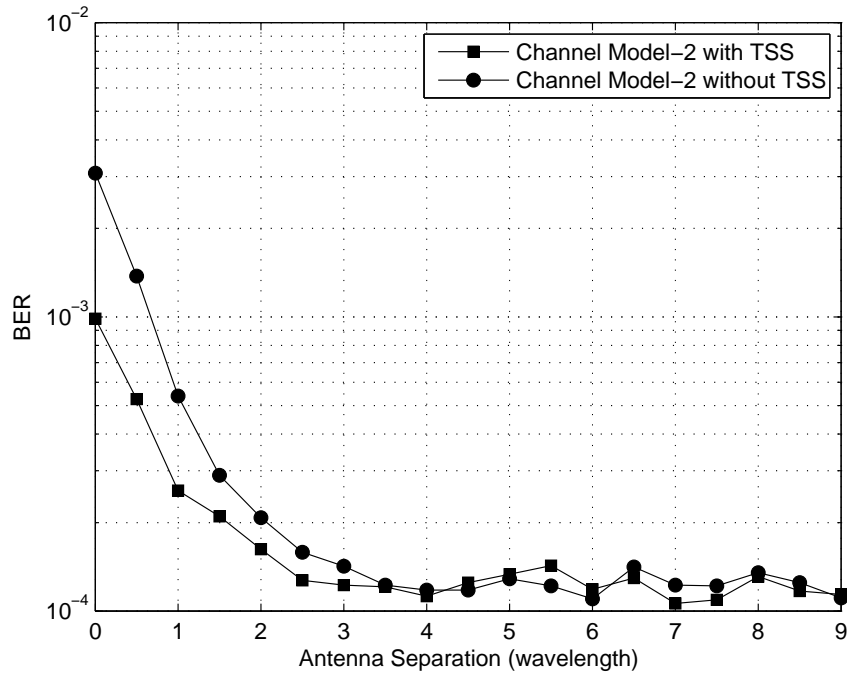


Figure 2.9: BER performance improvement with TSS for Channel Model-2 vs. Antenna Separation. E_b/N_0 is 20 dB. Spatial parameters for the Channel Model-2 is given in Table 2.2. Delay of the second path is $T_s/2$. Sampling delay at the second antenna is $T_s/2$.

In Figure 2.10, the angular spreads of the clusters are changed from 0° to 90° for both clusters. When the rays in clusters arrive within less than 20° , there is performance improvement observed with TSS. After 20° , the correlation is already low and the system achieves diversity so TSS can not add more improvement after that point.

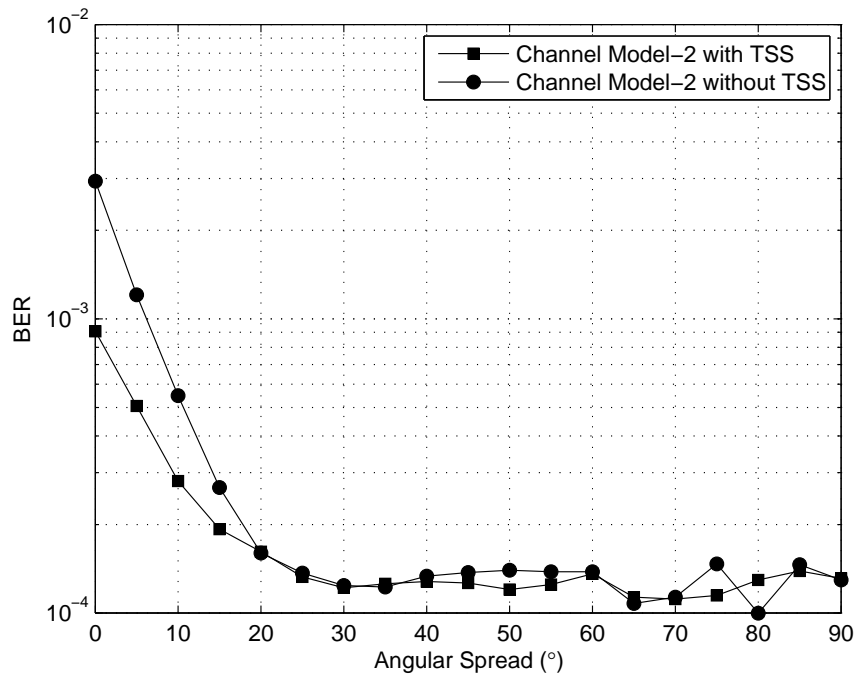


Figure 2.10: BER performance improvement with TSS for Channel Model-2 vs. Angular Spread. E_b/N_0 is 20 dB. Spatial parameters for the Channel Model-2 is given in Table 2.2. Delay of the second path is $T_s/2$. Sampling delay at the second antenna is $T_s/2$.

In Figure 2.11, the angles of arrivals of both clusters are changed from 0° (broad-side direction) to 90° (end-fire direction). At any value of the angle of arrival, there is improvement with TSS. It has been mentioned in Section 1.2 that when the angle of arrival is close to 0° , the correlation is low and the performance is better. When the angle of arrival gets close to 90° the performance decreases. For every angle of arrival, the array with TSS outperforms the conventional system. When the arriving angle is 90° , system performance with TSS is the same as it is 0° for the conventional arrays.

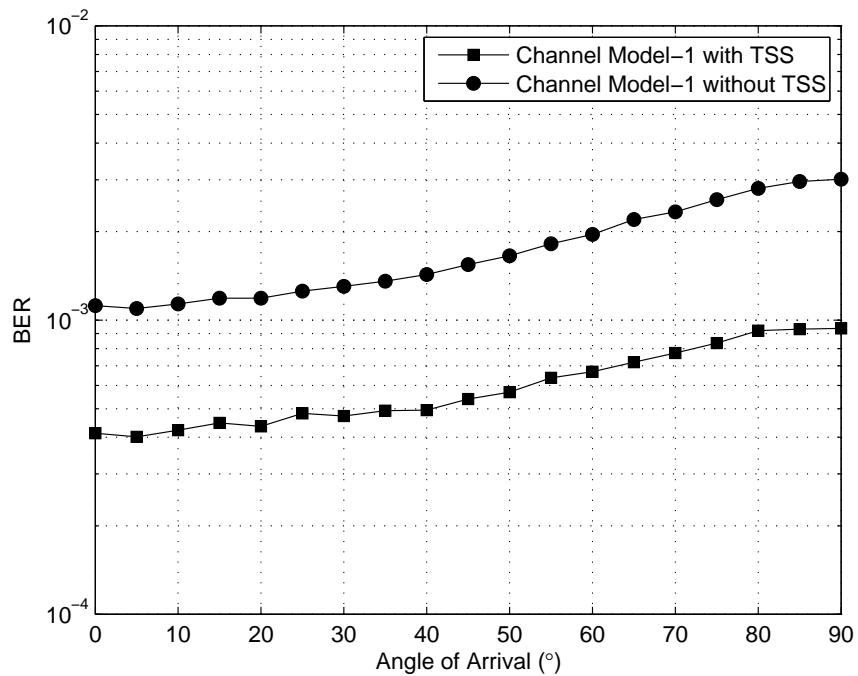


Figure 2.11: BER performance improvement with TSS vs. Angle of Arrival. E_b/N_0 is 20 dB. Spatial parameters for the Channel Model-1 is given in Table 2.2. Delay of the second path is $T_s/2$. Sampling delay at the second antenna is $T_s/2$.

The effect of the Doppler frequency on the system performance can be found in Figure 2.12. Simulations are performed under the time variant channels during one OFDM symbol for faster fading channels with normalized Doppler frequencies $f_D T_s$ from 10^{-4} to 10^{-1} . The system with TSS outperforms the conventional system under the both spatial channel models for the faster varying fading channels.

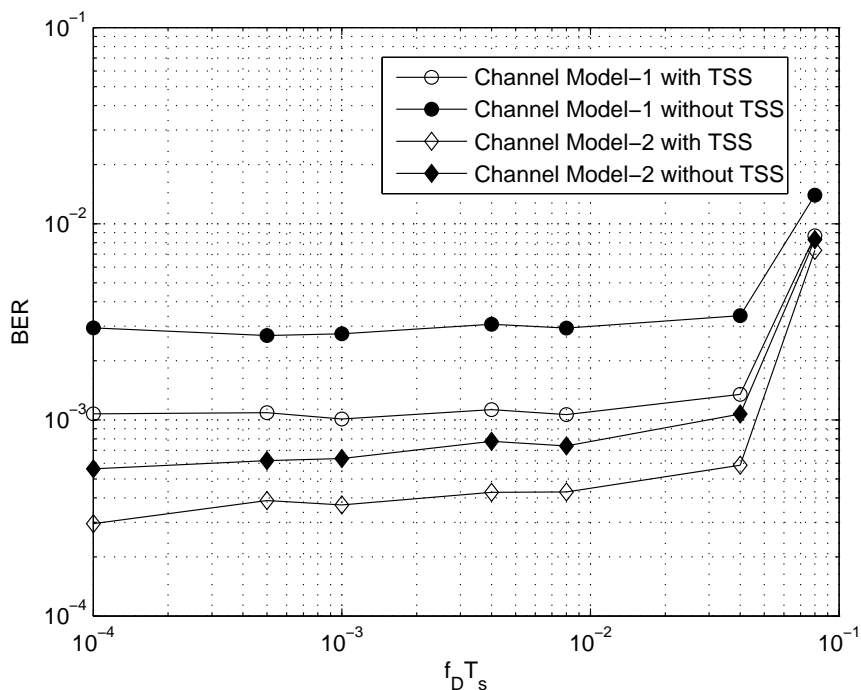


Figure 2.12: Effect of the Normalized Doppler Frequency on the BER Performance. E_b/N_0 is 20 dB. Spatial parameters for the Channel Model-1 and Model-2 are given in Table 2.2. Delay of the second path is $T_s/2$. Sampling delay at the second antenna is $T_s/2$.

In previous results, the delay of the second path and the delay at the second antenna for TSS receivers were both $T_s/2$ where the sampling point is optimized with the incoming second path. Figure 2.13 shows the BER performance improvement with TSS when the delay of the second path is $T_s/4$ and $3T_s/4$. The delay at the sampler of the second antenna is $T_s/2$. It is seen that the reduced correlation with TSS can improve the performance of the system for different delay profiles.

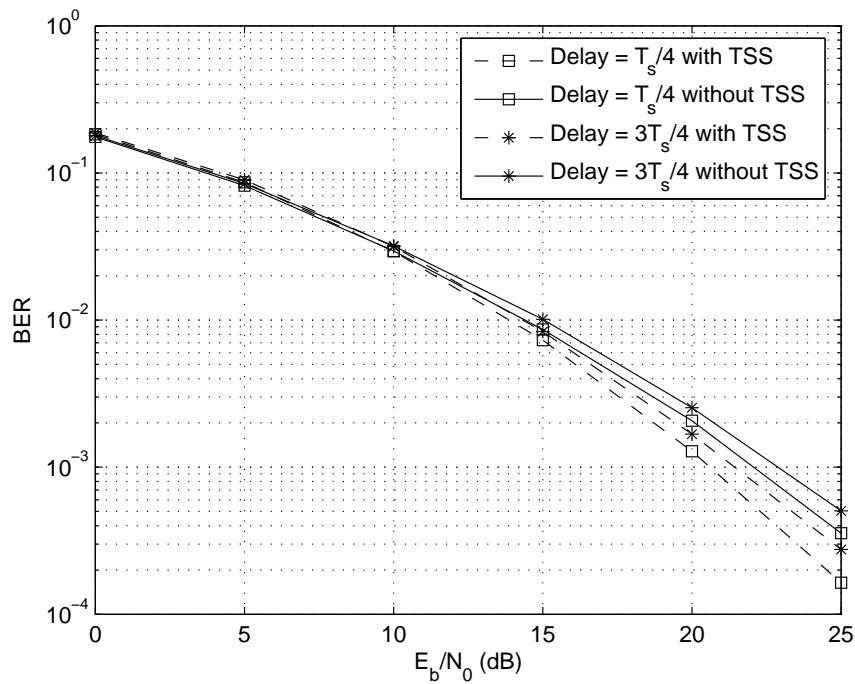


Figure 2.13: BER performance improvement with TSS for Channel Model-1. Spatial parameters for the Channel Model-1 is given in Table 2.2. Delay of the second path is taken as $T_s/4$ and $3T_s/4$. Sampling delay at the second antenna is $T_s/2$.

In Figure 2.14, BER performance is plotted for different delays at the sampler of the second antenna. The delay of the second path is fixed at $T_s/2$ and Channel Model-1 is considered. It is seen that the performance is maximized when the delay of the second antenna is $T_s/2$. For the delays different than $T_s/2$, there is still a performance gain when the TSS is employed. If there is no delay at the second antenna, the performance of TSS receiver is the same as the conventional receiver array's performance. Due to the cyclic property of DFT, the delay of T_s at the sampler will result the same frequency response as there were no delay. Therefore, the performance as a function of delay of the second antenna is periodic with T_s .

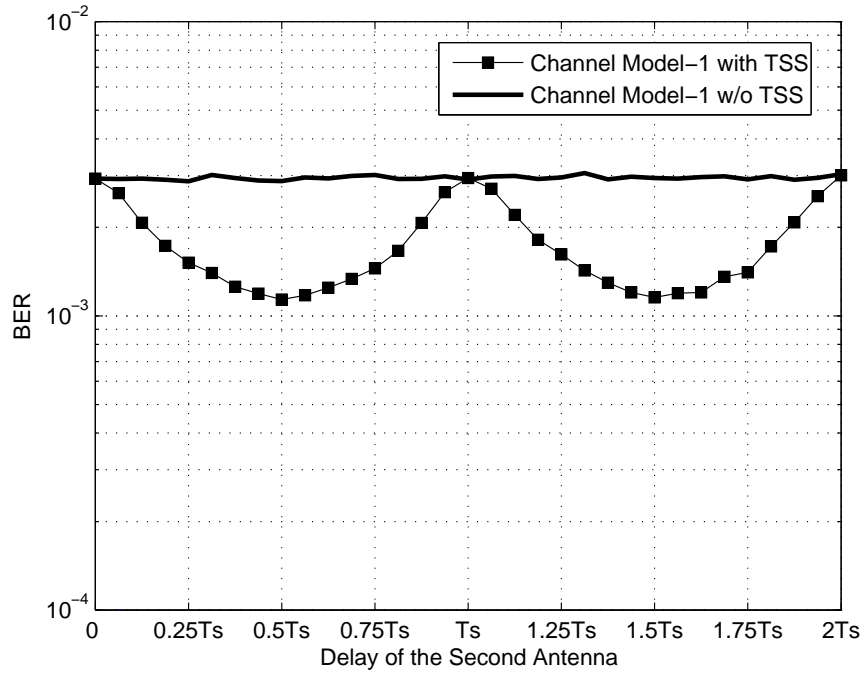


Figure 2.14: BER performance improvement with TSS for Channel Model-1 for different sampling delay at the second antenna. E_b/N_0 is 20 dB. Spatial parameters for the Channel Model-1 is given in Table 2.2. Delay of the second path is taken as $T_s/2$.

In Figure 2.15, simulation is run for the same conditions in Table 2.1 and Table 2.2, however this time number of elements in array is taken as four. Again, the system with TSS can take more advantage of diversity reception and improve system performance.

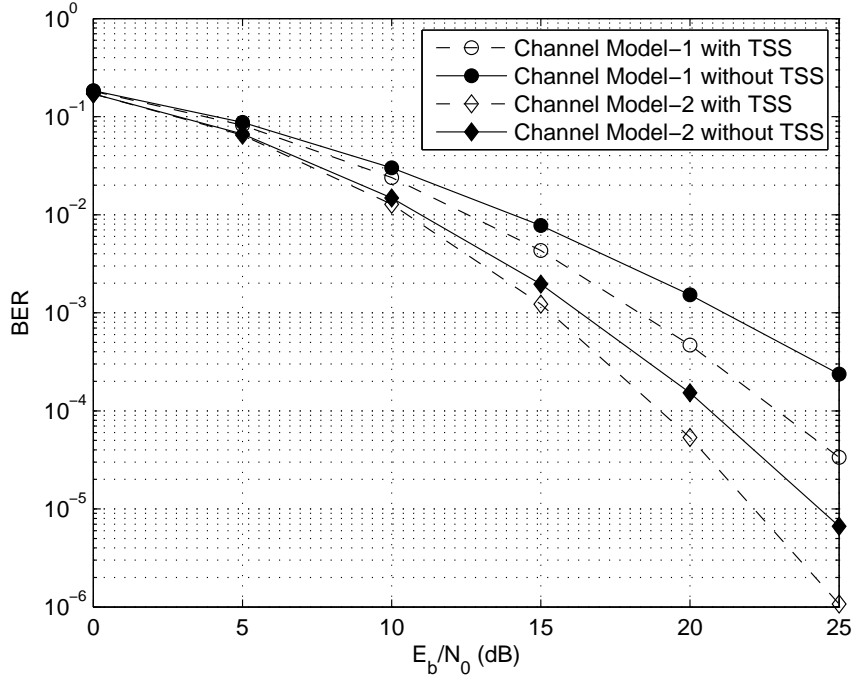
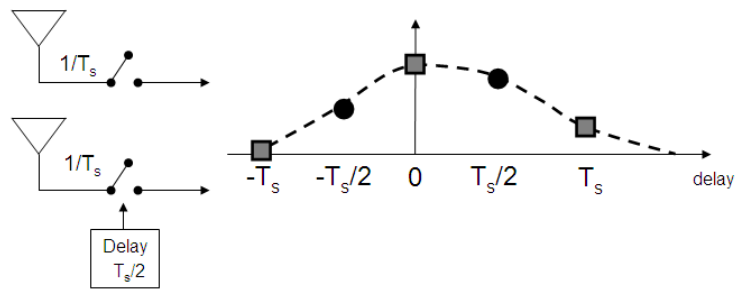


Figure 2.15: BER performance improvement with TSS for four elements antenna array. Spatial parameters for the Channel Model-1 and Model-2 are given in Table 2.2. Delay of the second path is $T_s/2$. Sampling delays at the second, third and fourth antennas are $T_s/4$, $2T_s/4$ and $3T_s/4$ respectively.

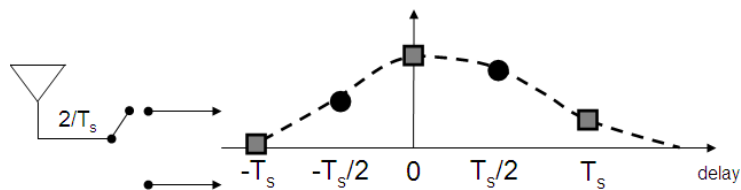
2.5 Discussions and Conclusion

TSS is a way to reduce the spatial correlation between the subcarriers of the OFDM symbol at the adjacent antennas. TSS can be considered as oversampling the multipath channel with different antennas. In extremely high correlated case, say all the antennas see the same channel, combining the time shifted samples from different antennas would result the same performance as oversampling the

channel with a single antenna. Figure 2.16 compares the TSS with 2 antennas and Oversampling with ratio of 2. Oversampling receiver samples 2 times faster than the Nyquist rate and obtains the same discrete channel samples as 2 element antenna array with TSS. The oversampling ratio is equal to the number of antennas in the TSS receiver.



(a) 2 element antenna array with TSS.



(b) OOFDM with ratio of 2.

Figure 2.16: Comparison of 2 element antenna array with TSS and Oversampling with ratio of 2. Discrete sequences to be transformed into the frequency domain and then combined are pointed as circles and squares.

OOFDM and TSS schemes are in common to sample the different points of the multipath channel which exploits the path diversity; OOFDM samples faster than the Nyquist rate and TSS shifts the sampling points. However, they provide different gains to their systems.

OOFDM, when it is compared to single antenna conventional OFDM systems, has additional replicas of the transmitted signal over the multipath channel.

OOFDM system achieves diversity by successfully combining these replicas. On the other hand, in antenna arrays the diversity gain is expected from the spatial diversity. The different replicas of the transmitted signal already exist in different channels to each antenna. If these diversity branches are already independent, TSS can not add any additional gain to the system. When the antennas are correlated, TSS takes the benefit of the path diversity and reduces the correlation. In summary, both OOFDM and TSS take the advantage of the path diversity. OOFDM system leads to SIMO (single-input multi-output) whereas TSS reduces the correlation between the antennas of the spatial diversity systems. The structures of the OOFDM and TSS receivers have already been discussed in Section 1.4.1.

Similar to applying OOFDM to MIMO systems [2.2], TSS can also be applied to MIMO. The capacity per subcarrier of MIMO-OFDM system is defined as [2.1]

$$C[k] = E[\log_2 \det(\mathbf{I}_{M_R} + \frac{E_s}{N_0} \mathbf{R}_r[k]^{1/2} \mathbf{H}_w[k] \mathbf{R}_t[k] \mathbf{H}_w[k]^H \mathbf{R}_r[k]^{H/2})] \quad (\text{bps/Hz}) \quad (2.15)$$

where $\mathbf{H}_w[k]$ is spatially white MIMO channel for subcarrier k , M_T is the number of antennas at the transmitter and M_R is the number of antennas at the receiver site. \mathbf{I}_{M_R} is the identity matrix of size $M_R \times M_R$. $\mathbf{R}_r[k]$ and $\mathbf{R}_t[k]$ are the $M_R \times M_R$ and $M_T \times M_T$ receive and transmit correlation matrices. Assume there is correlation only at the receiver and there are two antennas at the receiver array. Then, $\mathbf{R}_r[k]$ becomes

$$\mathbf{R}_r[k] = \begin{bmatrix} 1 & \rho[k] \\ \rho[k] & 1 \end{bmatrix}. \quad (2.16)$$

Hence, the reduced correlation by TSS per subcarrier can increase the capacity of MIMO systems.

In conclusion, the spatial fading correlation is the main limitation factor in multiple antenna reception. For some cases, although the antenna elements are

separated several times the wavelength, fading correlation is still high. Simulation results showed that TSS is effective technique to overcome the degradations in performance due to the spatial correlation. By TSS, it is possible to place antennas closer to each other for the same performance outcome or system performs better with the existing antenna placement. The proposed technique can be applied to arrays with any number of elements and MIMO systems as well.

References

- [2.1] H. Bolcskei, D. Gesbert, and A. J. Paulraj, “On the capacity of OFDM-based spatial multiplexing systems,” *IEEE Trans. on Communications*, vol. 50, pp. 225-234, Feb. 2002.
- [2.2] C. Tepedelenlioglu, R. Challagualla, “Low complexity multipath diversity through fractional sampling in OFDM,” *IEEE Trans. on Signal Processing*, vol. 52, No. 11, pp. 3104-3116, Nov. 2004.
- [2.3] H. Nishimura, M. Inamori, and Y. Sanada, , “sampling rate selection for fractional sampling in OFDM,” in Proc. *Int. Symp. on Personal Indoor and Mobile Radio Communications*, pp. 1-5, Sept. 2007.
- [2.4] D. Shiu, G. J. Foschini, M. J. Gans, J. M. Kahn, “Fading correlation and its effect on the capacity of multielement antenna systems,” *IEEE Trans. on Communications*, vol. 48, pp. 502-5133, March 2000.
- [2.5] G. J. Foschini, M. J. Gans , “On limits of wireless communication in a fading environment when using multiple antennas,” *Wireless Personal Commun.*, vol. 6, no. 3, pp. 311-335, Mar. 1998.
- [2.6] J. Salz, J. H. Winters, “Effect of fading correlation on adaptive arrays in digital mobile radio,” *IEEE Trans. Vehicular Technology*, vol. 43, No. 4, pp. 1049-1057, Nov. 1994.
- [2.7] R. B. Ertel, P. Cardieri, K. W. Sowerby, T. S. Rappaport and J. H. Reed, “Overview of spatial channel models for antenna array communication systems,” *IEEE Personal Commun.*, vol. 5, No.1, pp. 10- 21, Feb. 1998.

- [2.8] W. C. Jakes “Microwave Mobile Communications,” New York: Wiley, 1974, pp. 60-65.
- [2.9] T. L. Fulghum, K. J. Molnar, A. Duel-Hallen, “Jakes fading model for antenna arrays incorporating azimuth spread,” *IEEE Trans. Vehicular Technology*, vol. 51, No. 5, pp. 968-977, Sep. 2002.
- [2.10] A. F. Molisch, “Effect of far scatterer clusters in MIMO outdoor channel models ,” in Proc. *IEEE Vehicular Technology Conference*, vol.1, pp. 534-538 , Apr. 2003.
- [2.11] P. Pajusco, “Experimental Characterization of DOA at the base station in rural and urban area ,” in Proc. *IEEE Vehicular Technology Conference*, vol.2 , pp. 993 - 997, May 1998.
- [2.12] L. Fang, B. Guoan, and A.C. Kot, “New method of performance analysis for diversity reception with correlated Rayleigh-fading signals,” *IEEE Trans. on Vehicular Technology* , vol. 49, No. 5, pp. 1807-1812, Sept. 2000.

Chapter 3

Adaptive Modulation Scheme Incorporating Spatial Fading Correlation for OFDM with Time Shifted Sampling

In the previous chapter, it has been shown that the spatial correlation is not the same for each subcarrier of the OFDM symbol and it varies according to the pulse shaping filter, channel delay profile and the spatial correlation between each individual delayed paths. When the TSS technique is employed, the correlation coefficient for different subcarriers can vary dramatically depending on the channel conditions.

Since the channel correlation is the main factor on the system performance, the transmitter should know the correlation coefficient when it needs to optimize the transmission rate. In conventional adaptive systems that optimize the transmission rate, the transmitter decides the modulation scheme with respect to carrier-to-noise ratio (CNR) at each subcarrier. However, especially when the TSS technique is employed, correlation changes dramatically for different subcarriers. Therefore, the transmitter should also know the correlation coefficient for

each subcarrier to optimize the transmission rate.

In this chapter, selecting an appropriate modulation scheme for Adaptive OFDM (AOFDM) systems based on a given channel condition incorporating the spatial fading correlation is proposed. The numerical results through computer simulation show that the proposed decision chart outperforms the conventional systems in achieving the target BER and establishing reliable communication when the antennas are correlated.

This chapter is organized as follows. Section 3.1 gives an introduction. In Section 3.2, spatial fading correlation on subcarrier-by-subcarrier basis is given. Then in Section 3.3, the proposed scheme is introduced and numerically evaluated in Section 3.4. Section 3.5 gives the result for coded transmission. Finally, this chapter is concluded in Section 3.5.

3.1 Introduction

Future radio communication systems are expected to provide variety of multimedia services to mobile users. In order to meet these requirements, radio systems must be able support high capacity, variable bit rate transmission and high-bandwidth efficiency. One of the challenges to satisfy these high demands is to mitigate the effects of fading and multi-path phenomenons. OFDM is a good candidate because of its ability to convert a frequency selective multipath channel into a set of parallel frequency-flat fading channels. Also, it is possible to eliminate inter-symbol interference (ISI) due to multipath delay by inserting guard interval longer than the delay spread [3.1][3.2]. For these reasons, OFDM has been adopted in many wireless standards such as DAB/DVBT, 802.11 WLAN and 802.16 WMAN.

OFDM has also found to be advantageous in terms of ergodic capacity in rich multipath environments for antenna arrays [3.3]. In such performance analysis for OFDM antenna arrays, it is typically assumed that the fading is independent across diversity branches. This independence assumption can be valid for some

cases, while there are several cases where fading is correlated [3.4]. For instance, when the antenna elements can not be placed sufficiently apart due to the physical constraints. It is well known that the correlation degrades the diversity gain.

For correlated OFDM antenna array systems, Time Shifted Sampling (TSS) has been proposed which reduces correlation coefficients for some of the subchannels of the OFDM symbol in Chapter 2. Since, combining is usually done in the frequency domain on a subcarrier-by-subcarrier basis, this low correlation for some subcarriers turns into performance gain. In this work, an adaptive modulation scheme is proposed for OFDM based on the joint effect of the signal-to-noise ratio (SNR) and the correlation coefficient since the less correlated subchannels have more potential to transmit higher order modulated symbols.

Some early works on adaptive modulation in [3.5][3.6][3.7] propose burst-by-burst adaptive QAM (AQAM) for exploiting time-variant Shannonian capacity for narrowband fading channels. The associated AQAM schemes are adopted for Adaptive OFDM (AOFDM) systems in [3.8][3.9][3.10]. In the AOFDM transmission each carrier in the OFDM system can transmit different modulation schemes depending on its channel condition where in the non-adaptive OFDM systems use fixed modulation across all the subcarriers.

AOFDM transmission can be applied to duplex communication systems since it requires additional signaling including steps; (i) the transmitter should reliably estimate the channel quality, (ii) select the appropriate modulation scheme and (iii) the receiver should know which modulation scheme is applied to which subcarrier.

For the step (i); the channel quality should be predicted reliably in order to select the transmission parameters. In previous literatures, there are works related to AOFDM for reliable channel condition prediction [3.11][3.12][3.13]. Then in the step (ii), with the obtained channel knowledge, an appropriate modulated scheme has to be chosen. Each modulation scheme provides a tradeoff between spectral efficiency and a bit error rate (BER). Choosing the highest modulation scheme that will give an acceptable BER would maximize the spectral efficiency. At the final step (iii), for successful demodulation, the receiver has to be informed

as which modulation scheme parameters are used at the transmitter site. This can be done by transmitting this information directly to receiver with the cost of transmission capacity or the receiver may attempt to estimate which modulation scheme is used by itself.

In this work, the focus is given to the step (ii) which is selecting an appropriate modulation scheme for a given channel condition incorporating spatial fading correlation when the receiver site employs the TSS technique. A new modulation decision chart is proposed and the numerical results through computer simulation show that the proposed scheme is superior over the conventional systems in achieving a target BER and establishing reliable communication while having almost the same transmission rate.

3.2 Subcarrier-by-Subcarrier Spatial Correlation for TSS Receivers

In this section, the derivation for the correlation coefficient for each subcarrier for TSS is given. Suppose the OFDM symbol is transmitted and the information symbol on the k^{th} subcarrier is $s[k]$ ($k = 0, 1, \dots, N - 1$). Then OFDM symbol is the IDFT of the information symbols

$$u[n] = \frac{1}{N} \sum_{k=0}^{N-1} s[k] e^{j2\pi nk/N} \quad (3.1)$$

where n ($n = 0, 1, \dots, N - 1$) is the time index and N is the IDFT length. The baseband signal at the output of the filter is given by $x(t) = \sum_{n=0}^{P-1} u[n] p(t - nT_s)$ where $p(t)$ is the impulse response of the pulse shaping filter, T_s is the symbol duration and P is the sum of the IDFT length and the length of cyclic prefix. Then this signal is transmitted over a multi-path channel to the destination antenna m with an impulse response $c_m(t)$. The received signal by each antenna m then becomes

$$y_m(t) = \sum_{n=0}^{P-1} u[n] h_m(t - nT_s) + v_m(t) \quad (3.2)$$

where $h_m(t)$ is the impulse response of the channel seen by the antenna m and is given by $h_m(t)=p(t)\star c_m(t)\star p(-t)$, \star denotes convolution. $v_m(t)$ is the total additive white Gaussian noise at the receiver m . $h_m(t)$ can be expressed in a baseband form as

$$h_m(t) = \sum_{\ell=0}^{L-1} \alpha_{m,\ell} p_2(t - \tau_\ell). \quad (3.3)$$

$p_2(t) = \int p(t')p(t+t')dt'$ is the auto correlation of $p(t)$, L is the number of path components, $\alpha_{m,\ell}$ is the complex gains of the ℓ^{th} component at the m^{th} antenna and τ_ℓ is the path delay.

In TSS receiver, the signal is sampled at the baud rate of $1/T_s$ with a delay of $(m-1)T_s/M$ at antenna m over total of M antennas. The received signals in the discrete-time are expressed as

$$y_m[n] = \sum_{l=0}^{P-1} u[l]h_m[n-l] + v_m[n] \quad (3.4)$$

where $y_m[n] = y_m(nT_s + (m-1)T_s/M)$, $h_m[n] = h_m(nT_s + (m-1)T_s/M)$, $v_m[n] = v_m(nT_s + (m-1)T_s/M)$. At each antenna, noise samples are still independent and white. However the fading correlation between any antenna elements m and m' , $h_m[n]$ and $h_{m'}[n]$ is reduced. Channel gains in discrete-time at each antenna are given by

$$h_m[n] = \sum_{\ell=0}^{L-1} \alpha_{m,\ell} p_2(nT_s + (m-1)T_s/M - \tau_\ell). \quad (3.5)$$

By taking the DFT of (3.5), the channel gains for each subcarrier in frequency domain are

$$H_m[k] = \sum_{n=0}^{N-1} e^{-j2\pi nk/N} \sum_{\ell=0}^{L-1} \alpha_{m,\ell} p_2(nT_s + (m-1)T_s/M - \tau_\ell) \quad (3.6)$$

where N is the DFT size.

The basic input-output relationship in the OFDM-antenna array system is

$$\mathbf{z}[k] = \mathbf{H}[k]s[k] + \mathbf{w}[k] \quad (3.7)$$

where $\mathbf{z}[k]$, $\mathbf{H}[k]$ and $\mathbf{w}[k]$ are the $M \times 1$ column vectors of the received symbols, the channel gains and the Gaussian noises at each subcarrier, respectively. Then the estimate of $s[k]$ through MRC combining is

$$\check{s}[k] = \frac{\check{\mathbf{H}}^H[k]\mathbf{z}[k]}{\check{\mathbf{H}}^H[k]\check{\mathbf{H}}[k]} \quad (3.8)$$

where $\check{\mathbf{H}}[k]$ is the estimated $M \times 1$ channel column vector. Since MRC is employed in the frequency domain, the amount of spatial correlation is also derived in the frequency domain. Spatial correlation between any antenna elements m, m' can be written as

$$\rho[k]_{m,m'} = \frac{\text{Cov}[H_m[k]H_{m'}[k]^*]}{\sqrt{\text{E}[|H_m[k]|^2]\text{E}[|H_{m'}[k]|^2]}} \quad (3.9)$$

where $\text{Cov}[\cdot]$ is the covariance operator. The covariance at the numerator of Eq.(3.9) can be further expressed in terms of covariances of the individual path components as

$$\begin{aligned} \text{Cov}[H_m[k]H_{m'}[k]^*] = & \quad (3.10) \\ & \sum_{n_1=0}^{N-1} \sum_{n_2=0}^{N-1} e^{-j2\pi(n_2-n_1)/N} \sum_{\ell=0}^{L-1} p_2(n_1T_s + (m-1)T_s/M \\ & - \tau_\ell)p_2(n_2T_s + (m-1)T_s/M - \tau_\ell)\text{Cov}[\alpha_{m,\ell}, \alpha_{m',\ell}^*]. \end{aligned}$$

$\text{Cov}[\alpha_{m,\ell}, \alpha_{m',\ell}^*]$ is the product of correlation between the same path components and the variance of the fading waveform; $\text{Cov}[\alpha_{m,\ell}, \alpha_{m',\ell}^*] = \rho_\ell \sigma_\ell^2$. Therefore, correlation per subcarrier is a function of the delay of the paths, channel gains of each path and antenna correlation for each path. In Section 4, the performance of the time shifted sampling technique and correlation reduction for some subcarriers are presented.

3.3 Proposed Adaptive Modulation Scheme

For single antenna communication systems, the AOFDM systems in literature usually rely on the estimated CNR knowledge to choose the modulation scheme

[3.11][3.12]. In [3.12], in addition to the CNR value, the estimation of the delay spread has also been considered and then the modulation scheme is selected based on the joint effect of the CNR and the delay spread.

3.3.1 Conventional Modulation-Scheme Selection Chart

In this work, the antenna array receiver is considered instead of single antenna transmission. In antenna array receivers, in order to maintain the same bit-error-rate, the required combined CNR for antenna arrays is less than that for the single branch receiver. Therefore, the modulation scheme selection charts based on the CNR should be modified for the diversity reception case.

In Table 3.1, the conventional modulation scheme selection chart is given for the target BER of 10^{-3} for a 2 branch independent diversity receiver based on the received average CNR values. However, when the antennas are correlated, it is difficult to reach the target BER value.

Table 3.1: Conventional Modulation-Scheme Selection Chart based on CNR for target BER 10^{-3}

Modulation Scheme	Required CNR (dB)
BPSK	$-\infty$
QPSK	14.2 dB
16-QAM	17.2 dB
64-QAM	24.2 dB

3.3.2 Proposed Modulation-Scheme Selection Chart

In order to reach the target BER, in the proposed scheme, the mobile unit decides the modulation scheme based on the knowledge of the average CNR and the correlation coefficient which are fed back from the base station. Figure 3.1 illustrates the signaling in the proposed scheme. The correlation coefficient at the destination can be measured or statistically estimated [3.14][3.15].

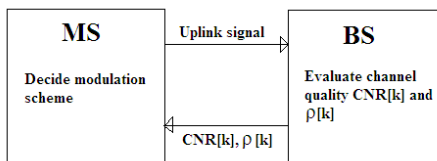


Figure 3.1: Signaling scenario in proposed scheme.

Figure 3.2 shows the relationship between the correlation coefficient and the CNR for the target BER of 10^{-3} for four different modulation schemes when the destination has two antennas. The optimum modulation scheme regions are obtained for the CNR and the correlation coefficient ($\rho[k]$) based on the BER plots which are prepared before. The chart is prepared in advance as follows. First, the channel propagation characteristics have been defined; Rayleigh fading is considered. Then computer simulations have been performed to obtain the relationship between the CNR and BERs for several correlation coefficients. Then, after a required BER is defined, optimum modulation scheme region is cleared that can obtain a BER performance lower than a required BER. Depending on the correlation coefficient and the CNR value, in the region of the modulation scheme, the spectral efficiency is maximized for the acceptable target BER of 10^{-3} . In the chart, when the target BER can not be achieved, BPSK is selected.

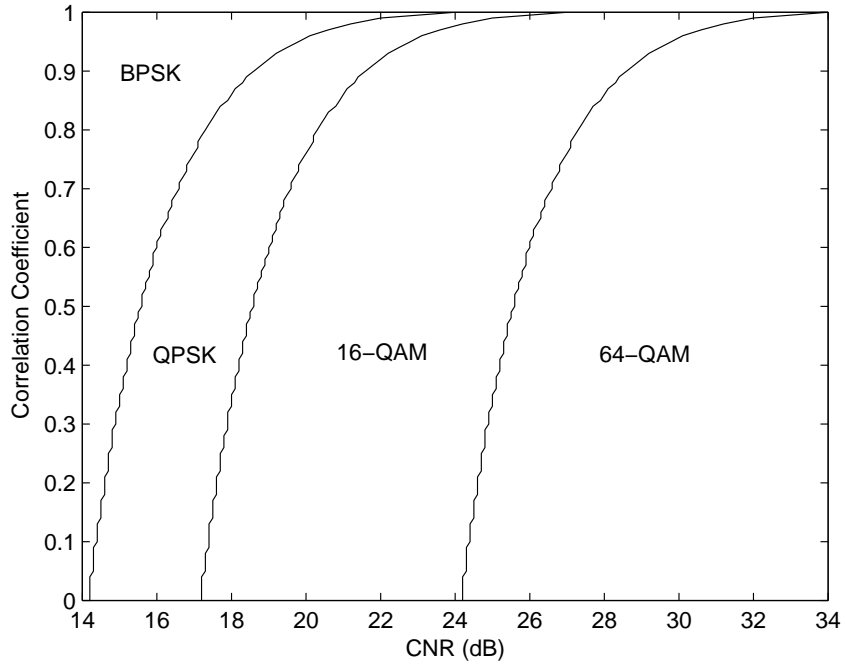


Figure 3.2: Proposed Modulation-Scheme Selection Chart based on CNR and correlation coefficient for target BER 10^{-3} .

3.4 Performance of the Proposed Scheme

3.4.1 Simulation Conditions

The results presented in previous sections are applied to simulations that provide the impacts of different parameters on the spatial fading correlation over subcarriers such as the delay spread and the path correlations. The first set of simulations is run in a 2 path Rayleigh fading channel for its simplicity, then the second set of simulations is run for a more realistic channel model that is 6-ray GSM Typical urban channel model. BER results are given in order to see the impact of the proposed adaptive scheme and its approach to the target BER. Simulation conditions are summarized in Table 3.2.

Table 3.2: Simulation Conditions

Number of Antenna Elements	2
FFT size	64
Number of Subcarriers	64
Guard Interval	$16 T_s$
DFT Sampling frequency	5 MHz
Data Modulation	BPSK/QPSK/16-QAM/64-QAM
Channel Model	Rayleigh fading (a) 2 path uniform (b) GSM Typical urban model
OFDM Symbol Duration	$64 T_s$
Doppler Frequency	50 Hz
Combining Scheme	MRC
Channel Coding	No Code/Convolutional Code
Channel Estimation	Ideal

3.4.2 Channel Models

The first set of simulations is run for a 2 path Rayleigh fading model in order to clarify the parameters which affect the spatial correlation distribution over subcarriers. Figure 3.3 shows the delay profile of the 2 path channel. In simulations, the delay τ_1 is set to $T_s/2$. Different spatial characteristics are defined for the clusters. In both cases, all the paths are coming from 0° and angular spreads of the first and the second paths are 5° and 10° . Table 3.3 summarizes the spatial properties of the assumed channel. Therefore, in Case-1, we expect high correlation due to the insufficient antenna separation. On the other hand, in Case-2 fading distributions are independent due to the adequate antenna separation.

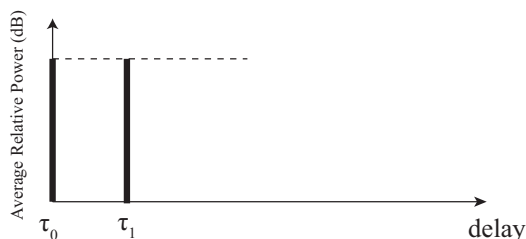


Figure 3.3: 2 path Rayleigh fading model with uniform delay spread.

Table 3.3: Spatial Channel Models Used for 2 Path Rayleigh Channel

	Case-1	Case-2
Antenna Separation	1λ	10λ
Angular Spread of the First Path	5°	10°
Angular Spread of the Second Path	5°	10°
Angle of Arrival of the First Path	0°	0°
Angle of Arrival of the Second Path	0°	0°

Then the second set of simulations is run for the 6-ray typical urban model. The 6-ray typical urban model is one of the propagation models that are mentioned in the main body of 3GPP TS 45.005 [3.16]. Figure 3.4 shows the delay profile of the 6-ray GSM channel model. The parameters of the model are given in Table 3.4. The amplitudes of the paths follow Rayleigh distribution. As for the spatial characteristics, the angle of arrivals for all the paths are set to 0° . The angular spread depends on the propagation environment and usually it is assumed to be independent of delay spread [3.17]. However, some measurement results have indicated a clear correlation between the delay spread and the angular spread [3.18].

In both models, the channel response is assumed to be constant during one OFDM symbol.

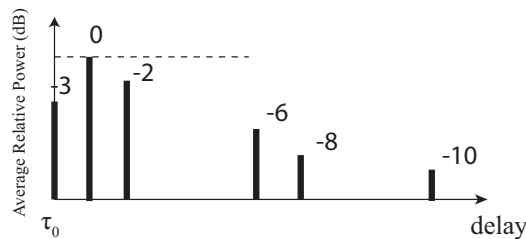


Figure 3.4: 6-ray GSM Typical Urban model.

Table 3.4: 6-ray GSM Typical Urban Model

Tap Number	Relative time(μsec)	Average Relative Power (dB)
1	0.0	-3.0
2	0.2 (T_s)	0.0
3	0.5 ($2.5T_s$)	-2.0
4	1.6 ($8T_s$)	-6.0
5	2.3 ($11.5T_s$)	-8.0
6	5.0 ($25T_s$)	-10.0

3.4.3 Effect of Time Shifted Sampling for 2 path Rayleigh Channel

Time Shifted Sampling can reduce the correlation coefficient for some of the subcarriers when it is employed at the receiver. Considering the cases defined in Table 3.3, computer simulation is run to observe the correlation coefficient on the subcarrier-by-subcarrier basis. Figure 3.5 shows the correlation coefficient over the subcarriers for both Case-1 and Case-2. In Case-1, antennas are placed by the wavelength distance which introduces high correlation over the subcarriers. When TSS is employed, correlation is reduced for some subcarriers, mainly around $k = \mp N/2$ as shown in Chapter 2. In Case-2, antennas are placed by the distance 10 times of the transmission wavelength, which provides uncorrelated fading distributions at each antenna. When TSS is employed, the correlation is still low.

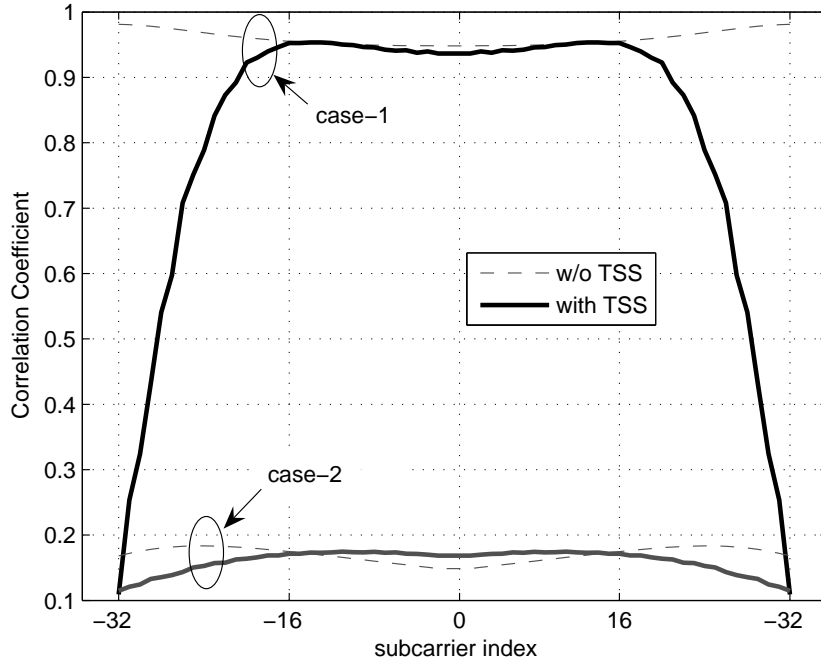


Figure 3.5: Correlation coefficient over subcarriers for 2-path Rayleigh channel.

In this chapter, throughput(η) is defined as [3.11]

$$\eta = R_b \frac{N_{suc}}{N_{trans}} \quad (3.11)$$

where R_b is the carrier bit rate, N_{trans} and N_{suc} are the transmitted and successfully received OFDM symbols, respectively. Using BPSK, QPSK, 16-QAM and 64-QAM, the carrier bit rate is 12, 24, 48 and 72 Mbps, respectively.

Figure 3.6 shows the throughput performance of the system with and without the TSS technique employed at the receiver site. Only Case-1 is considered where the impact of the TSS is more apparent. Fixed BPSK, QPSK, 16-QAM and 64-QAM are considered as modulation schemes. When the TSS technique is employed, since the correlation coefficient is low for some of the subcarriers, transmission suffers less from spatial fading correlation and performance gain is observed. When the CNR is high enough so that the throughput reaches its limit, employing the TSS does not make difference in the system performance.

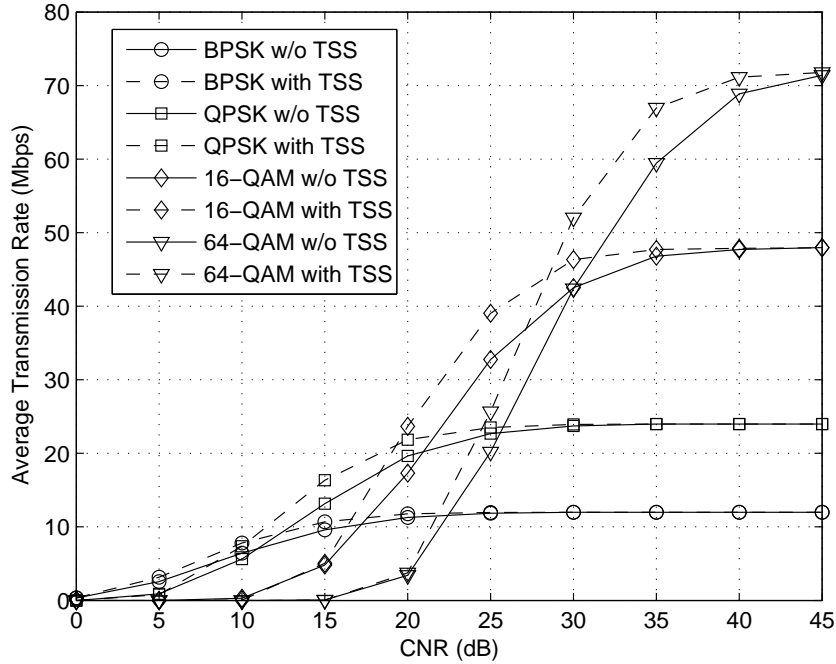


Figure 3.6: Impact of TSS on system throughput performance for 2-path Rayleigh channel Case-1.

As seen in Figure 3.6, employing the TSS to the correlated channels is an effective way to increase the system throughput. Hence, in the following results, only the receivers with the TSS are considered and the discussions on the proposed scheme are given for the TSS receivers.

3.4.4 Performance of the Proposed Adaptive Modulation Scheme for 2 path Rayleigh Channel

In this section, performance of the proposed scheme is presented. The 2-path Rayleigh channel is considered. Perfect knowledge of the channel condition at the transmitter site and of the set of demodulation parameters at the receiver site is assumed. The target BER is taken as 10^{-3} .

First, Case-1 is considered where correlation coefficients for some subcarriers are low. Figure 3.7 shows the BER performances of the transmission with fixed

modulation schemes, the adaptive modulation scheme based on the CNR values given in Table 3.1 as the conventional scheme and the proposed scheme which is based on the joint effect of the CNR and the spatial correlation given in Figure 3.2. Since, the conventional scheme has no knowledge about the spatial fading correlation, it chooses the modulation scheme as the receiver antennas were uncorrelated. Therefore, it makes more errors for the correlated subchannels. On the other hand, the proposed scheme can easily reach the target BER since it has both the CNR and the spatial correlation coefficients for every subcarriers. For instance, when the average CNR[k] is 20 dB the conventional scheme transmits 16-QAM symbol over a correlated subchannel and it makes more errors than the target BER 10^{-3} . The proposed scheme has superiorly in choosing a modulation scheme; when CNR[k] is 20 dB, it chooses QPSK for correlated subchannels, and 16-QAM for uncorrelated subchannels.

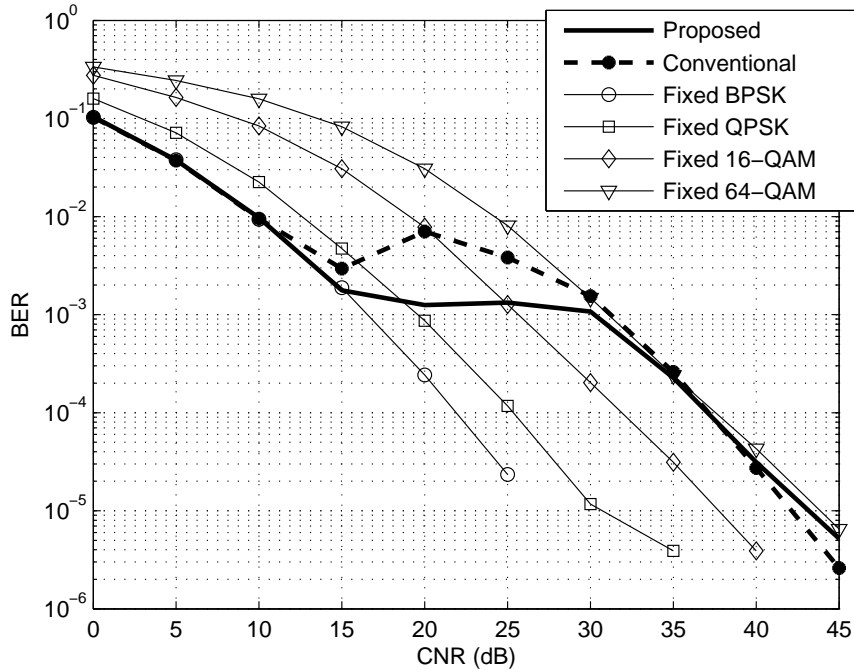


Figure 3.7: BER performance of the proposed scheme for 2-path Rayleigh channel Case-1.

Figure 3.8 shows the throughput performance of the proposed scheme with comparison to the conventional and fixed modulation schemes. The conventional adaptive modulation based on the CNR values in Table 3.1 and the proposed adaptive modulation scheme have the similar throughput performance. Up to the CNR of 10 dB they both choose BPSK. Between the CNRs of 10 dB and 20 dB, the conventional scheme chooses higher modulation schemes and achieves 2-3 Mbps throughput gain over the proposed scheme with the cost of more bit error rate as the proposed scheme has as shown in Figure 3.7. Therefore, the proposed scheme outperforms the conventional systems in achieving the target BER and establishing reliable communication while having almost the same transmission rate.

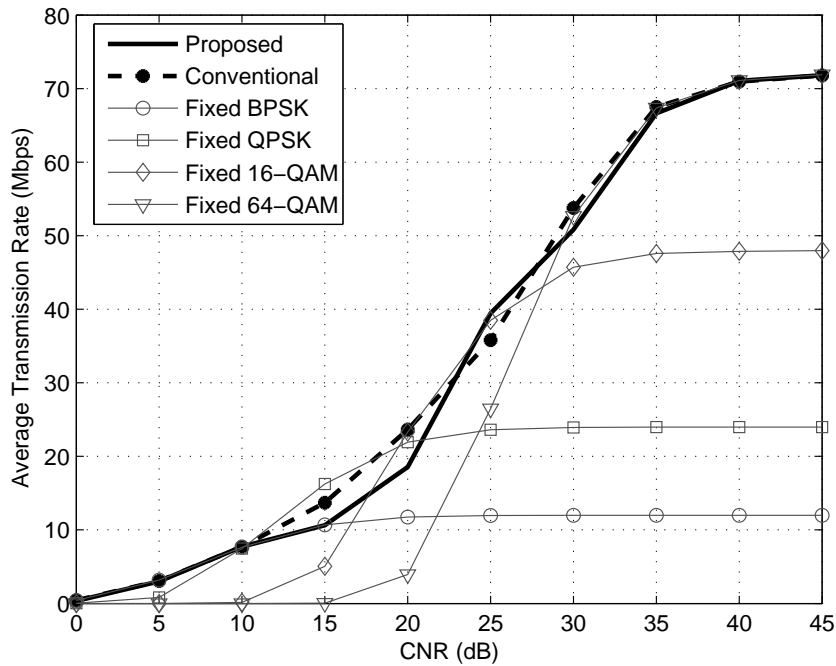


Figure 3.8: Throughput performance of the proposed scheme for 2-path Rayleigh channel Case-1.

Figures 3.9 and 3.10 show the BER and throughput performances of the proposed scheme in the 2 path Rayleigh channel Case-2 where the channel is uncorrelated for all the subcarriers. The modulation selection chart in Table 3.1 for the conventional scheme is already driven for uncorrelated channels and system performance is optimum. The proposed scheme can easily adapt the uncorrelated channel as well and reach the same performance as in Figures 3.9 and 3.10.

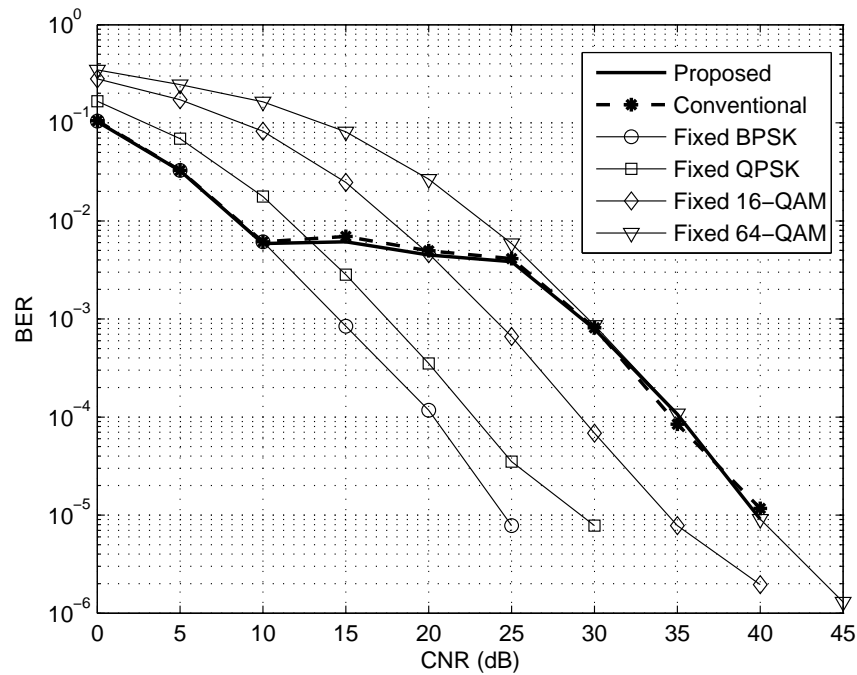


Figure 3.9: BER performance of the proposed scheme for 2-path Rayleigh channel Case-2.

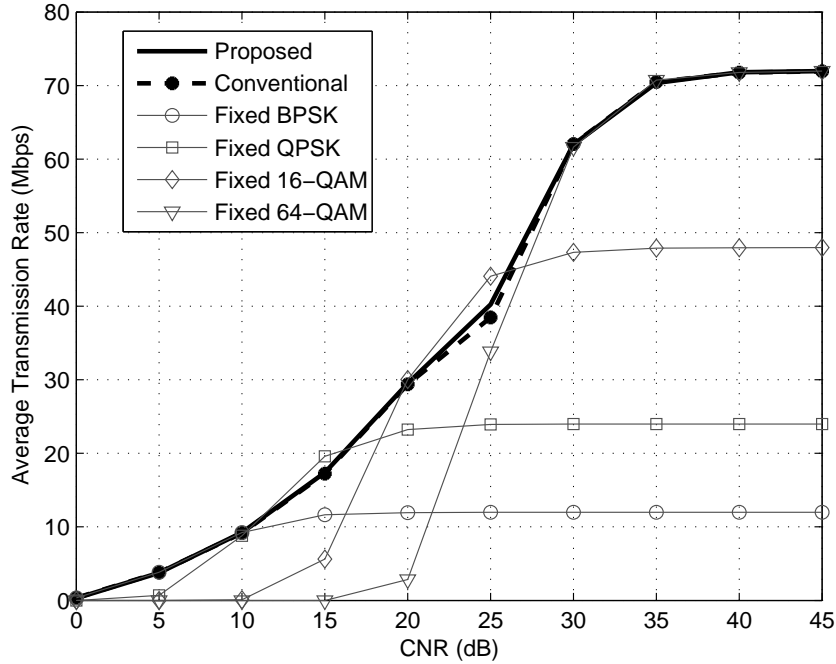


Figure 3.10: Throughput performance of the proposed scheme for 2-path Rayleigh channel Case-2.

3.4.5 Effect of Time Shifted Sampling for 6-ray GSM Channel Model

In the second set of simulations, a more realistic channel model is studied to observe the system performance. 6-ray GSM Channel Model is assumed. The original model does not include the cluster properties of the paths such as their angle of arrivals and angular spreads. In practice, the angle of arrival depends on the position of the receiver, the transmitter and the scattering environment. In the simulations, the angle of arrival of all 6 paths are set to 0° . The angular spread is increased with respect to the delay spread according to [3.18] in which authors show the correlation between the angular spread and the delay spread. In this study, the angular spreads are increased from very small angular spread from 2° to 12° , $\Delta_\ell = [2^\circ \ 2.5^\circ \ 3.7^\circ \ 5.4^\circ \ 7.8^\circ \ 12^\circ]$. The small angular spread is also the interest of some works [3.19][3.20] since it reduces diversity effect dramatically for antenna array communication. The performances of the proposed scheme

and the conventional scheme are compared under this realistic channel condition. Antenna separation is taken as equal to the transmission wavelength. Figure 3.11 shows the correlation values for different subcarriers under these assumptions. It is seen that when the TSS technique is applied the correlation coefficient is lowered for the subcarriers. Given this correlated channel, the average transmission rates for fixed modulation schemes with and without the TSS technique are given in Figure 3.12. When the TSS technique is applied under this channel condition, throughput performance improves.

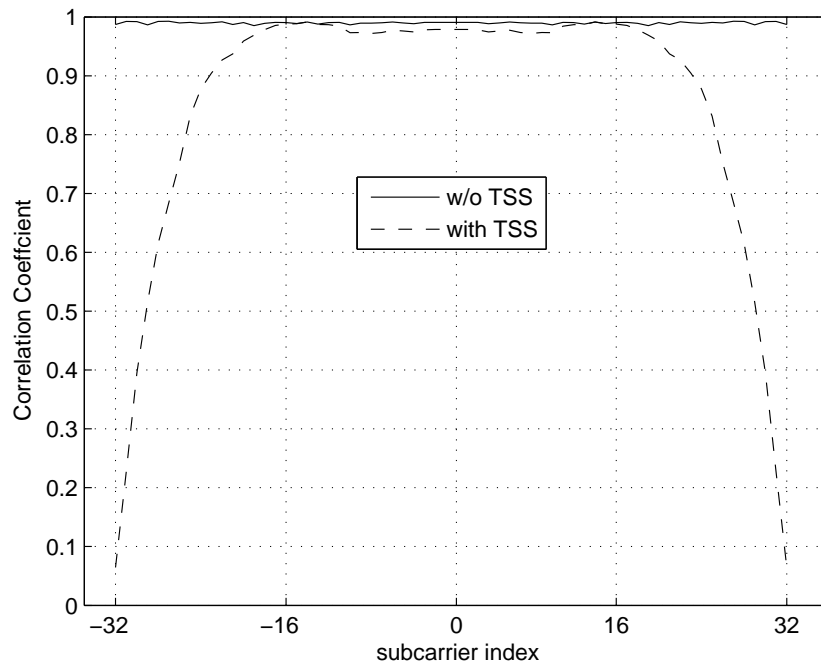


Figure 3.11: Correlation coefficient over subcarriers for 6-ray GSM Channel Model.

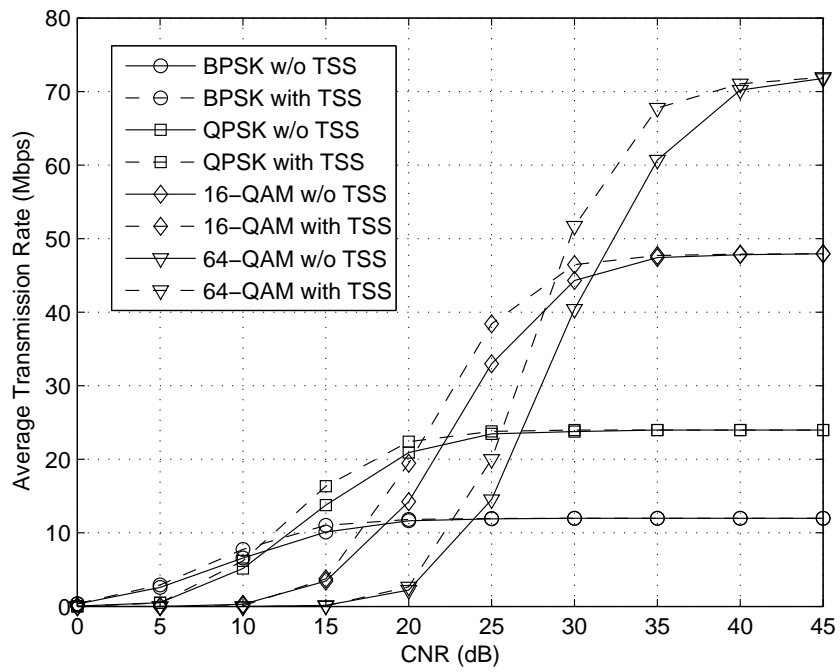


Figure 3.12: Impact of TSS on system throughput performance for 6-ray GSM Channel Model.

3.4.6 Performance of the Proposed Adaptive Modulation Scheme for 6-ray GSM Channel Model

The performance of the proposed scheme is evaluated under this correlated 6-ray GSM Channel Model. Only the receiver with the TSS is considered. Figure 3.13 shows the BER performance of the proposed scheme and the conventional scheme which is based on the CNR values only. Under this channel, again the target BER is achieved with the proposed scheme while the conventional scheme makes more errors than the target BER. The BER curves of the fixed modulation schemes are also given as a reference.

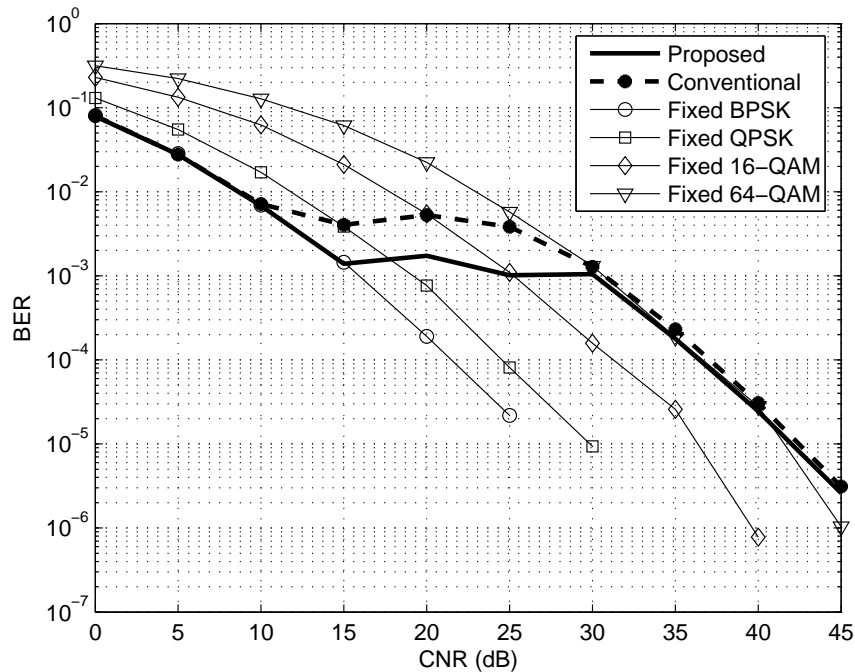


Figure 3.13: BER performance of the proposed scheme for 6-ray GSM Channel Model.

Figure 3.14 gives the average transmission rate achieved by the proposed scheme. While achieving the acceptable target BER rate, the proposed scheme gives higher transmission rate than the conventional scheme. The conventional scheme fails in successful transmission under this channel condition because of narrow angular spreads which introduce very high correlation at some subcarriers shown in Figure 3.11. On the other hand, the proposed scheme chooses the modulation schemes according to the chart in Figure 3.2 and it is more sensitive for higher correlation coefficients. For instance, for the CNR value around 24 dB, for correlated subcarriers the proposed scheme chooses 16-QAM where the conventional scheme chooses 64-QAM which is hard to transmit through the highly correlated channel. Therefore, for very highly correlated channels ($\rho[k]>0.98$), the proposed scheme overcomes the conventional scheme in terms of the transmission rate as well.

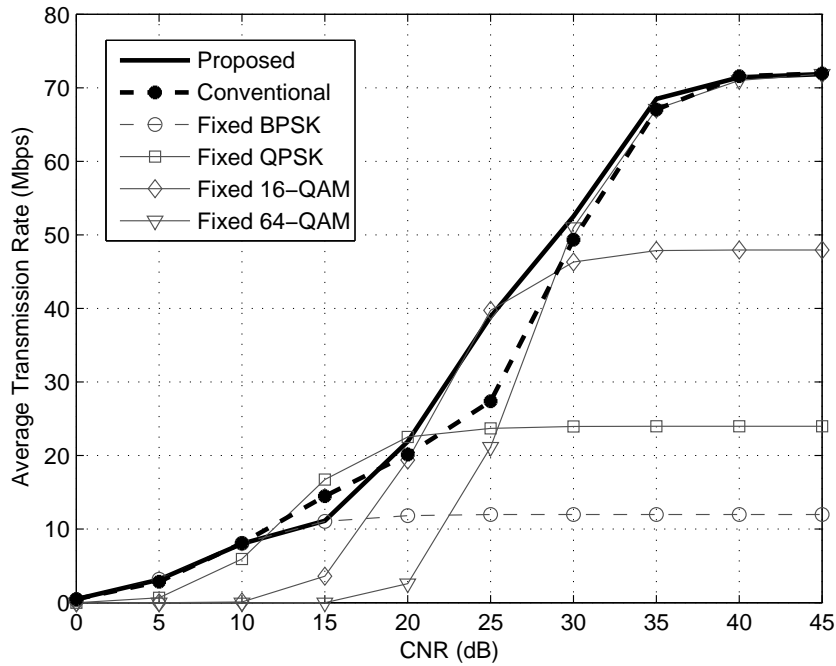


Figure 3.14: Throughput performance of the proposed scheme for 6-ray GSM Channel Model.

3.5 Effect of Error Correcting Code

To observe the effect of an error correction, error correction code is used and BER curves are calculated. A convolutional error correction code is considered with the rate $R_c = 1/2$ and the constraint length $Kc = 7$. Viterbi soft decoding is also assumed at the receiver side. Figure 3.15 shows the BER performance of the proposed scheme for the 2 path Rayleigh channel model Case-1 when the TSS is applied. For this channel condition, from Figures 3.7 and 3.8 it has been shown that the proposed scheme and the conventional scheme have almost the same transmission rate and the proposed scheme has better BER performance. By applying the error correcting code, the proposed scheme achieves more reliable communication than the conventional scheme while having very close transmission rate. The proposed scheme chooses BPSK until 15 dB, then it chooses QPSK and 16-QAM at 20 dB, 16-QAM and 64-QAM at 25 dB. On the other hand, the conventional scheme transmits QPSK and 16-QAM symbols at 15 dB, 16-QAM and 64-QAM symbols at 20 dB and these decisions result in more error. The results in Fig. 3.15 is consistent with the the uncoded results in Fig. 3.7. Hence, the throughput for the conventional scheme for coded transmission is also around 10% higher than the proposed scheme for the CNR values 15 dB and 25 dB. This is because the conventional decision chart can not optimize the throughput for a given target BER and it increases the throughput while having a high BER performance.

3.6 Discussions and Conclusion

A new decision chart for spatially correlated AOFDM systems has been proposed. In the proposed decision chart, when the antennas at the receiver end are correlated, modulation scheme is selected based on both the CNR and the correlation coefficient for each subcarrier.

In the discussions above, the feedback information of the CNR and the correlation coefficient are both long-term average values. When MRC is employed

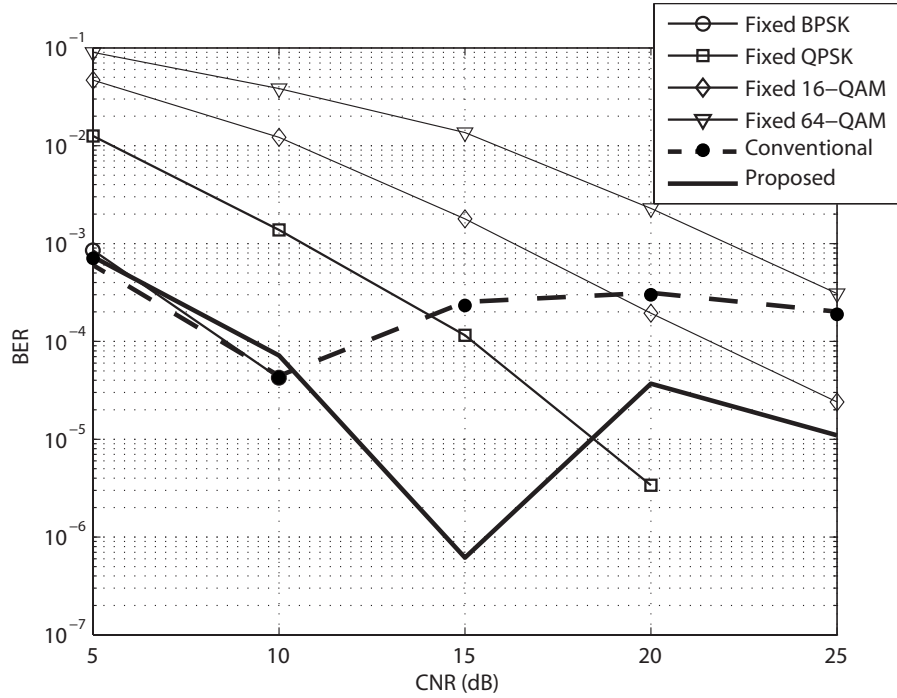


Figure 3.15: BER performance of the proposed scheme with error correcting code for 2-path Rayleigh Case-1.

at the antenna array receiver, the long-term average CNR value at the output of the MRC does not depend on the correlation coefficient. This is the main reason of why the correlation coefficient information should be sent back to the transmitter to optimize the transmission rate. If other combining schemes such as Selection Combining (SC) are used, the long-term CNR value will depend on the antenna correlation and in that case the long-term CNR information would suffice to optimize the transmission rate [3.21].

Correlation coefficient is already a long-term statistics. However, the feedback information of CNR value for each subcarrier can be an instantaneous value. The instantaneous CNR at the output of MRC is affected by the antenna correlation. Hence, if the transmitter knows the instantaneous CNR, correlation information is not needed and the conventional decision chart can optimize the transmission rate.

Figure 3.16 shows the probability density function of the CNR at the output

of MRC for different correlation coefficients. The average CNR is fixed at 20 dB and it does not depend on the correlation coefficient. As seen in Fig. 3.16 the probability of low CNR increases when the correlation increases. Therefore, in the case of available instantaneous CNR at the transmitter, modulation scheme can be selected based on the conventional modulation selection chart. However, the instantaneous feedback information can load the uplink traffic.

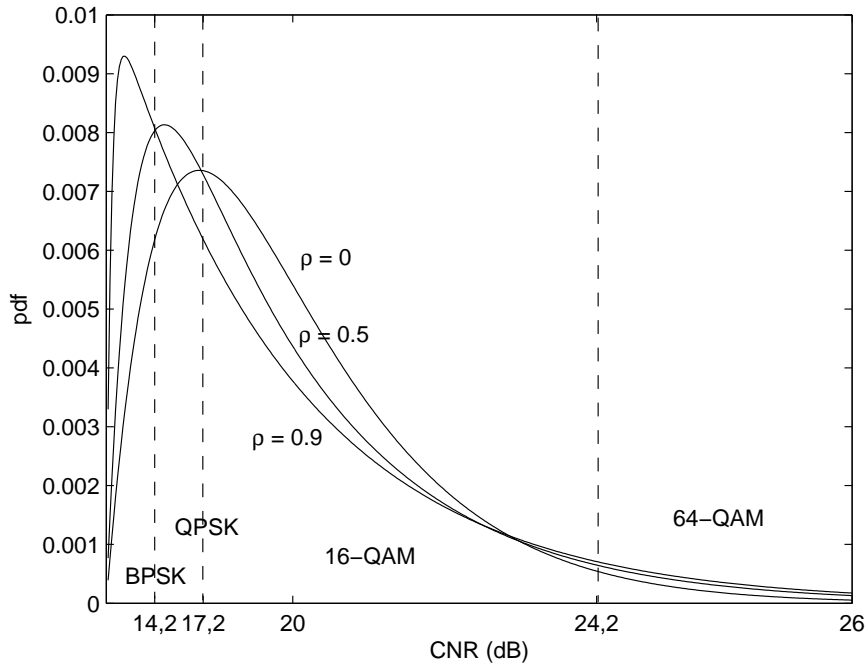


Figure 3.16: The probability distribution function of the CNR at the output of MRC combiner for different correlation coefficients. The mean of CNR is 20 dB.

In Figures 3.17 and 3.18, the proposed decision chart which is based on both long-term CNR and the correlation coefficient information is compared with the conventional decision chart based only on instantaneous CNR. Feedback period T_{fb} is taken as every 1, 6, 24 and 60 OFDM symbols. TSS is employed at the receiver. The same simulation conditions in Table 3.2 and 2-path Rayleigh channel Case-1 are considered. When the transmitter has very frequent instantaneous CNR knowledge, after each OFDM symbol $T_{fb} = 1$, both the throughput and the BER performances of the conventional decision chart is better than the proposed decision method. However, this much frequent channel knowledge at the transmitter is not feasible in real applications. In [3.22], for WiMAX the feedback

information period (T_{fb}) is defined as every 6,24, and 60 OFDM symbols. From Figures 3.17 and 3.18, it is seen that the proposed decision method outperforms the conventional scheme for T_{fb} is every 6,24 and 60 OFDM symbols. Therefore, when the antennas are correlated, even frequent CNR feedback knowledge ($T_{fb} = 6, 24, 60$) can not guarantee the optimum transmission. For optimum transmission, long-term CNR and the correlation coefficient knowledge should be fed back to the transmitter.

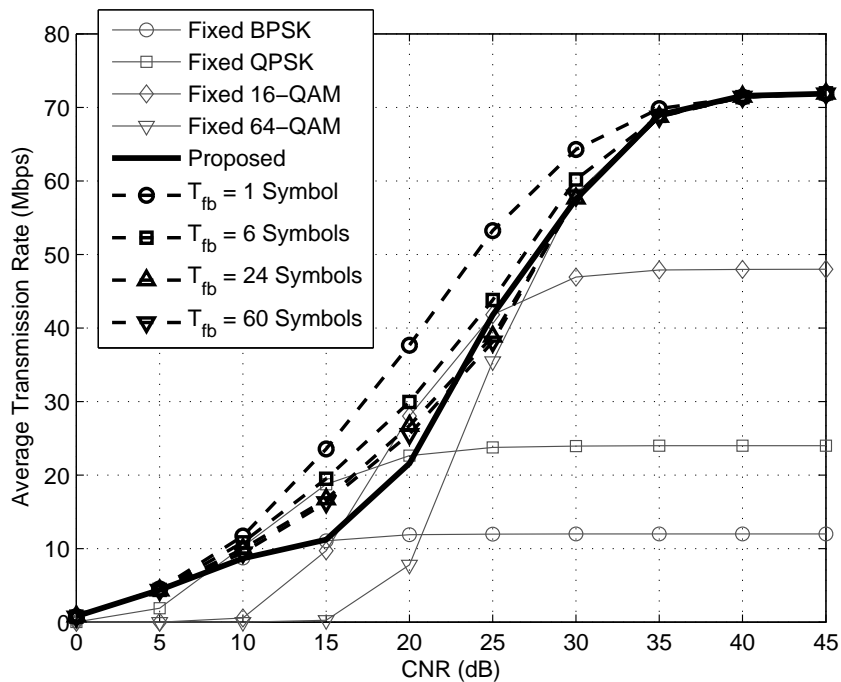


Figure 3.17: Comparison of the throughput performances of the proposed scheme based on long-term CNR and correlation information and the conventional scheme based on instantaneous channel information. 2-path Rayleigh channel Case-1 is considered.

In conclusion, a new adaptive modulation scheme for OFDM incorporating the spatial fading correlation has been proposed. The method is based on using the knowledge of antenna correlation in addition to the CNR value. In the TSS receiver, correlation coefficient changes dramatically over the subchannels. In such a condition, deciding a modulation scheme based only on the CNR value fail to achieve the target BER. Numerical results showed that by using the proposed technique, it is possible to achieve the target BER under the correlated channels

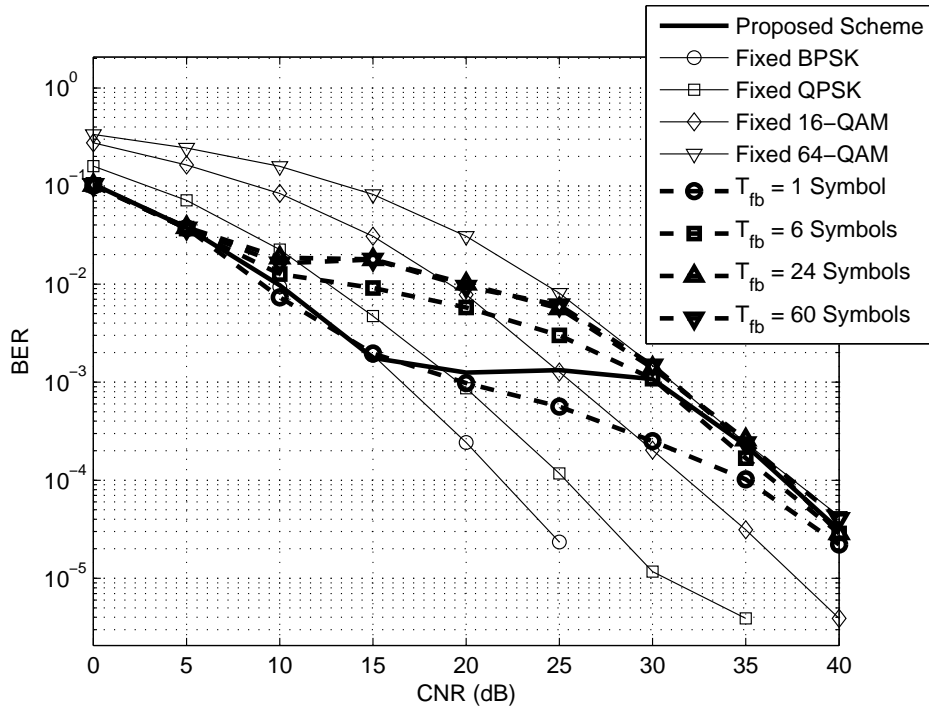


Figure 3.18: Comparison of the BER performances of the proposed scheme based on long-term CNR and correlation information and the conventional scheme based on instantaneous channel information. 2-path Rayleigh channel Case-1 is considered.

while having transmission rate comparable to existing adaptive algorithms. Only the receiver with the TSS was considered because of its resistance to correlated channels. The proposed scheme can also be applied to receiver arrays which do not employ the TSS where all the subcarriers experience almost the same correlation coefficient. In that case, the knowledge of the correlation coefficient is still important to decide the modulation scheme.

References

- [3.1] L. Cimini, "Analysis and simulation of a digital mobile channel using OFDM," *IEEE Trans. on Comm.*, vol.33, pp.665-675, July 1985.
- [3.2] J.A. C. Bingham, "Multicarrier modulation for data transmission: an idea whose time has come," *IEEE Comm. Mag.*, vol.28, pp.5-14, May, 1990.
- [3.3] H. Bolcskei, D. Gesbert, and A. J. Paulraj, "On the capacity of OFDM-based spatial multiplexing systems," *IEEE Trans. on Communications*, vol. 50, pp. 225-234, Feb 2002.
- [3.4] R. B. Ertel, P. Cardieri, K. W. Sowerby, T. S. Rappaport, J. H. Reed, "Overview of spatial channel models for antenna array communication systems," *IEEE Personal Commun.*, vol. 5, pp. 10- 21, Feb 1998.
- [3.5] W. Webb, R. Steele, "Variable rate QAM for mobile radio," *IEEE Trans. on Communications*, vol. 43, no.7, Jul. 1995, pp. 2223-2230.
- [3.6] L. Hanzo, W. Webb, "Single and multicarrier Quadrature Amplitude Modulation," Wiley-IEEE Press, 2000.
- [3.7] I H. Masuoka, S. Sampei, N. Morinaga, Y. Kamio, "Adaptive modulation system with variable coding rate concatenated code for high quality multimedia communication systems," in Proc. *IEEE Vehicular Technology Conference*, pp.815-819, Piscataway, NJ,USA, 1996.
- [3.8] T. Keller, L. Hanzo, "Adaptive orthogonal frequency division multiplexing schemes," in Proc. *ACTS Summit*, pp. 794799, June 1998.

- [3.9] A. Czylik, "Adaptive OFDM for wideband radio channels," in Proc. *IEEE Int. Global Telecom. Conference*, pp. 713718, 1996.
- [3.10] R. F. H. Fischer, J. B. Huber, "A new loading algorithm for discrete multitone transmission," in Proc. *IEEE Int. Global Telecom. Conference*, 1996.
- [3.11] C.J. Ahn, I. Sasase, "The effects of modulation combination, target BER, doppler frequency, and adaptive interval on the performance of adaptive OFDM in broadband mobile channel," *IEEE Trans. Consumer Electronics* vol. 48, no.1, pp. 167-174, Feb. 2002.
- [3.12] H. Harada, T. Yamamura, Y. Kamito, M. Fujise, "Adaptive modulated OFDM radio transmission scheme using a new channel estimation method for future broadband mobile communication systems," *IEICE Trans. Commun.* VOL.E-85B, No.12, Dec. 2002.
- [3.13] T. Keller, L. Hanzo, "Adaptive modulation techniques for duplex OFDM transmission," *IEEE Trans. Vehicular. Tech.*, vol.49, no.5 pp.1893-1906, Sep. 2000.
- [3.14] Liang-bin Li, Zong-xin Wang, "A novel spatial correlation estimation technique for MIMO communication system," *Vehicular Technology Conference*, pp. 1-5, Sept. 2006.
- [3.15] N. Czink, G. Matz, D. Seethaler, F. Hlawatsch, "Improved MMSE estimation of correlated MIMO channels using a structured correlation estimator," in Proc. *IEEE Signal Processing Advances in Wireless Communications, Workshop on* pp. 595-599, June 2005.
- [3.16] 3GPP TS 45.005 v.6.8.0 (2005-1), Radio Access Network; Radio Transmission and Reception (Release 6).
- [3.17] P. Almers, et al., "Survey of Channel and Radio Propagation Models for Wireless MIMO Systems," *EURASIP Journal on Wireless Communications and Networking*, Volume 2007, Article ID 19070.

- [3.18] K.I. Pederson, P.E. Mogensen, B.H. Fleury, "A Stochastic Model of the temporal and azimuthal dispersion seen at the base station in outdoor propagation environments," *IEEE Trans. Vehicular Technology*, vol. 49, no. 2, pp. 437-447, 2000.
- [3.19] Y. Zhang, Z. Wang, D. Li, "A simulation study on the MIMO channel capacity for small angle spread correlated fading signals," in Proc. *IEEE Int. Conf. on Communications, Circuits and Systems, ICCAS* vol. 1, pp. 158-161, 2000.
- [3.20] W.C. Jeong, J.M. Chung, "Analysis of macroscopic diversity combining of MIMO signals in mobile communications," *Int. Journal on Electron. Commun. (AEU)*, pp. 454-462, 2005.
- [3.21] Y.C. Ko, M.S. Alouini, M. K. Simon, "Average SNR of dual selection combining over correlated Nakagami-m fading channels," *IEEE Communications Letters*, vol. 4, No. 1, Jan 2000.
- [3.22] M.I. Rahman, S.S. Das, Y. Wang, F.B. Frederiksen, R. Prasad, "Link adaptation strategies for multi-antenna assisted WiMAX-like system," in Proc. *IEEE Mobile and Wireless Communications Summit* pp. 1-6, 2007.

Chapter 4

Performance Analysis of OFDM Repeater Networks with Spatial Fading Correlation

In Chapters 2 and 3, the TSS technique has been proposed for OFDM systems and applied to the AOFDM systems, respectively. In Chapter 3, a new modulation decision chart has been proposed to optimize the transmission rate when the receiver array employs the TSS. It has been shown that the TSS receiver arrays outperform the conventional receiver arrays in correlated channels; and the proposed decision chart optimizes the transmission rate when the receiver employs TSS. The discussions have been given for point-to-point communication systems.

However, the next generation wireless systems are expected to operate at higher frequency ranges which will cause high propagation losses between the terminals. In order to increase the uplink coverage while maintaining a high bit rate level, repeaters are employed in the networks. In this chapter, wireless repeater networks are analyzed when the base station antenna array is correlated. TSS technique is also applied and it is found to be effective to reduce the correlation effect and improve the system performance.

The remainder of this chapter is as follows. Section 4.1 gives the introduction. Section 4.2 describes the system model and the effect of repeating on the fading correlation. OFDM signal model is introduced in Section 4.3 and then numerical results are given in Section 4.4. Finally, conclusion is presented in Section 4.5.

4.1 Introduction

In order to increase the uplink coverage while maintaining a high bit rate level, repeaters are employed in the networks. The concept of repeater can be found in cellular systems, WLANs, and digital broadcasting systems which are based on OFDM [4.1]-[4.8].

Recently, relay network structure is in demand for similar purposes. Relaying function can be provided by another mobile terminal or by a fixed dedicated station [4.1][4.2]. The main difference between the relay networks and the networks with repeaters is that the relay station usually can not listen and transmit at the same time and needs additional scheduling algorithms, which will cost a part of the capacity. On the other hand, repeaters can be deployed on the existing networks without any prior work. However, they are expected to increase the amount of interference in the network. Some papers investigated the performance of RF repeaters in cellular systems [4.2]-[4.5]. It is expected that repeaters will enhance the cell size and it might increase the capacity for some applications [4.5].

An RF repeater receives and amplifies the signal almost at the same time. The delay between the reception and the transmission is as low as 5-6 μ sec [4.6]. In some applications, the replica of the transmitted signal may reach the destination from the direct path. Therefore, the received signal consists of the signal from the main transmitting station and the signal from the repeater, and each regarded as delayed multipath signal [4.7][4.8]. Hence, the repeater channel can be considered as an artificial multipath channel if the signal reaches the destination from both the source (direct path) and the repeater (relayed path). When

OFDM is considered, guard interval should be long enough to mitigate the inter-symbol interference due to the delay of the relayed path [4.8]. Moreover, when an antenna array is employed at the destination, delay spread channels turn into a capacity gain [4.9].

When the destination is equipped with an antenna array, spatial fading correlation causes degradation in the performance of the system. Spatial fading correlation occurs when there is an insufficient displacement between the antennas. The correlation coefficient also depends on the physical channel characteristics such as the angle of arrivals and the angular spreads of the incoming paths. For OFDM transmission, in multipath channels spatial correlation varies over subcarriers depending on the channel delay profile and the spatial correlation between each individual delayed paths. In order to overcome the degradations due to the high correlation Time Shifted Sampling (TSS) technique has been proposed in Chapter 2. In TSS receiver array, the received signals are sampled at the same rate at all antennas, however the sampling points are shifted at each antenna. TSS makes it possible to benefit from the multipath diversity and reduce the correlation between the subchannels of an OFDM symbol. This technique has been originally proposed for natural multipath channels and in this study it is applied to the multipath channels generated by the repeater.

The goal of this chapter is to analyze the performance of spatially correlated antenna array receivers when an RF repeater is added into the network. For the wireless channels without repeaters, spatial fading correlation is well studied in literature [4.10]-[4.15] and in this work, by generating a multipath channel with the aid of the repeated signal, spatial fading correlation per each subcarrier at the destination antenna array is analyzed. In the generated multipath channel, direct path's fading distribution can be modeled by one of the well known fading statistics such as Rayleigh distribution. The fading distribution on the relayed path follows the multiplicative property of two fading channels, channels from the source to the repeater ($S \rightarrow R$) and from the repeater to the destination ($R \rightarrow D$). Recently, modeling the channel as a product of fading distributions has gained interest, one study can be found in [4.15] for double-Rayleigh channels in amplify-and-forward networks. After generating the multipath channel, the

effects of repeater on the antenna correlation per subchannel and the OFDM system performance is studied for both conventional arrays and the arrays which employ TSS. In repeater networks, arriving angles of the incoming paths are governed by the positions of the repeater and the source. In this study, it is shown that for some specific positions of the repeater and the source, although the antennas are not well separated, fading correlation at the destination is low and the performance degradation is limited. For some other positions of the repeater and the source, when the antennas experience high correlation TSS technique is applied.

4.2 System Model

4.2.1 Amplify-and-Forward Repeater System

Consider the communication system in Figure 4.1. The source terminal (S) is communicating with the destination terminal (D) through the repeater station (R).

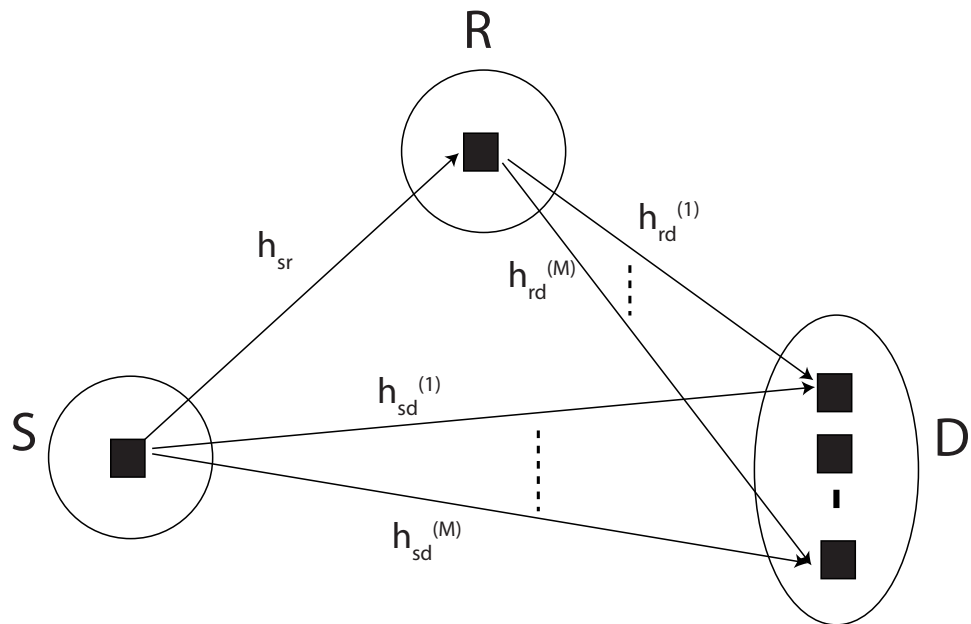


Figure 4.1: Transmission model.

If the total power consumed by the source and the repeater is constraint to ε , the received signal at the antenna m from the direct path can be written as

$$r_{d1}^{(m)} = \sqrt{\varepsilon/2}sh_{sd}^{(m)} + n_{d1}^{(m)} \quad (4.1)$$

where s is the transmitted symbol, $\varepsilon/2$ is the signal energy, $h_{sd}^{(m)}$ is the channel response between the source and the destination antenna m . $n_{d1}^{(m)}$ is the noise added at the antenna m with variance N_0 . On the direct path, the correlation between the receiver antennas m and m' depends on the correlation between the channel responses $h_{sd}^{(m)}$ and $h_{sd}^{(m')}$. Additive noises are independent at each antenna.

For the relayed path, the received signal at the terminal R is

$$r_r = \sqrt{\varepsilon/2}sh_{sr} + n_r \quad (4.2)$$

where h_{sr} is the complex channel response between S and R and n_r is the additive noise. At the repeater terminal, the received signal is then multiplied by the gain G then retransmitted to the destination with a delay of τ . At the destination antenna m , the received signal through the repeater terminal is

$$\begin{aligned} r_{d2}^{(m)} &= [\sqrt{\varepsilon/2}sh_{sr} + n_r]Gh_{rd}^{(m)} + n_{d2}^{(m)} \\ &= \sqrt{\varepsilon/2}sGh_{sr}h_{rd}^{(m)} + n_rGh_{rd}^{(m)} + n_{d2}^{(m)} \end{aligned} \quad (4.3)$$

where $h_{rd}^{(m)}$ is the channel response between the repeater and the destination, $n_{d2}^{(m)}$ is the additive noise at the destination antenna m with variance N_0 . Several different choices of the amplification gain G have been proposed in literature; such as fixed gain relaying and variable relaying. The choice of G ,

$$G^2 = \frac{(\varepsilon/2)}{(\varepsilon/2)\sigma_{h_{sr}}^2 + N_0} \quad (4.4)$$

is proposed in [4.16] in order to invert the effect of path loss while limiting the output power of the relay to $\varepsilon/2$. The gain in Eq.(4.4) is called fixed gain relaying and requires average power received by the repeater instead of instantaneous

channel knowledge for variable gain relaying [4.17]. The gain in Eq.(4.4) has been widely used in literature [4.18]-[4.21]. This gain normalizes the received signal to maintain average unit energy and then retransmits with fixed transmission power. Since, fixed gain relays are simpler to implement, our analysis assumes fixed gain amplification. If the gain is fixed, correlation between the received signals will be governed by the correlation between $h_{sr}h_{rd}^{(m)}$ and $h_{sr}h_{rd}^{(m')}$.

The delay spread channel can be constructed as the direct path be the first path component and the relayed path be the second path component. The spread of the channel is equal to the delay introduced by the RF repeater hardware and additional propagation delay. Figure 4.2 illustrates the delay profile at the adjacent antennas.

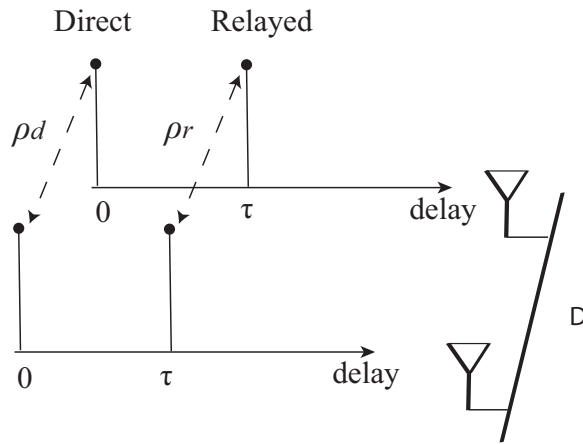


Figure 4.2: Multipath delay profile at adjacent antennas.

Let ρ_d and ρ_r be the correlation coefficients between the direct path components and the relayed path components between the adjacent antennas respectively. It is well known that the spatial fading correlation coefficient significantly depends on the physical channel characteristics such as angle of arrival (ϕ), angular spread (Δ) and antenna separation (δ). Figure 4.3 shows the cluster model with rings of scatterers for the paths from S and R. The amounts of correlations ρ_d and ρ_r will be governed by their corresponding clusters. If antennas are not well separated or the signal propagates within a small spread, the system will suffer from high correlation. Angle of arrivals will depend on the positions of S and R with respect to D.

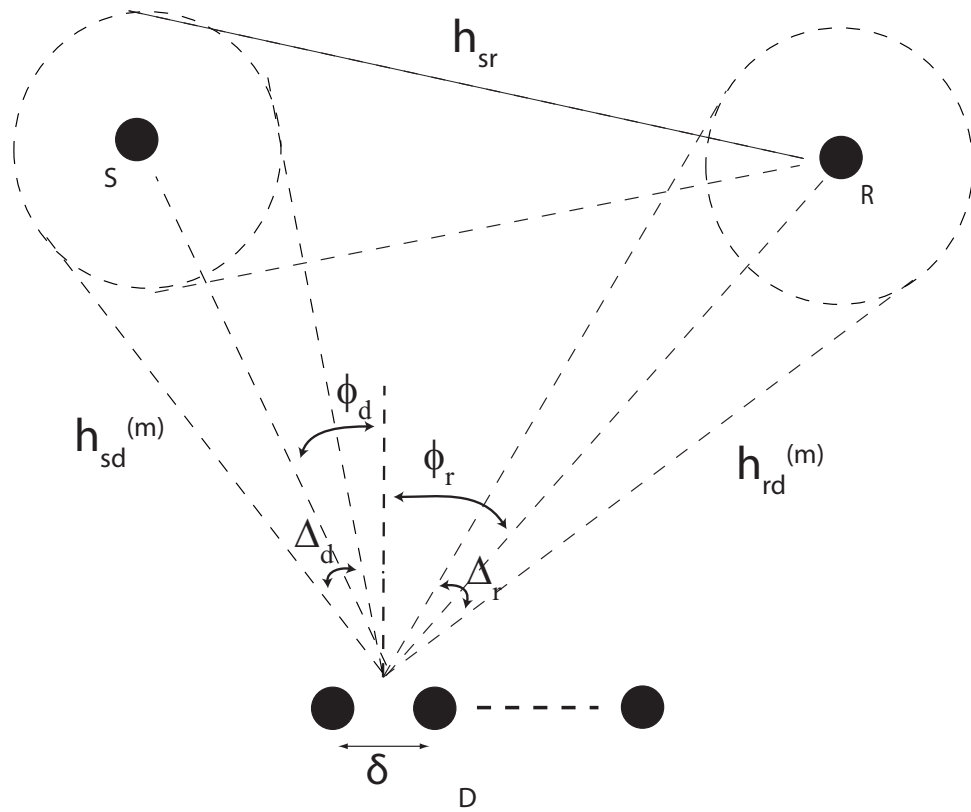


Figure 4.3: Simplified illustration of antenna separation, angular spread and angle of arrival.

4.2.2 Spatial Correlation on the Direct-Path (ρ_d)

When S is moving and D is fixed, the fading distribution is characterized by Rayleigh statistics since generally non-line-of-sight (NLOS) is expected between these terminals.

Figure 4.4 shows the correlation coefficient in magnitude (ρ_d) at the adjacent antennas for different antenna separations and angle of arrivals. Angular spread (Δ_d) is taken 10° since some measurement results indicated that when the base station is placed over the rooftop level, angular spread is usually around 10° [4.22]. In order to generate a set of correlated fading waveforms, the method in [4.13] is followed which is the extension of Jakes' ring model [4.23] for antenna arrays.

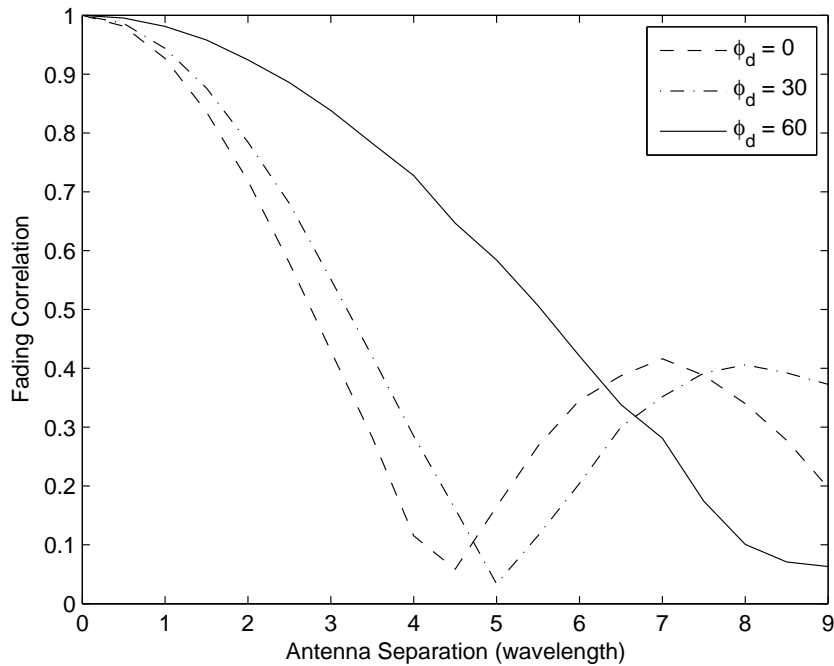


Figure 4.4: Spatial fading correlation coefficient (ρ_d) between the antennas for the direct path.

4.2.3 Spatial Correlation on the Relayed-Path (ρ_r)

In fixed gain relaying, the fading experienced by the received signal at the repeater is transferred to the relayed path. Fading statistics for the channel S→R follow Rayleigh distribution since NLOS is expected between these terminals. On the other hand, the terminals R and D are fixed and there will be a strong LOS path, which is modeled as Ricean distribution. Previous studies have shown that Ricean K -factors for fixed links are significantly higher than those in mobile channels [4.24]. Reported values for the K -factor in fixed wireless links can exceed 20 dB [4.25]. Therefore, end-to-end channel fading distribution at the destination antenna is the product of independent Rayleigh and Ricean distributions. Spatial correlation (ρ_r) between the product of Rayleigh and Rice channels at the adjacent antennas is expected to be very high due to the strong LOS.

The spatial correlations ρ_d and ρ_r are the correlation coefficients between the fading envelopes at different antennas. For OFDM systems, combining is usually done in the frequency domain. Hence, the correlation between the different sub-channels in frequency domain should be considered which is a subject of sampling points and the FFT property at the demodulators. Sections 3 and 4 investigate the spatial correlation in the frequency domain in more detail.

4.3 Signal Model

Suppose the OFDM symbol is transmitted and the information symbol on the k^{th} subcarrier is $s[k]$ ($k = 0, 1, \dots, N - 1$). Then OFDM symbol is the IDFT of the information symbols

$$u[n] = \frac{1}{N} \sum_{k=0}^{N-1} s[k] e^{j2\pi nk/N} \quad (4.5)$$

where n ($n = 0, 1, \dots, N - 1$) is the time index and N is the IDFT length. The baseband signal at the output of the filter is given by $x(t) = \sum_{n=0}^{P-1} u[n] p(t - nT_s)$ where $p(t)$ is the impulse response of the pulse shaping filter, T_s is the symbol duration and P is the sum of the IDFT length and the length of cyclic prefix.

Then this signal is transmitted over artificial multi-path channel to the destination antenna m with impulse responses $c_m(t)$. The received signals by each antenna m then become

$$y_m(t) = \sum_{n=0}^{P-1} u[n]h_m(t - nT_s) + v_m(t) \quad (4.6)$$

where $h_m(t)$ is the impulse response of the channel seen by antenna m and is given by $h_m(t) = p(t) \star c_m(t) \star p(-t)$, \star denotes convolution. $v_m(t)$ is the total additive white Gaussian noise at the receiver m including the noise forwarded from repeater. $h_m(t)$ can be expressed in a baseband form as

$$h_m(t) = \sum_{\ell=0}^{L-1} \alpha_{m,\ell} p_2(t - \tau_\ell). \quad (4.7)$$

$p_2(t) = \int p(t')p(t+t')dt'$ is the auto correlation of $p(t)$, L is the number of path components, $\alpha_{m,\ell}$ is the complex gains of the ℓ^{th} component at the m^{th} antenna and τ_ℓ is the path delay. In this work, channels h_{sr} , h_{rd} and h_{sd} are assumed frequency flat channels, so that $L = 2$, $\alpha_{m,0} = h_{sd}^{(m)}$ and $\alpha_{m,1} = Gh_{sr}h_{rd}^{(m)}$. The notation of $\alpha_{m,\ell}$ is used in this Section for a general case regardless of the fading distributions.

In TSS receiver, the signal is sampled at the baud rate of $1/T_s$ with a delay of $(m-1)T_s/M$ at antenna m over total of M antennas. The received signals in the discrete-time are expressed as

$$y_m[n] = \sum_{l=0}^{P-1} u[l]h_m[n-l] + v_m[n] \quad (4.8)$$

where $y_m[n] = y_m(nT_s + (m-1)T_s/M)$, $h_m[n] = h_m(nT_s + (m-1)T_s/M)$, $v_m[n] = v_m(nT_s + (m-1)T_s/M)$. At each antenna, noise samples are still independent and white. However the fading correlation between any antenna elements m and m' , $h_m[n]$ and $h_{m'}[n]$ is reduced. Channel gains in discrete-time at each antenna are given by

$$h_m[n] = \sum_{\ell=0}^{L-1} \alpha_{m,\ell} p_2(nT_s + (m-1)T_s/M - \tau_\ell). \quad (4.9)$$

By taking the DFT of Eq.(4.9), the channel gains for each subcarrier in frequency domain are

$$H_m[k] = \sum_{n=0}^{N-1} e^{-j2\pi nk/N} \sum_{\ell=0}^{L-1} \alpha_{m,\ell} p_2(nT_s + (m-1)T_s/M - \tau_\ell) \quad (4.10)$$

where N is the DFT size.

The basic input-output relationship in OFDM-antenna array systems is

$$\mathbf{z}[k] = \mathbf{H}[k]s[k] + \mathbf{w}[k] \quad (4.11)$$

where $\mathbf{z}[k]$, $\mathbf{H}[k]$ and $\mathbf{w}[k]$ are the $M \times 1$ column vectors of the received symbols, the channel gains and the Gaussian noises at each subcarrier, respectively. Then the estimate of $s[k]$ through MRC combining is

$$\check{s}[k] = \frac{\check{\mathbf{H}}^H[k]\mathbf{z}[k]}{\check{\mathbf{H}}^H[k]\check{\mathbf{H}}[k]} \quad (4.12)$$

where $\check{\mathbf{H}}[k]$ is the estimated $M \times 1$ channel column vector. Since MRC is employed in the frequency domain, the correlation coefficient is also derived in the frequency domain. Spatial correlation between any antenna elements m, m' can be written as

$$\rho[k]_{m,m'} = \frac{\text{Cov}[H_m[k]H_{m'}[k]^*]}{\sqrt{\text{E}[|H_m[k]|^2]\text{E}[|H_{m'}[k]|^2]}} \quad (4.13)$$

where $\text{Cov}[\cdot]$ is the covariance operator. The covariance at the numerator of Eq.(4.13) can be further expressed in terms of covariances of the individual path components as

$$\begin{aligned} \text{Cov}[H_m[k]H_{m'}[k]^*] = & \sum_{n_1=0}^{N-1} \sum_{n_2=0}^{N-1} e^{-j2\pi k(n_2-n_1)/N} \sum_{\ell=0}^{L-1} p_2(n_1T_s + (m-1)T_s/M - \tau_\ell) \\ & p_2(n_2T_s + (m-1)T_s/M - \tau_\ell) \text{Cov}(\alpha_{m,\ell}, \alpha_{m',\ell}^*). \end{aligned} \quad (4.14)$$

$\text{Cov}[\alpha_{m,\ell}, \alpha_{m',\ell}^*]$ is the product of correlation between the same path components and the variance of the fading waveform; $\text{Cov}[\alpha_{m,\ell}, \alpha_{m',\ell}^*] = \rho_\ell \sigma_\ell^2$. Therefore,

correlation per subcarrier is a function of the delay of the paths, channel gains of each path and antenna correlation for each path.

4.4 Numerical Results

The computer simulations are run to observe the effect of repeater on the spatial correlation at the destination antenna array. The OFDM parameters are listed in Table 4.1. Number of antennas at the receiver site is 2. Maximum Doppler frequency is 100Hz for all channels. The delay added by the repeater is taken as $5.5 \mu\text{sec}$ which is equal to $62.5T_s$ [4.6][4.8]. Fading statistics for the channels S→R and S→D follow Rayleigh distribution and the channel R→D follows Rician distribution as explained in Sections 4.2.2 and 4.2.3. Normalizing the path-loss in S→D to be unity $\sum_m |h_{sd}^{(m)}|^2=1$, the relative channel powers of the S→R and R→D links are $|h_{sr}|^2=(d_{sd}/d_{sr})^\eta$ and $\sum_m |h_{rd}^{(m)}|^2=(d_{sd}/d_{rd})^\eta$. The propagation exponent η is 4. All the channels are flat and constant during one OFDM symbol. Noise variances at the destination and the repeater are the same.

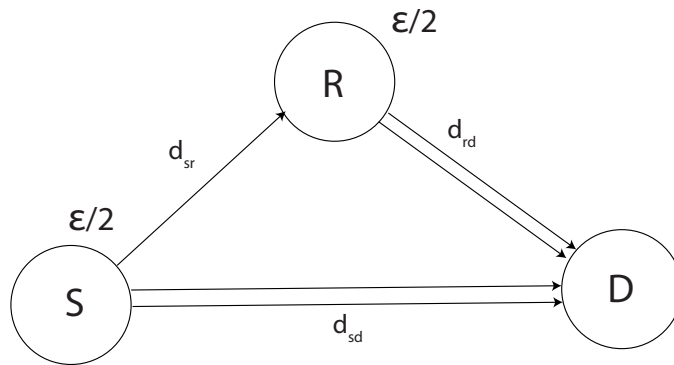
Table 4.1: OFDM Parameters

Modulation	QPSK
FFT size	1024
Number of subcarriers	1024
Sampling Frequency ($1/T_s$)	11.24 MHz
OFDM Symbol Duration	91.13 μsec
Guard Interval	1/8 (11.39 μsec)
Channel Estimation	ideal
$p_2(t)$	Truncated Sinc
Combining Scheme	MRC

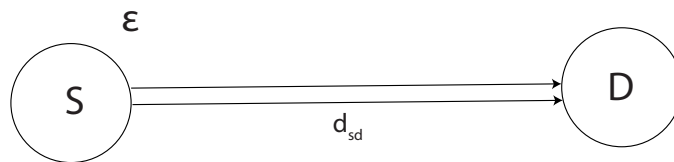
4.4.1 Impact of the Repeater

First set of simulations is run to observe the performance of the correlated channels with the repeater. The results are compared with the singlehop reference

channel where the source communicates with the destination directly over a frequency flat channel from a distance of d_{sd} . The total consumed powers are constraint to ε in the reference channel and the channel with the repeater. Figure 4.5 illustrates the channel models. For the simulations, angle of arrivals, angular spreads, antenna separation and the K -factor for the Rice channel are given in Table 4.2.



(a) Repeater Channel



(b) Singlehop Reference Channel

Figure 4.5: Wireless repeater channel and singlehop reference channel models. Double lines indicate multi-antenna channel links.

Azimuth of the signal from Source ϕ_d	60°
Azimuth of the signal from Repeater ϕ_r	0°
K -factor	20 dB
Antenna Separation δ	1λ
Angular Spread of Direct path Δ_d	10°
Angular Spread of Relayed path Δ_r	10°

Figure 4.6 shows the BER performances for the reference channel and the repeater channel. BER results are given versus total received E_b/N_0 in the singlehop reference channel. The probability of error results for the repeater channel are plotted such that the E_b/N_0 in the direct path (S→D) is half of the E_b/N_0 in the singlehop reference channel due to the power constraints. For the parameters in Table 4.2, in the singlehop channel, the correlation between the antenna elements is 0.97 ($\phi_d = 60^\circ$, $\delta = 1\lambda$, $\Delta_d = 10^\circ$) and the BER performance is given in Figure 4.6. 2-branch independent channel performance is also given as a reference.

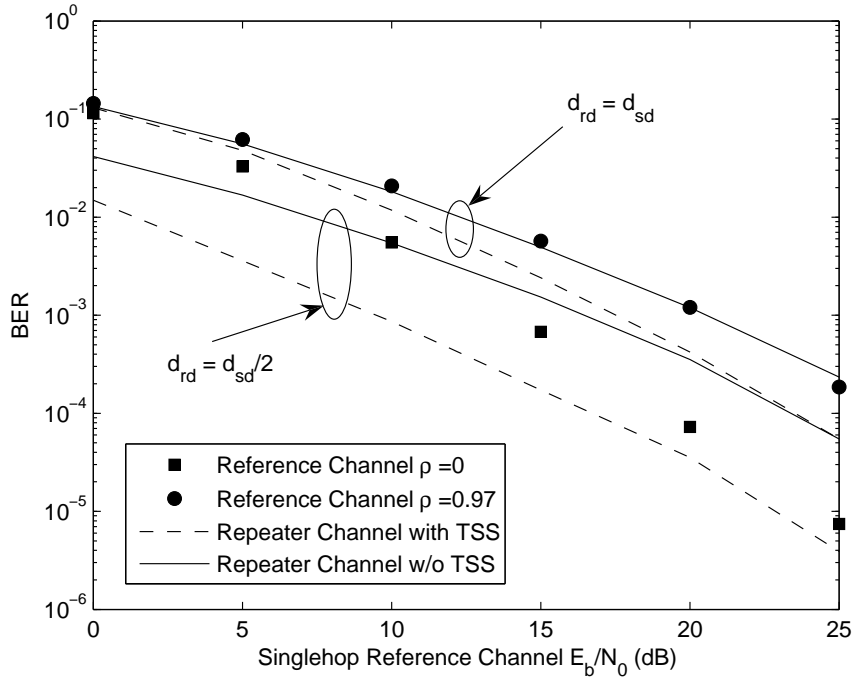


Figure 4.6: BER performance improvement with TSS for repeater wireless channel.

When an RF repeater is added to the network ($\phi_r=0^\circ$) at a distance equal to the distance between the source and the destination ($d_{rd}=d_{sd}$) as in Figure 4.7(a), almost the same BER performance as the transmission in the reference channel is obtained. The performance gain is observed when the destination employs TSS. The improvement with TSS can be explained with the spatial correlations per each subchannels of the OFDM symbol. In Figure 4.8, for the conventional arrays correlation is high for all subchannels and when TSS is applied it is reduced partially for some subchannels which turns into a performance improvement. Note that when d_{rd} is equal to d_{sd} , with the gain in Eq.(4.4) path energies from the repeater and the source are equal. Distance between the source and the repeater d_{sr} will affect the SNR transferred to the destination.

Repeaters gain significance when they are placed closer to the destination. When the repeater terminal is placed at $d_{rd}=d_{sd}/2$ as in Figure 4.7(b), BER performance improves significantly for the conventional arrays due to the SNR increase on the relayed path. High signal energy on the relayed path also increases

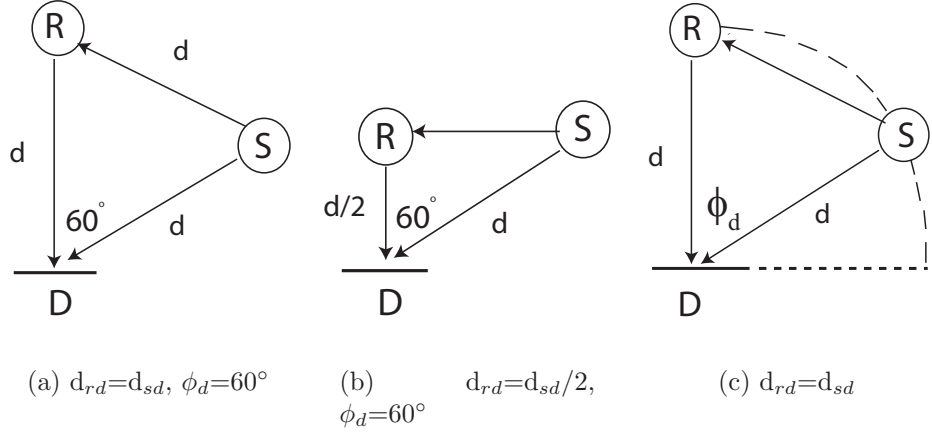


Figure 4.7: Different placements of the repeater and the source.

the correlation per subchannel as in Figure 4.8 since the relayed path is highly correlated. When TSS is applied, in addition to the gain from reducing the correlation, shifting the sampling points at one antenna gathers more energy from the relayed path which provides additional gain.

In Figure 4.8 when TSS is employed correlation is mostly reduced around $k = \mp N/2$. For conventional arrays, channel responses for each subcarrier are

$$H_1[k] = h_{sd}^{(1)} + h_{sr}h_{rd}^{(1)}p_2(-T_s/2) + e^{-j2\pi k/N}h_{sr}h_{rd}^{(1)}p_2(T_s/2) \quad (4.15)$$

$$H_2[k] = h_{sd}^{(2)} + h_{sr}h_{rd}^{(2)}p_2(-T_s/2) + e^{-j2\pi k/N}h_{sr}h_{rd}^{(2)}p_2(T_s/2). \quad (4.16)$$

When $k = \mp N/2$, $H_1[N/2] = h_{sd}^{(1)}$ and $H_2[N/2] = h_{sd}^{(2)}$. Therefore, correlation at $k = \mp N/2$ is equal to the correlation between the first path components (ρ_d) which is 0.97. With TSS, the frequency responses are

$$H_1[k] = h_{sd}^{(1)} + h_{sr}h_{rd}^{(1)}p_2(-T_s/2) + e^{-j2\pi k/N}h_{sr}h_{rd}^{(1)}p_2(T_s/2) \quad (4.17)$$

$$H_2[k] = e^{j2\pi k/N}h_{sd}^{(2)}p_2(-T_s/2) + h_{sd}^{(2)}p_2(T_s/2) + h_{sr}h_{rd}^{(2)}. \quad (4.18)$$

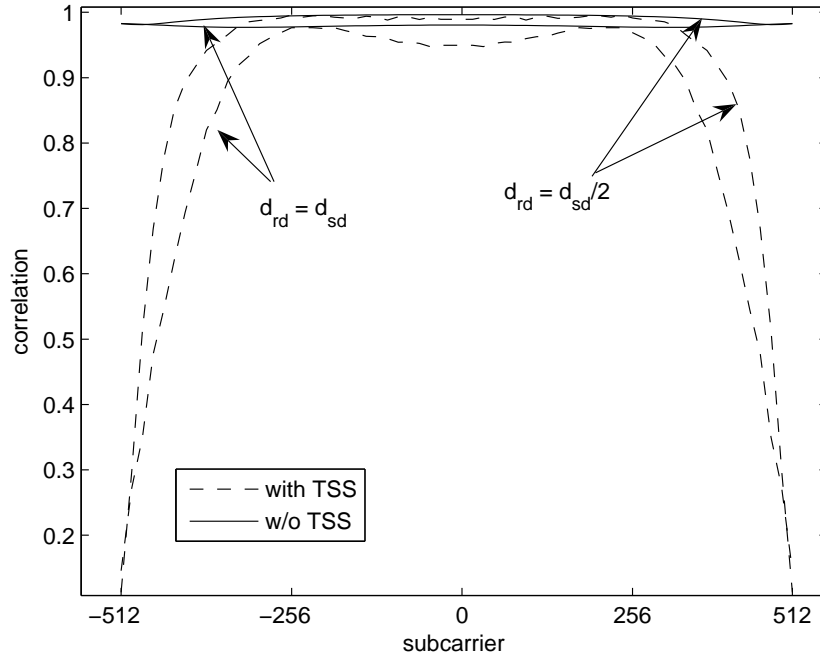


Figure 4.8: Spatial fading correlation between the subcarriers for repeater wireless channel.

When $k = \mp N/2$, $H_1[N/2] = h_{sd}^{(1)}$ and $H_2[N/2] = h_{sr}h_{rd}^{(2)}$. The spatial correlation at $k = \mp N/2$ is equal to the correlation between $h_{sd}^{(1)}$ and $h_{sr}h_{rd}^{(2)}$ which are independent.

Figure 4.9 shows the BER performance of the system for different transmission powers in terms of ϵ for the source and the repeater terminals. The repeater and the source terminals are placed as in Figure 4.7(a). Noise power at the repeater and the destination terminals are the same. Noise power is fixed at when E_b/N_0 for the singlehop reference channel is 10 dB for the transmission power ϵ . It is seen that the performance of both conventional receiver and the receiver with TSS is more sensitive to the transmission power of the source terminal. It is because the transmission power of the source both affects the received powers at the destination and the repeater terminals. Therefore, when the source transmission power increases, the repeater receives higher SNR signal and then transmits to the destination with its transmission power. The receiver which employs TSS outperforms the conventional array for most of the transmission power

distributions. When both the transmission powers of the repeater and the source are weak, the TSS receiver makes more error than the conventional one. This result is expected since that time the received SNR from both paths are very low. The SNR on the second path is more significant for TSS and it can be seen in the Figure 4.9 that when the transmission power of the repeater increases the performance of the TSS receiver improves.

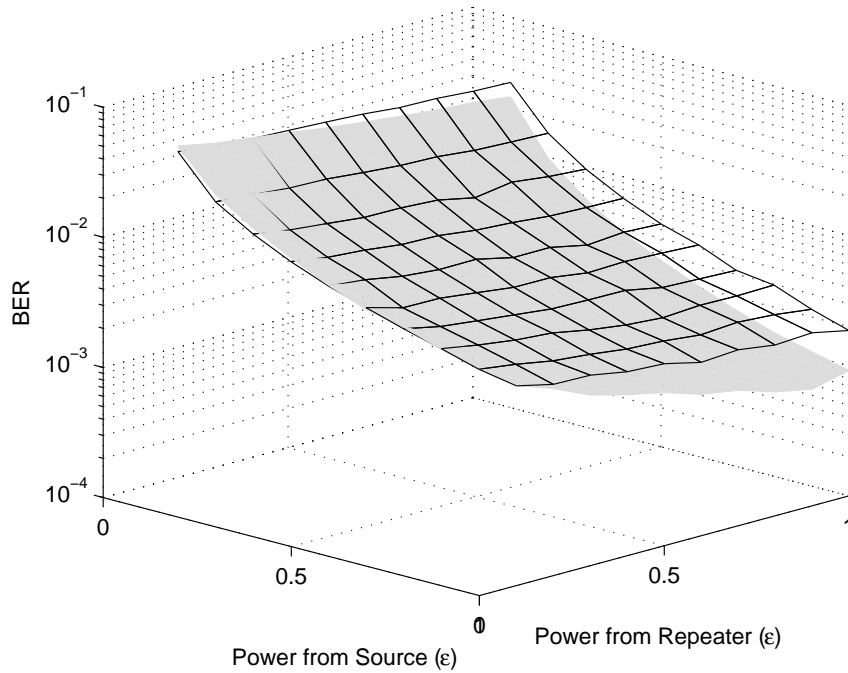


Figure 4.9: BER performance improvement with TSS for different transmission powers in terms of ϵ for the source and the repeater terminals. The gray surface is the performance for the TSS receiver. The black grid is the performance for the conventional receiver.

4.4.2 Impact of Location of the Source

The second set of simulations is run to observe the effect of the source location on the spatial correlation at the destination array. The source terminal is placed at different locations, 30° and 60° and the repeater terminal is placed at 0° , $\phi_r = 0^\circ$ as in Figure 4.7(c). It is assumed that for every location of the source, all terminals are in the range to establish a link so that the network topology does

not change. Indeed, changing the repeater location will not affect the correlation coefficient on the relayed path (ρ_r) since the received Rayleigh waveforms are transferred via the strong LOS components to the receiver antenna array which causes very high correlation on the relayed path. Figures 4.10 and 4.11 show the BER performances and the spatial correlation for each subcarrier for different source locations, respectively. Under these cluster models, the special case occurs when the source terminal is at 30° . For this case, the spatial correlation for some subchannels are already low for conventional arrays and when the TSS technique is applied the spatial correlation is found to be very low for all subchannels. The frequency responses of the channels when the TSS is applied were given in Eqs.(17) and (18).

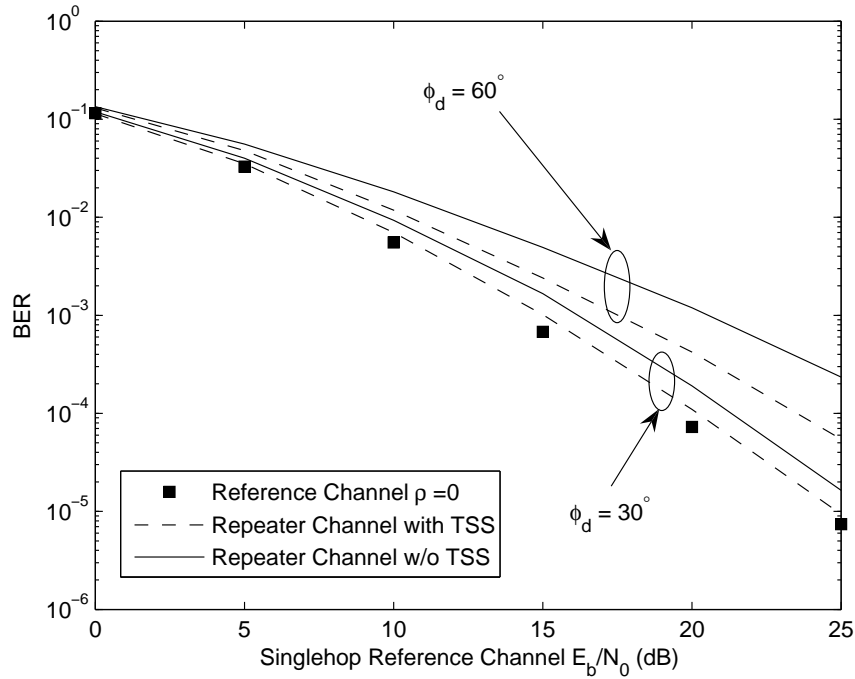


Figure 4.10: BER performance improvement with TSS for repeater wireless channel.

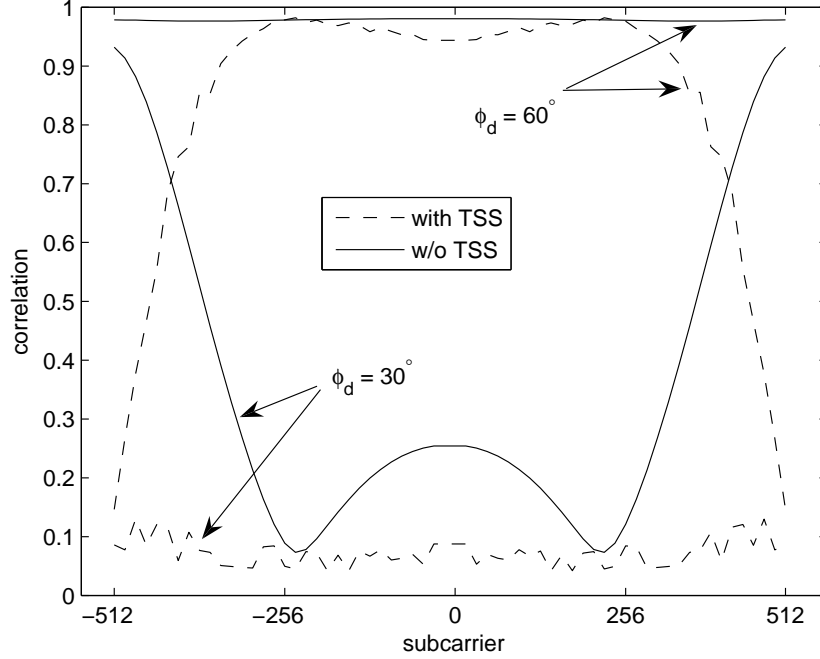


Figure 4.11: Spatial fading correlation between the subcarriers for repeater wireless channel.

The covariance between $H_1[k]$ and $H_2[k]$ becomes

$$\begin{aligned} \text{Cov}[H_1[k]H_2[k]^*] &= (e^{j2\pi k/N}p_2(-T_s/2) + p_2(T_s/2))\text{Cov}[h_{sd}^{(1)}, h_{sd}^{*(2)}] \\ &+ (p_2(-T_s/2) + p_2(T_s/2)e^{j2\pi k/N})\text{Cov}[h_{sr}h_{rd}^{(1)}, h_{sr}^*h_{rd}^{*(2)}]. \end{aligned} \quad (4.19)$$

Covariances of the independent pairs such as $\text{Cov}[h_{sd}^{(m)}, h_{sr}^*h_{rd}^{*(m')}]$ are neglected. When $\phi_r = 0^\circ$ and $\phi_d = 30^\circ$, $\text{Cov}[h_{sd}^{(1)}, h_{sd}^{*(2)}]$ and $\text{Cov}[h_{sr}h_{rd}^{(1)}, h_{sr}^*h_{rd}^{*(2)}]$ have almost the same value but with opposite signs. In other words, from the direct path antennas are negatively correlated and from the relayed path antennas are positively correlated. Hence, for any subcarrier $\text{Cov}[H_1[k]H_2[k]^*]$ is found to be very low. The effect of low correlation when $\phi_d = 30^\circ$ can be observed in BER performance in Figure 4.10. It is known that with the correlation value less than 0.7, system performs very close to the independent 2-branch receiver performance [4.26]. When TSS technique is applied, performance improvement is observed for any location of the source.

Figure 4.12 shows the spatial correlation on the adjacent antennas for the subcarriers $k=0, \pm N/4$ and $\pm N/2$ for different source locations when the repeater is placed at $\phi_r = 0^\circ$. The spatial fading correlation for the subcarrier $k=\pm N/2$ is found to be high for any source locations. When TSS is applied, the correlation is lowered for all locations of the source. For the subcarrier $k=\pm N/4$ the spatial correlation remains the same for both conventional arrays and arrays with TSS. Moreover, the correlation is found to be the lowest around $\phi_d=30^\circ$. Spatial fading correlation on the subcarrier $k=0$ can be lowered by the TSS technique and the amount of reduction is more for the source location ϕ_d between 20° and 30° .

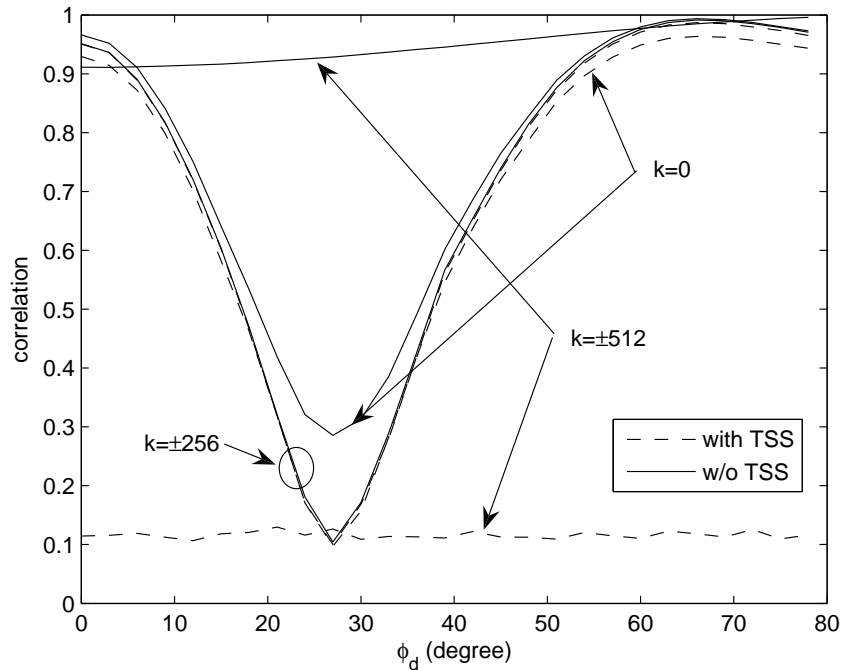


Figure 4.12: Spatial fading correlations for subcarriers $k=0, \pm N/4$ and $\pm N/2$ vs. different source locations.

4.5 Conclusion

The spatial fading correlation has been analyzed for the OFDM diversity receivers in wireless channels with an RF repeater. A multipath channel is constructed with the aid of repeated signal and the spatial correlation between the subchannels of

an OFDM symbol is studied. It is observed that depending on the source location spatial correlation can be partially low for conventional diversity receivers and can be further reduced by the Time Shifted Sampling technique. It is shown that the TSS technique can provide performance enhancement under correlated channels when the network includes an RF repeater.

References

- [4.1] R. Raulefs, A. Damman, “Repeating or relaying in wireless systems,” *in Proc. IEEE Wireless Communications and Networking Conference*, pp. 506-510, 2008.
- [4.2] M. Qingyu, A. Osseiran, “Performance comparison between DF relay and RF Repeaters in the cellular system,” *in Proc. IEEE Vehicular Tech. Conference*, pp. 2021 - 2025, May. 2008.
- [4.3] K. Hiltunen, “Using RF repeaters to improve WCDMA speech coverage and capacity inside buildings,” *in Proc. IEEE Vehicular Tech. Conference*, pp. 1-5, Sep. 2006.
- [4.4] M. N. Patwary, P. B. Rapajic, I. Oppermann, , “Capacity and coverage increase with repeaters in UMTS urban cellular mobile communication environment,” *IEEE Transactions on Communications*, Vol.53, No. 10, October 2005.
- [4.5] W. Choi, B.Y. Cho, T.W. Ban, “Automatic on-off switch repeater for DS/CDMA reverse link capacity improvement,” *IEEE Commun. Lett.*, vol. 4, no. 5, pp. 138-141, Apr. 2001.
- [4.6] “UTRA Repeater: Planning guidelines and system analysis,” *3GPP TR 25.956*
- [4.7] S.W. Choi, H.J. Hong , “A Study on the interference in single frequency network and On-Channel Repeater,” *Progress In Electromagnetics Research Symposium*, Cambridge, USA 2008

- [4.8] “Repeater issues for MBWA,” *IEEE 802.20 working group on mobile broadband wireless Access*
- [4.9] H. Bolcskei, D. Gesbert, A. J. Paulraj, “On the capacity of OFDM-based spatial multiplexing systems,” *IEEE Trans. on Communications*, vol. 50, pp. 225-234, Feb 2002.
- [4.10] D. Shiu, G. J. Foschini, M. J. Gans, J. M. Kahn, “Fading correlation and its effect on the capacity of multielement antenna system,” *IEEE Trans. on Communications*, vol. 48, pp. 502-5133, March 2000.
- [4.11] J. Salz, J. H. Winters, “Effect of fading correlation on adaptive arrays in digital mobile radio,” *IEEE Trans. Vehicular Technology*, vol. 43, N. 4, pp. 1049-1057, Nov. 1994.
- [4.12] G. J. Foschini, M. J. Gans, “On limits of wireless communication in a fading environment when using multiple antennas,” *Wireless Personal Commun.*, vol. 6, no. 3, pp. 311-335, Mar. 1998.
- [4.13] T. L. Fulghum, K. J. Molnar, A. Duel-Hallen, “Jakes fading model for antenna arrays incorporating azimuth spread,” *IEEE Trans. Vehicular Technology*, vol. 51, N. 5, Sep. 2002.
- [4.14] R. B. Ertel, P. Cardieri, K. W. Sowerby, T. S. Rappaport, J. H. Reed, “Overview of spatial channel models for antenna array communication systems,” *IEEE Personal Commun.*, vol. 5, pp. 10- 21, Feb 1998.
- [4.15] C.S. Patel, G. L. Stuber, T. G. Pratt, “Statistical properties of amplify and forward relay fading channels,” *IEEE Trans. on Vehicular Tech.*, vol. 55, no. 1, pp. 1-9, Jan. 2006.
- [4.16] R.U Nabar, H. Boelcskei, F.W. Knueubhueler, “Fading relay channels: Performance limits and space-time signal design,” *IEEE J. Sel. Areas Commun.*, vol. 22, No. 6, pp. 1099-1100, 2000.
- [4.17] J.N. Lenaman, D. Tse, G.W. Wornell, “Cooperative diversity in wireless networks: Efficient protocols and outage behavior,” *IEEE Trans. on Information Theory*, vol. 40, No. 12, pp. 3062-3080, 2004.

- [4.18] B. Gedik, M. Uysal, "Two channel estimation methods for Amplify-and-Forward relay networks," *in Proc. Canadian Conference on Electrical and Computer Engineering* pp. 615-618, 2008.
- [4.19] S.A.Fares, F.Adachi, E.Kudoh, "A novel cooperative relaying network scheme with inter-relay data exchange," *IEICE Trans. Commun.*, vol. E92-B, No. 5, pp. 1786-1795, 2009.
- [4.20] M. Hasna, M.S. Alouini "A performance study of dual-hop transmissions with fixed gain relays," *IEEE Trans. Wireless Comm.*, vol. 3, No. 6, pp. 1963-1968, 2004.
- [4.21] M. Hasna, M.S. Alouini "End-to-end performance of transmission systems with relays over Rayleigh fading channels," *IEEE Trans. Wireless Comm.*, vol. 2, No. 6, pp. 1126-1131, 2003.
- [4.22] P. Pajusco, " Experimental characterization of DOA at the base station in rural and urban area ," *in Proc. IEEE Vehicular Technology Conference VTC 2003 Spring*, pp. 993 - 997, vol.2 , May 1998.
- [4.23] W. C. Jakes "Microwave mobile communications," New York: Wiley, pp. 60-65, 1974.
- [4.24] L. J. Greenstein, S. Ghassemzadeh, V. Erceg, D. G. Michelson, "Ricean K-factors in narrowband fixed wireless channels," *in Proc. Int. Conf. Wireless Personal Multimedia Commun.*, Sept. 1999.
- [4.25] L. Ahumada, R. Feick, R. A. Valenzuela, C. Morales, "Measurement and characterization of the temporal behavior of fixed wireless links," *IEEE Trans. Vehicular Tech.*, vol. 54, pp. 13913-1922, Nov. 2005.
- [4.26] L. Fang, B. Guoan, A.C. Kot, "New method of performance analysis for diversity reception with correlated Rayleigh-fading signals," *IEEE Trans. on Vehicular Technology*, vol. 49, pp. 1807-1812, No. 5, September 2000.

Chapter 5

Conclusions

Future wireless systems are expecting to use OFDM as an air-interface technology combined with multi-antennas employed at both transmitter and receiver ends. It has been shown that multi-antenna systems significantly improve the performance of transmission in terms of higher capacity with the same power consumption and in a reasonable bandwidth. However, the primary problem of the antenna array communications is that the performance of the diversity receiver heavily depends on the fading correlation between different branches. In order to have low correlation, antenna elements should be well separated (a few times the transmission length) and the wireless channel should be rich in scattering. In some cases, although the antennas are sufficiently separated, signal may reach the array within very small angular spread because of the poor scattering environment which introduces high correlation. This case is likely to happen at the base station array, since the base station is usually placed on high vantage and very far from the mobile. The problem is not so severe for mobile devices since they are usually surrounded by scatterers. Therefore, the spatial fading correlation stands as a significant challenge in antenna array communications and determines the motivation of this dissertation. The goal of this work is to combat the degradations in the performance due to the spatial fading correlation in OFDM antenna array receivers for future wireless systems.

Time Shifted Sampling (TSS) as a novel signal processing technique has been

proposed in Chapter 2 in order to reduce the effects of high spatial correlation at the receiver array. TSS has been proposed for OFDM systems and based on the multipath diversity. In multipath channels, although the same channel taps are correlated at the adjacent antennas, between the different taps correlation is still low (for instance; the first path component at one branch and the second path component at another branch). Based on this fact, in Time Shifting Sampling receiver, during analog-to-digital conversion every branch samples the received signal at different time instants. Whereas the sampling rate is kept the same for all branches. Therefore, every branch gathers less correlated signal samples from different multipath components. Since, the combining is usually employed in frequency domain for OFDM systems, when these digital samples are Fourier transformed into frequency domain, the correlation is found to be low for some subcarriers.

Even small reduction in correlation coefficient gives performance improvement. The relationship between the correlation coefficient and the BER performance is not linear. For instance, the BER performance difference is not much for correlation coefficients 0.7 and 0.8. On the other hand, BER performances are very different for correlation coefficients 0.92 and 0.98. Therefore, especially for very high correlated case, even small reductions with TSS for some subcarriers improves the BER performance. It is shown that for some subcarriers, with TSS correlation coefficient can be lower than 0.7 which gives very close performance as uncorrelated case. The reduction is limited for other carriers, however even small reduction can cause performance improvement.

Future wireless networks are expected to employ (combined with antenna arrays) adaptive OFDM (AOFDM) schemes and repeaters/relays as well. In those systems, again the spatial fading correlation is expected to be the main limitation on the system performance. In this dissertation, the effects of fading correlation on the AOFDM and OFDM repeater networks are also analyzed.

In the AOFDM transmission, each carrier in the OFDM system can transmit different modulation schemes depending on its channel condition whereas in the conventional OFDM systems fixed modulation across all the subcarriers is

used. Selection of the modulation scheme usually depends on the estimated carrier to noise ratio (CNR) at the AOFDM transmitter. The transmitter chooses modulation scheme to achieve a reasonable BER while maximizing the throughput. There is a tradeoff between the selected modulation scheme and the system throughput. Depending on the design issues, if the target BER is high (say 10^{-2}) system throughput can be maximized. On the other hand, for reliable communication (low target BER such as 10^{-5}) throughput can be optimized for given target BER. However, when the antenna array is employed at the receiver end, the knowledge of CNR is not enough to decide the modulation scheme to achieve the target BER due to the possibility of spatial correlation. Transmitter may know the number of antennas employed and can decide the modulation scheme with CNR and the number of diversity branches. However, if the antennas are correlated, system would fail to achieve the target BER. In Chapter 3, a new modulation decision chart based on joint effects of CNR and the correlation coefficient has been proposed. In the proposed scheme, the transmitter knows the CNR and the correlation coefficient, this knowledge can be fed back to transmitter from the receiver. The receiver may measure the correlation or estimate it with statistical techniques which are already reported in literature. Therefore, with this knowledge transmitter can decide the modulation scheme successfully in order to achieve the target BER. We have also applied TSS technique to the receiver array in order to reduce the correlation effects. TSS is found to be effective in both conventional AOFDM and the proposed AOFDM schemes. Since TSS reduces correlation for different subcarriers, the subcarrier based knowledge of CNR and correlation becomes more significant to decide the modulation order.

As mentioned earlier, future wireless systems are also expected to employ repeaters in the network. This is due to the compensate the propagation losses at high frequencies in order to keep the cell size. Another application might be to fill the gaps in coverage area as in current DVB-T networks. Relays are also in demand for similar purposes, but they require additional signaling in order to provide relay diversity (or multihop diversity). Whereas, the repeaters can be employed without any prior work into any network. Again the problem of spatial correlation arises when the base station employs an antenna array in

repeater networks. In Chapter 4, we have analyzed the OFDM repeater networks when the base station antennas are correlated. It is shown that depending on the repeater and the mobile terminal locations, accordingly their angle of arrivals, the spatial correlation on subcarrier basis changes dramatically at the base station antenna array. In this work, a multipath channel is constructed by the repeated signal instead of natural multipath due to cluttered environments. Direct path is set as the first path component and the repeated path is set as the second path component. Therefore, in this multipath channel, the TSS receiver performance has been analyzed and it is shown that the TSS receiver can work properly in the wireless repeater networks to reduce the effects of high correlation.

Acknowledgements

I would like to express my deep gratitude to my supervisor Assoc. Prof. Dr. Yukitoshi Sanada for his patient guidance, endless support and encouragement throughout my thesis research.

I would like to express my special thanks and gratitude to Prof. Dr. Iwao Sasase, Prof. Dr. Tomoaki Otsuki and Assoc. Prof. Dr. Hiroki Ishikuro for showing keen interest to the subject matter and accepting to read and review the thesis.

I would like to thank all the former and present members of the Sanada Laboratory for their support and close working relationships.

The financial supports from the Ministry of Education, Culture, Sports, Science and Technology of Japan (MEXT) and Keio Leading-Edge Laboratory (KLL) are thankfully acknowledged.

Finally, I would like to express my thanks to my family for their trust, encouragement and support throughout my life.

List of Achievements

Journal Articles:

[1] R.C. Kizilirmak and Y. Sanada, "Multipath Diversity through Time Shifted Sampling for Spatially Correlated OFDM-Antenna Array Systems," IEICE Trans. on Fundamentals, Vol. E91-A, No. 11, pp. 3104-3111, Nov. 2008

[2] R.C. Kizilirmak and Y. Sanada, "Performance Analysis of OFDM Repeater Networks with Spatial Fading Correlation" accepted to Wireless Personal Communications.

International Conference Articles:

[1] R.C. Kizilirmak and Y. Sanada, "Multipath Diversity through Time Shifted Sampling in Spatially Correlated OFDM-Antenna Array Systems," in Proc. the 68th IEEE Vehicular Technology Conference, Calgary, Canada, Sept. 2008.

[2] R.C. Kizilirmak and Y. Sanada, "Multipath Diversity through Time Shifted Sampling in Repeater Assisted Spatially Correlated OFDM Systems," in Proc. IEEE International Symposium on Intelligent Signal Processing and Communication Systems 2009, Kanazawa, Dec. 2009.

Presentations at Domestic Meetings:

[1] R.C. Kizilirmak and Y. Sanada "On the Capacity of Spatially Correlated MIMO-OFDM Systems in Multipath Environments" IEICE Society Conference BS-4-13 Sep. 2008.

[2] R.C. Kizilirmak and Y. Sanad "Diversity Gain through Time Shifted Sampling in Repeater assisted Spatially Correlated OFDM Systems" IEICE Technical Report WBS2009-3 June 2009.

[3] R.C. Kizilirmak and Y. Sanada" Spatial Fading Correlation for OFDM Antenna Arrays on a per Subcarrier Basis" IEICE Society Conference ABS1-8 Sep. 2009.

[4] R.C. Kizilirmak and Y. Sanada" Multihop Relaying with Polarization Diversity for OFDM" IEICE Technical Report RCS2009-138 Nov. 2009.

[5] R.C. Kizilirmak and Y. Sanada "Adaptive Modulation Scheme Incorporating Spatial Fading Correlation for OFDM with Time Shifted Sampling " IEICE Technical Report SR2009-** March 2010.

Awards:

[1] IEEE VTS Japan 2008 Young Researcher's Encouragement Award

[2] IEICE 2009 WBS Student Paper Awards